2014

The Role of MicroRNA in Staphylococcal Enterotoxin B-Induced Inflammation and Acute Lung Injury

Roshni Rao
University of South Carolina - Columbia

THE ROLE OF MICRORNA IN STAPHYLOCOCCAL ENTEROTOXIN B-INDUCED INFLAMMATION AND ACUTE LUNG INJURY

By

ROSHNI RAO

Bachelor of Science
Bangalore University, 2006

Master of Science
University of Otago, 2008

Submitted in Partial Fulfillment of the Requirements

For the Degree of Doctor of Philosophy in

Biomedical Science

School of Medicine

University of South Carolina

2014

Accepted by

Mitzi Nagarkatti, Major Professor

Prakash Nagarkatti, Chairman, Examining Committee

Cory Robinson, Committee Member

Angela Murphy, Committee Member

Raja Fayad, Committee Member

Lacy Ford, Vice Provost and Dean of Graduate Studies

DEDICATION

This work is dedicated to my family - my mother, who has been a source of unconditional love and strength. My father, whose words of wisdom resonate with me in times of need and my brother, who always makes me laugh.

ACKNOWLEDGEMENTS

"It is good to have an end to journey toward; but it is the journey that matters, in the end".

As I ponder over the last five years of graduate school, I clearly see the faces of the people who have willingly and sometimes unknowingly made what would seem to be a long, treacherous road ahead, a journey of immense growth, laughter, love and learning and I would like to take the opportunity to acknowledge them.

First, I thank my mentors Dr Prakash and Dr Mitzi Nagarkatti for providing me with many opportunities to grow in Science and in leadership. Inspired by their hard work and dedication they have equipped me with the tools to face the challenges that the next phase of a scientific career will bring. I am grateful for their support, encouragement and training.

While laboratory work has sometimes yielded triumphs and most times been frustrating, it was counting the small blessings that helped persist forward. I owe that encouragement and consistent support to my fellow graduate students and lab members who I now consider family. Thank You to my sisters Sadiye Rieder, and Jessica Sido, my friends Austin Jackson, Brandon Busbee and Sunil Tomar for consistently having my back and a special Thank You to Michael Rouse for being my pillar of strength, my guide and confidant in the best and darkest of times. I would like to acknowledge Dr Narendra Singh for his anecdotes and bits of wisdom that allowed me to stay positive and a Thank You to Dr Venkatesh Hegde for teaching me the importance of quality of work. A very

special Thanks to Lee Ann Fauling, Tina Akers, Ansley Roberts and Judy Lawrence for their patience and kindness in taking care of me and the incessant administrative questions I might have posed. Thank You to Chakira Hogan for a friendship and strength you provided to face my challenges.

I would like to thank my committee members, Dr Angela Murphy for her guidance, patience and constant encouragement for the last five years. Dr Cory Robinson and Dr Raja Fayad for being inspiring scientists and whose guidance and input during my comprehensive exam I greatly appreciate.

While my time at the University has mainly revolved around the lab, I cannot forget the friends outside the confines of the School of Medicine who have encouraged, cheered and egged me on towards completion. My friend Amrita, whose intelligence and mostly her goodness will always make me want to strive further. Pallavi and Shraddha whose simplicity and joyfulness keeps me grounded. While you have all journeyed with me today, know that it is what has shaped me to be better tomorrow.

Finally, my dearest family, Mom, Dad, Karan, Tadeep, Chichi and Suraj for all the sacrifices that they have made. It is because of all of them and their blessings that I am excited to begin a brand new chapter of my life.

ABSTRACT

Staphylococcal enterotoxin B (SEB) is a potent activator of the Vβ8+T-cells leading to the proliferation of nearly 30% of the T-cell pool. As a consequence, excessive amounts of cytokine mediators are released leading to extensive tissue damage and sometimes toxic shock and death. Due to the ease with which SEB can be aerosolized anddisseminated, it is considered a biological weapon. In the current study, we investigated the pro-inflammatory effects of SEB in two mouse models of acute inflammatory lung injury. Specifically, while inflammatory cues are known to elicit changes in key transcriptional factors and gene expression, we explored for the first time, the role of microRNA following SEB exposure. We found that C57BL/6 mice exposed to a single dose (50 μg/mouse) of SEB demonstrated symptoms of pulmonary inflammation characterized by cellular infiltration, histopathological damage and the release of copious amounts of IFN-γ. Upon conducting microRNA microarray analysis and applying cutting-edge bioinformatics analysis, we identified the overexpression of miR-155 and the subsequent repression of its target gene *Socs1* following SEB exposure. Further, through the use of miR-155$^{-/-}$ mice, we demonstrated the critical role for SEB-induced miR-155 in mediating damage. In a more severe model of acute inflammatory lung injury, C3H/HeJ mice were exposed to two smaller quantities (2 μg and 5μg/ mouse) of SEB given two hours apart. As a result, mice succumb to vascular leak, excessive cellular infiltration and exaggerated cytokine and chemokine release. Pulmonary damage is associated with the dysregulation of several miRNA. Those miRNA that were

overexpressed were found to target key regulators of inflammation and those that were underexpressed allowed for the expression of pro-inflammatory genes demonstrating that several SEB-inducing miRNA act in concert to orchestrate inflammation. Therapeutic strategies to combat inhalation exposure to SEB are either lacking in their efficacy or with regards to acute inflammatory lung injury, limited to supportive care. As a result, we investigated the role of the marijuana cannabinoid- Delta-9-Tetrahydrocannabinol(THC), a known anti-inflammatory agent in the treatment of SEB-triggered inflammation. Interestingly, C3H/HeJ that succumbed to SEB toxicity, were completely protected by THC treatment. Upon investigation of the anti-inflammatory nature of THC, we demonstrated for the first time the ability of THC to modulate a prominent inflammatory miRNA cluster (miR-17-92) involved in activation of the PI3K/AKT signaling pathway THC, by acting as an inhibitor of this pathway, via the downregulation of the cluster, induces T-regulatory cells, reduces cellular proliferation and decreases IFN-γ production. Taken together, our studies highlight the importance of miRNA in SEB-induced inflammatory damage. Moreover, we provide further insight into the anti-inflammatory properties of THC and emphasize its potential as a powerful therapeutic agent.

TABLE OF CONTENTS

LIST OF FIGURES

CHAPTER I: INTRODUCTION

1.1 STAPHYLOCOCCAL ENTEROTOXIN B (SEB)

The gram positive bacterium *Staphylococcus aureus* is an opportunistic pathogen that persistently colonizes up to 20% of healthy humans thereby increasing their susceptibility to infections (Kuehnert *et al.*, 2006; Wertheim *et al.*, 2005). Some of the most common infections caused by the pathogen are, bacteremia, endocarditis, septic shock, food-borne gastroenteritis and toxic shock syndrome making *Staphylococcus aureus* a leading cause of community and hospital acquired morbidity (Frank *et al.*, 2010; Huang *et al.*, 1998).

The bacterium possesses an arsenal of virulence factors that contribute to its pathogenesis. Some of these factors include the expression of surface proteins to aid in adhesion, the formation of biofilms to enable persistence , the secretion of enzymes such as proteases and lipases to ensure immune evasion and importantly, the production of inflammation inducing- enterotoxins (Archer, 1998; Gordon *et al.*, 2008).

Staphylococcal enterotoxins (SEs) are a group of ~23-30 kDA secreted, acid and heat stable proteins that share amino-acid sequence homology and are functionally similar (Balaban *et al.*, 2000). Structurally, although these proteins all comprise of tightly packed β-sheets and α-helical domains separated by a shallow groove, they differ in their interaction with the major histocompatibility class II (MHC II) and in their T-cell receptor specificity (Argudin *et al.*, 2010). Amongst the large group of SEs (SE A-V and toxic shock staphylococcal toxin-1, the TSST-1), SEA and SEB are the best studied.

While, SEA is the most common toxin associated with staphylococcal food poisoning (Pinchuk *et al.*, 2010), the focus of our study is SEB. SEB is the only SE studied with regards to its role as a potential biological weapon. Since it is easy to produce in the laboratory, is a stable and robust protein and can be easily aerosolized, the Center for Disease Control and Prevention (CDC) has classified SEB as a 'select' agent (Pinchuk *et al.*, 2010). In fact, the study of SEB was carried out in the 1960's when the USA had an active offensive biological warfare program. Since then, a number of facets of SEB exposure have been elucidated.

SEB exposure elicits a wide range of symptoms depending on the site of entry. Ocular exposure to SEB leads to conjunctivitis, while the ingestion of SEB results in nausea, vomiting and diarrhea within 6 hours of exposure. The inhalation of the toxin can lead to fever, respiratory damage, acute respiratory distress syndrome (ARDS) and death. Furthermore, exposure to the toxin under battlefield-induced stress exacerbates the severity of symptoms which include vasodilation and drop in blood pressure.

The potency of SEB stems from the fact that it is a superantigen, a term used to describe antigens that hyper-activate the immune system. Unlike conventional antigens that undergo antigen processing by an Antigen Presenting Cell (APC) and are displayed to a T-cell via the MHC II, leading to the activation of a fraction (~0.001%) of T-cells, a superantigen, strongly stimulates T-cells comprising the Vβ8 domain of the T-cell receptor independent of antigen recognition and processing. As a result, up to 30% of the T-cells are activated and clonally expanded. This initial binding is followed by engagement of co-stimulatory molecules such as CD69, CD28, CD80 that help sustain activation and trigger downstream signaling cascades such as the MAPK, PI3K/AKT,

NFκB pathways. It is well established that several cytokines such as IL-1, TNF-α, IL-2, IFN-γ, IL-6, MCP-1 are induced upon activation of these key inflammatory signaling pathways. The release of these cytokines after SEB exposure results in further proliferation of T-cells and the recruitment of other immune cell subsets. Thus, SEB exposure involves the activation of the immune system and the establishment of a strong inflammatory environment that can now mediate extensive tissue damage.

Treatment against the harmful effects of SEB exposure has previously been explored and has shown some therapeutic promise. For example, the use of a combination of monoclonal antibodies confers protection from SEB-induced toxic shock in HLA DR3 transgenic mice (Varshney *et al.*). The use of synthetic peptides elicits anti-SEB antibodies (Visvanathan *et al.*, 2001) and mimetic peptides of CD28 decrease production of IL-2, IFN-γ thereby protecting mice from SEB-induced shock (Chen *et al.*).In addition, the use of immunosuppressive glucocorticoids such as Dexamethasone and Rapamycin have demonstrated protective effects in mice exposed to SEB by blocking SEB-induced cytokines and chemokines and suppressing NFκB activation. On the other hand, several other therapeutic strategies to combat SEB exposure have been limited in their efficacy. For example, SEB-peptide antagonists are unable to prevent T-cell activation and cytokine production *in vitro* and *in vivo* in HLA II transgenic mice (Tilahun *et al.*, 2011). The use of TCR Vβ8 mimics that interfere with the binding of SEB have short half-lives in rabbits and would prove ineffective in the clinic (Strandberg *et al.*).

In conclusion, SEB, by virtue of being a superantigen, elicits a strong immune response characterized by cellular proliferation, excessive release of cytokines and

chemokines and the simultaneous activation of several key inflammatory pathways. As a result, exposure to the toxin has a number of far reaching effects in humans ranging from food poisoning to death. While a number of treatment modalities have been studied to combat the toxicity induced by SEB, therapeutic interventions that are efficacious and manage inflammation in the clinical setting is still lacking.

1.2 microRNA

Cells contain a number of non-coding RNA (ncRNA) that are structural, catalytic or regulatory in function but do not encode protein (Eddy, 2001). One such class of small regulatory non-coding RNAs that are newly discovered and have generated significant interest in the scientific community is microRNA (miRNA).

The first miRNA- *lin-4* and *let-7* were identified in *C. elegans* and found to be critical in the developmental stages of the nematode. It was observed that *lin-4* was partially complimentary to the 3' Untranslated region (UTR) of *lin-14 and lin28,* genes that encode protein necessary for the progression of larval stages. Similarly, *let 7* bound to the 3'UTR of *lin-41* and *hbl-1,* hindering development of the worm (Lin *et al.*, 2003; Sasaki *et al.,* 2010; Vella *et al.,* 2004). This discovery, hinted towards a novel form of gene regulation that could influence development and prompted the exploration of these miRNA in other species. Since then, hundreds of miRNA have been identified in plants, animals, viruses and unicellular algae and at least a thousand miRNA have been found in humans likely regulating 30-90% of genes (Dai *et al.*, 2011; Molnar *et al.*, 2007). These miRNA serve as key regulators of genes in myriad biological processes such as cellular proliferation, differentiation, signal transduction, development of organs, apoptosis and immune response (Sonkoly *et al.,* 2008).

The biogenesis of miRNA begins with the transcription of primary miRNA transcripts (pri-miRNA) by RNA polymerase II that are up to thousands of nucleotides long and contain hairpin structures. Classically, the pri-miRNA is processed and cleaved in the nucleus by a complex known as the Microprocessor comprising of RNase III enzyme Drosha and the double-stranded RNA binding domain protein DGCR8 yielding a ~70 nt precursor miRNA (pre-miRNA). Exportin 5 subsequently transports the pre-miRNA into the cytoplasm where it is cleaved by RNase III enzyme Dicer to yield a ~22 nucleotide mature miRNA: miRNA* duplex product. This duplex is loaded into the Argonaute (Ago) protein to form a RNA-inducing silencing complex (RISC). Following the degradation of the miRNA* strand within the RISC, the miRNA strand that remains, guides the RISC to mRNA targets and allows for the interaction of the miRNA with the 3'UTR of target mRNA. 2-8 nucleotide regions within the 3'UTR, known as seed sequences are important for the miRNA recognition of the target gene. Consequently, mRNA is cleaved and degraded if the miRNA displays perfect or near-perfect complementarity to the 3'UTR, otherwise, as is the case with most miRNA, the miRNA and its respective target base-pair imperfectly resulting in the repression of translation (Bushati *et al.*, 2007; Plaza *et al.*, 2004).

As mentioned above, miRNA have been found to regulate almost every cellular process in the body. This includes actively participating and orchestrating the development and function of the innate and adaptive arm of the immune system. A few studies have identified miRNA in the regulation of hematopoietic stem cells (HSC), where CD34+ human stem and progenitor cells express numerous miRNA (Georgantas *et al.*, 2007; Mandal *et al.*, 2005). The Homeobox (HOX) family of genes which are

important in the regulation of HSC stem cells, are targeted by individual miRNA such as miR-196b, miR-126 (Shen *et al.*, 2008; Yekta *et al.*, 2004). Furthermore, the role of miRNA has also been established in the function and development of dendritic cells (DC), macrophages, Natural killer (NK) cells, granulocytes and monocytes. For example, miR-223 targets transcription factor E2F1, which results in increased granulocyte differentiation (Pulikkan *et al.*). miR-424 enhances monocyte differentiation by binding NFI-A which in turn causes the activation of macrophage colony-stimulating factor receptor (M-CSFR) (Rosa *et al.*, 2007). Similar to their roles in the innate system, miRNA control the development, differentiation and function of cells of the adaptive arm. For example, the miR-17-92 cluster increases T-cell survival during the double negative 2 (DN2) stage of thymopoiesis. The absence of this cluster, also leads to the lymphoproliferation of B and T-cells (Xiao *et al.*, 2008). miR-181a functions to enhance TCR signaling strength (Greenhough *et al.*, 2007), while miR-155 promotes Th1 differentiation (Plaza *et al.*, 2007). Furthermore, the conditional deletion of Dicer or Drosha in T-regulatory (T-regs) cells causes lethal autoimmune inflammatory disease (Zhou *et al.*, 2008). Thus, given that miRNA are critical regulators of gene expression, it is not surprising that they also control aspects of the immune system. By serving as fine tuners of important stages of development and differentiation, they maintain and enable proper immune response and homeostasis. However, what is interesting to this study is the possibility of a strong dysregulation of miRNA. For instance, what is the role of miRNA during inflammatory response and disease? By regulating important inflammatory genes and transcription factors, can miRNA be implicated in inflammation? Can we target key miRNA involved in inflammatory disease and thus

prevent inflammatory damage? While several studies have already sought to answer some of these questions a brief overview of miRNA in inflammation is presented below.

Inflammation is important for host defense against pathogens. However, the hyperactivation of the inflammatory response triggered by exposure to bacterial LPS, peptidoglycan, enterotoxins such as SEB can cause host tissue damage and disease. It is important that molecules that govern the initiation, progression and resolution of inflammation be properly regulated. While an inflammatory insult elicits intricate changes in the transcriptional landscape, we have now learned that the dysregulation of miRNA accompany these molecular changes. For example, murine macrophages activated with Poly (I:C) and interferon β results in the activation of the MAP kinase JNK, which in turn leads to the induction of miR-155(O'Connell *et al.*, 2007). Similarly, the overexpression of miR-21 in myeloma cells is dependent on the expression of STAT3 (Loffler *et al.*, 2007). miR-146a is induced upon lipopolysaccharide (LPS) stimulation in human monocytes to function as a negative regulator of Toll-like receptor (TLR) signaling by targeting TRAF6 and IRAK4 (Baltimore *et al.*, 2008).

Evidently, inflammatory cues alter the expression of several miRNA. Moreover, aberrant expressions of several miRNA have been implicated in inflammatory disease and autoimmunity. miR-326 is overexpressed in Multiple Sclerosis (MS) and plays a role in Th17 cell differentiation (Miethke *et al.*, 1993). Murine models of arthritis have demonstrated the role for miR-182 in regulating B and T-cell function (Stittrich *et al.*). Similarly, the introduction of synthetic let-7 mimic to mice in asthma represses IL-13 and ameliorates airway inflammation(Polikepahad *et al.*).

In summary, miRNA have arisen as important regulators of gene expression serving critical roles in mammalian inflammatory response. Given that several miRNA target a number of potential genes and owing to the infancy of the miRNA field, a number of features of miRNA-mRNA interactions remain to be uncovered. Nevertheless, we have begun to carefully study the role of individual miRNA in disease process to identify novel biomarkers, establish unique therapeutic agents that can directly modulate them with the ultimate goal of curing and preventing inflammation and disease.

1.3 DELTA-9 TETRAHYDROCANNABINOL (THC)

The flowering tops and leaves of the *cannabis sativa* (marijuana) plant contain biologically active constituents known as cannabinoids. Amongst the approximately 60 cannabinoids produced, Delta-9-Tetrahydrocannabinol (THC) is the major psychoactive component (Klein *et al.*, 2001). Although anecdotal evidence regarding its therapeutic properties has existed for thousands of years, it was the isolation and elucidation of its structure in 1964 that prompted its study. Since then, a number of synthetic analogues have been developed that mimic its analgesic, anti-emetic and immunomodulatory properties in *vivo.*

Cannabinoids mediate their action through the ligation of two main cannabinoid receptors, the CB1 and CB2. These receptors are G-protein coupled single polypeptides with an extracellular N-terminus and intracellular C-terminus with seven transmembrane helices. While the CB1 receptor is predominantly located on the hippocampus and basal ganglia in the brain, it is also expressed on peripheral tissues such as the liver, pancreas and immune cells. The CB2 receptor is mainly expressed in the

periphery and particularly in immune cells such as B-cells, NK cells, monocytes, Peripheral mononuclear cells (PMN) and T-cells (Klein *et al.*, 2003).

The presence of CB receptors on immune cells suggests that cannabinoids are immunomodulatory. THC in particular has demonstrated a number of anti-inflammatory properties such as the modulation of cytokines, the modulation of T-cells and the induction of apoptosis (Nagarkatti *et al.*, 2009). For example, splenocytes activated with pokeweed mitogen (PWM) and treated with THC lead to a decrease in Th1 cytokine IFNγ and simultaneous increase in Th2 cytokines IL-4 and IL-10 (Newton *et al.*, 1998). Similarly, THC treatment of mice given *Legionella pnuemophila* succumbed to infection due to the decrease in IFNγ and IL-12 and the increase in IL-4, suggesting that the THC mediated Th1 to Th2 cytokine shift contributed to enhanced infection (Klein *et al.*, 2000). THC has also been demonstrated to induce apoptosis in T-cells, B-cells and macrophages (Nagarkatti *et al.*). Furthermore, THC mediated apoptosis was found to be mediated through BCL2 and the activation of caspases (Nagarkatti *et al.*, 2009). Our laboratory has demonstrated that THC also induced immunosuppressive immune cells. For example, in a mouse model of Con-A induced hepatitis, THC treatment ameliorated liver injury by the induction of Foxp3+ T-regulatory cells(Hegde *et al.*, 2008). We have also observed that THC induces functional myeloid derived suppressor cells (MDSC) through the activation of the CB1 and CB2 receptors further demonstrating the potent anti-inflammatory properties of THC (Hegde *et al.*).

Recently, we have reported novel mechanisms of action for THC. It appears that THC can activate the expression of Th2 cytokine genes, while suppressing the signals to Th1 cytokines via histone modifications (Yang *et al.*). Moreover, we have also

found that THC-induced MDSCs displayed a distinct miRNA profile compared to MDSCs derived from naïve bone marrow, suggesting that THC induced miRNA may play a functional role in the development of these MDSCs (Hegde *et al.*).

In conclusion, although a number of studies have explored the role of THC as an anti-inflammatory agent and have established its efficacy in modulating immune response, we are only now discovering unique properties that underlie its mechanism, the examination of which will enable us to further exploit its therapeutic properties.

1.4 PROBLEM AND HYPOTHESIS

The superantigenic property of SEB makes it an ideal candidate to be used as a biological weapon. Studies have established that exposure to the toxin results in an exaggerated immune response due to the secretion of a number of inflammatory mediators. With the discovery that inflammatory cues can trigger the expression of a unique class of gene regulators, the miRNA, it was unclear if SEB exposure would affect the miRNA profile in mice and if the miRNA played a role in SEB-mediated damage to the lung. Therefore, we hypothesized that exposure to the toxin results in the dysregulation of miRNA. Furthermore, we also wanted to establish the role of the marijuana derived cannabinoid, THC, known for its anti-inflammatory properties in ameliorating SEB-induced acute inflammatory lung injury. Accordingly, we hypothesized that THC treatment would prevent SEB-mediated mortality of mice and does so by the modulation of inflammation specific miRNA.

CHAPTER II: Staphylococcal enterotoxin B (SEB) - induced microRNA-155 targets suppressor of cytokine signaling-1 (SOCS1) to promote acute inflammatory lung injury.

2.1 INTRODUCTION

Staphylococcal Enterotoxin B (SEB), a superantigen produced by *Staphylococcus aureus* has deleterious effects in humans such as food poisoning (Pinchuk *et al.*, 2010) and toxic shock (Savransky *et al.*, 2003). Because it can be easily aerosolized, SEB is classified as a Category B agent by the Centers for Disease Control and Prevention (Ulrich, 2001). Upon inhalation exposure, SEB can trigger acute inflammatory lung injury characterized by immune cell infiltration, excessive cytokine production, tissue damage and pulmonary edema (Neumann *et al.*, 1997; Saeed *et al.*).

Due to the distinct manner in which SEB binds to the non-polymorphic regions of MHC II on antigen presenting cells and the specific Vβ regions of the T-cell receptor (TCR) such as murine Vβ8 (Bavari *et al.*, 1995), SEB exposure leads to the activation and proliferation of a large population (5-30%) of T-lymphocytes (Kozono *et al.*, 1995). Activation of such a substantial number of T-lymphocytes results in the robust production of inflammatory cytokines such as IL-2, TNF-α and IFN-γ (Bette *et al.*, 1993; Miethke *et al.*, 1993). In most cases, IFN-γ is the main culprit in mediating the damaging and often lethal effects seen upon SEB exposure. For example, transgenic mice deficient in IFN-γ, were protected from SEB-mediated Toxic Shock Syndrome (TSS) and

subsequent mortality(Tilahun *et al.*, 2011). Additionally, the neutralization of IFN-γ, after SEB exposure was shown to prevent lethal systemic inflammation (Florquin *et al.*, 1995) further suggesting the importance of SEB-mediated IFN-γ production. While the interaction between SEB and TCR, along with the subsequent T-cell proliferation and cytokine secretion have been extensively studied (Fleischer *et al.*, 1991; Herman *et al.*, 1991; Saeed *et al.*, 2012), the role of miRNA in mediating SEB-induced inflammation has not yet been elucidated.

MicroRNA (miR) are ~21-23 nt long, single stranded non-coding RNA molecules that can translationally repress or target mRNA for degradation, thereby acting as primary modulators of gene expression (Cai *et al.*, 2009). Several studies have demonstrated a role for miR in modulating immune responses under various inflammatory conditions (O'Connell *et al.*, 2012). For example, while miR-125b is highly expressed in naïve CD4+ T-cells, it becomes significantly downregulated upon T-cell activation (Rossi *et al.*, 2011). Similarly, studies have demonstrated that overexpression of miR-17-92 cluster in T-cells leads to lymphoproliferative disorder due to the repression of the pro-apoptotic molecule, BIM (Xiao *et al.*, 2008). Furthermore, mice deficient in miR-155 are resistant to developing experimental autoimmune encephalomyeltis, a mouse model of multiple sclerosis (O'Connell *et al.*, 2010), while the overexpression of miR-155 exacerbates the symptoms associated with the disease.

Taken together, these studies strongly suggest that miRs play a major role in modulating immune cell activation, particularly T-cells, as well as promoting pro-inflammatory responses.

In the current study of SEB-induced acute inflammatory lung injury, we applied microarray analysis and quantitative real time PCR (q-RT PCR) to establish important miRs that are dysregulated in response to SEB. Further, our data identified miR-155 as a major contributor to SEB-mediated lung inflammation. While it is known that SEB exposure leads to inflammation and the production of copious amounts of IFN-γ, we provide mechanistic insight through gain and loss of function experiments, into the role of miR-155 in this process. Our results may present an opportunity to further therapeutically target miR-155 in the treatment of SEB-mediated acute inflammatory lung injury.

2.2 MATERIALS AND METHODS

Mice

Female C57BL/6 mice (6-8 weeks) were purchased from the National Cancer Institute (NCI). miR-155$^{-/-}$ (B6.Cg-*Mir155* $^{tm1.1\ Rsky}$/J) were purchased from The Jackson laboratory. All mice were housed under pathogen free conditions at the Animal Resource Facility (ARF), University of South Carolina (USC) School of Medicine. The use of vertebrate animals in the experiments performed was pre-approved by the Institutional Animal

Care and Use Committee (IACUC) at USC. This study was carried out in strict accordance with the recommendations in the Guide for the Care and Use of Laboratory Animals of the National Research Council (2011)

Induction of SEB-induced acute lung injury (ALI)

SEB was obtained from Toxin Technologies (Sarasota, Florida). SEB dissolved in sterile PBS (2 mg/mL) was administered by the intranasal (i.n) route in a volume of 25 µL for a dose of 50 µg per mouse, as described (Rieder *et al.*, ; Rieder *et al.*, ; Saeed *et al.*) . Mice were euthanized 48 hours after SEB exposure.

Lung histopathological analysis

At the time of euthanasia, lungs were obtained and fixed in 10% formalin. The tissue was then paraffin embedded and serial sections (5 µm) were made. The sections were subsequently deparaffinized by dissolving with xylene, followed by rehydration in several changes of alcohol (100%, 95%, and 90%). The slides were then stained with hematoxylin and eosin (H&E) and evaluated with a Nikon E600 light microscopy system.

Antibodies

Fluorescein isothiocyanate-conjugated anti-CD8 (clone: 53.6.7) and phycoerythrin-conjugated anti-CD4 (clone: GK1.5) Abs were purchased from Biolegend (San Diego, CA).

Preparation of lung-infiltrating cells and flow cytometry

Mice were exposed to SEB as described above. Forty eight hours after SEB exposure, lungs were harvested and homogenized using Stomacher® 80 Biomaster blender from Seward (Davie, FL) in 10 ml of sterile PBS. After washing with sterile PBS, the cells

were carefully layered on Ficoll - Histopaque ®-1077 from Sigma-Aldrich (St Louis, MO) and separated by density gradient centrifugation at 500 x g for 30 minutes at 24°C with brake off. The mononuclear cell layer isolated was then enumerated using the Trypan blue exclusion method. To determine the subsets of immune cells infiltrating the lung, cells were stained with fluorescent conjugated antibodies (anti-CD4, anti-CD8) and analyzed using the Beckman Coulter 500 Flow cytometer (Indianapolis, IN).

Recovery of broncheoalveloar lavage fluid (BALF) and cytokine detection

Forty-eight hours after SEB exposure, mice were euthanized and tracheae from vehicle or SEB exposed mice were tied with a suture and the lung was excised as an intact unit. With 1 ml sterile ice-cold PBS, the trachea was lavaged to collect the BALF fluid. Cytokine analysis for interferon-γ (IFN-γ) was carried out using BALF. All cytokines were measured using Biolegend (San Diego, CA) ELISA MAX™ Standard kits.

Total RNA isolation

Total RNA (including small RNAs) was isolated from lung-infiltrating mononuclear cells or *in vitro* from lymph nodes or splenocytes using miRNeasy kit from Qiagen (Valencia, CA) following manufacturer's instructions. The purity and concentration of the RNA was confirmed spectrophotometrically, while the integrity of miRNA was further assessed using Agilent 2100 BioAnalyzer (Agilent Tech, Palo Alto, CA).

miRNA expression profiling and analysis

To profile miRNA expression in the lung, the Affymetrix GeneChip ® miRNA 1.0 array platform was used. The array which comprises of 609 mouse miRNA probes makes use of FlashTag™ Biotin HSR hybridization technique and was carried out according to

manufacturer's instructions (Affymetrix, Santa Clara, CA). Fluorescent intensities obtained from hybridization were log-transformed and visualized in the form of a heatmap. Hierarchical clustering was carried out using Ward's method and Similarity measurement was calculated using half square Euclidean distance. miRNA expression fold change obtained from the microarray were then further analyzed using the commercially available analysis tool Ingenuity Systems®-Ingenuity Pathway analysis – (IPA), (Mountain View, CA, USA.) In brief, the dataset of 609 miRNA were uploaded into IPA and only miRNA that were 3 fold or higher were considered for analysis. Core analysis was carried out and a 'Top Network' of miRNA and its associated molecules was generated. All microRNA microarray data were deposited in ArrayExpress database (www.ebi.ac.uk/arrayexpress) under accession number E-MTAB-2379.

Analysis of miRNA target genes

IPA was also used to determine and collate the highly predicted, moderately predicted and experimentally observed mRNA target genes of those miRNA that were highly (≥3 fold) upregulated using IPA's miRNA target filter tool. These targets were further sorted based on their role in cytokine signaling, cellular growth and proliferation and cellular immune response. Additionally, to assign Immunological functions to our list of miRNA targets, Gene Ontology (GO) mapping of miRNA target genes was carried out using Cytoscape 3.0.1 equipped with ClueGO and CluePedia applications.

Quantitative real-time PCR (qRT-PCR)

Total RNA (miRNA and mRNA) were converted to cDNA using the miScript cDNA synthesis kit (Qiagen) according to manufacturer's instructions. For miRNA validation, the miScript SYBR Green PCR kit (Qiagen) was used and fold change of miRNA was

determined using $2^{-\Delta\Delta Ct}$ method. Snord 96a was used as small RNA endogenous control. For mRNA validation, SSO advanced™ SYBR Green PCR kit from Biorad (Hercules, CA) was used according to manufacturer's instructions and β-actin was used as the endogenous control. The following primers were used: *β-actin* (F) 5'-GGCTGTATTCCCCTCCAT G-3' and (R) 5'-CCAGTT GGTAACAATGCCATGT-3'; *SOCS-1* (F) 5'-GGTTGTAGCAGCTTGTGTC-3' and (R) 5'-AATGAAGCCAGAGACCCTC-3'; *IFN-γ* (F) 5'-GCGTCATTGAATCACACCTG-3' and (R) 5'-GAGCTCATTGAATGCTTGGC-3'

Transfection with miR-155 mimic and inhibitors

Lymph nodes (axillary and inguinal) from naïve C57Bl/6 mice were harvested and cultured in 10 ml of complete media at 37° C and 5% CO_2. Complete media comprised of RPMI 1640 medium (Gibco Laboratories, Grand Island, NY) supplemented with 10% FBS, 10mM L-glutamine, 10mM Hepes, 50 μM β-Mercaptoethanol , and 100 μg/mL penicillin. Cells were seeded at $2x10^5$ cells in 24 well plates and transfected with either 40 nM synthetic mmu-miR-155 -3p miScript miRNA mimic (CUCCUACCUGUUAGCAUUAAC) or AllStar negative control siRNA. For inhibition of miR-155, cells were activated with SEB (1 μg/ml) and treated with 100 nM Anti-mmu-miR-155-3p miScript miRNA inhibitor (CUCCUACCUGUUAGCAUUAAC) or miScript Inhibitor negative control for 24 hours using HiperFect transfection reagent(Qiagen) according to manufacturer's instructions.

Luciferase assay

The following plasmids were purchased from GeneCopoeia (Rockville, MD) – 3'UTR-*Socs1* (MmiT028883) and control plasmid (CmiT000001-MT01). Chinese Hamster

Ovary (CHO) cells were co-transfected with 100 ng of plasmid and 100nM of miRIDIAN microRNA mmu-miR-155-5p mimic or miRIDIAN microRNA mimic negative control using DharmaFECT DUO transfection reagent following manufacturer's instructions (Thermo Scientific, Pittsburgh, PA). 24 hr following transfection, Luciferase activity was measured using LucPair ™ miR-Duo Luciferase Assay kit from GeneCopoeia.

Statistics

All statistical analyses were carried out using GraphPad Prism Software (San Diego, CA). In all experiments, the number of mice used was 4-5 per group, unless otherwise specified. Results are expressed as means ± SEM. Student's t-test was used to compare WT and miR-155$^{-/-}$ data, whereas multiple comparisons were made using one-way analysis of variance (ANOVA), followed by *post hoc* analysis using Tukey's method. A p-value of <0.05 was considered statistically significant. Individual experiments were performed in triplicate and each experiment was performed independently at least three times to test reproducibility of results.

2.3 RESULTS

SEB exposure triggers inflammation in the lung.

Previously, a single dose of SEB (50 μg) by intranasal delivery was found to induce cellular infiltration, increase cytokine production, cause histopathological lesions and edema in C57BL/6 mice (Rieder *et al.*, ; Rieder *et al.*, ; Saeed *et al.*) mimicking the symptoms of acute inflammatory lung injury in humans (Wheeler *et al.*, 2007). In this study, we first sought to investigate the inflammatory effect of SEB-exposure in the lungs. Forty -eight hours after SEB exposure, H&E stained sections of the lungs from

SEB-exposed mice showed massive infiltration of cells and signs of edema as evidenced by fluid filled bronchioles (Figure 2.1A). Because SEB is a potent activator of T-cells, we examined the effect of SEB on T-cell subsets within the lung. Immediately after euthanasia, the lungs were harvested and mononuclear cells were isolated from the lungs by density gradient centrifugation to determine the phenotypic characteristics of the cells. SEB exposure not only led to an overall increase in mononuclear cells but specifically, an increase in CD4+ and CD8+ T cells (Figure 2.1B) was seen. Because SEB exposure triggers an increase in IFN-γ, a major pro-inflammatory cytokine previously reported to orchestrate the inflammatory cascade and cause tissue damage(Miyata *et al.*, 2008; Plaza *et al.*, 2007; Tilahun *et al.*, 2011), we analyzed the concentration of IFN-γ in the broncheoalveolar lavage fluid (BALF) and found a high concentration (upto 3000 pg/ml) of IFN-γ in the lungs of SEB exposed mice (Figure 2.1C). These data suggested that SEB administration via the intranasal route triggers acute inflammation in the lungs.

SEB exposure modulates miRNA expression in the lungs.

The dysregulation of specific miRs in response to SEB exposure has not been elucidated. Because miRs play a critical role in mediating inflammation, we examined the miR profile after SEB exposure. Total miR was isolated from lung-infiltrating mononuclear cells and the relative abundance of miR in SEB exposed and vehicle treated mice was determined using microarray miRNA analysis. A heatmap was generated based on hierarchical clustering of miRNA highlighting a stark difference between vehicle- and SEB-exposed mice (Figure 2.2A). Further examination of miR expression revealed that of the 609 miR assessed, most remained unchanged, but a few showed significant up- or downregulation as seen in the fold change distribution plot (Figure 2.2B). Ingenuity

Pathway Analysis (IPA) generated a 'Top Network' of miR that comprised of five upregulated miRs, including miR-155, miR-31, miR-182, miR-20b, and miR-222 and their associated molecules (Figure 2.2C). This network was characterized by IPA as responses involving inflammation, cellular development, cellular growth and proliferation. To assign significant Immunological functions to the genes in the aforementioned 'Top Network', Cytoscape (ClueGO+CluePedia application) was employed. Gene Ontology (GO) mapping revealed that the genes associated with the miR in the 'Top Network' were functionally relevant to T-cell activation (GO: 0042110) and proliferation (GO: 0042098), Interferon-γ signaling (GO: 0060333) and Toll-like receptor signaling (GO: 0002224) (Figure 2.2D). Next, we validated the expression levels of these miRs in lung infiltrating mononuclear cells by q-RT PCR , which corroborated the expression patterns seen using the microarray (Figure 2.2E). Amongst the miRs we validated, miR-155 was the most highly expressed (~ 8 fold) in the lungs upon SEB exposure. Based on this, the role of miR-155 in the development of SEB-induced ALI was further investigated.

miR-155 is important for SEB-mediated inflammation

Because miR-155 was highly upregulated in response to SEB, we hypothesized that it might play a crucial role in facilitating the inflammation observed during the disease. To that end, WT and miR-155 $^{-/-}$ mice were exposed to SEB to determine the effects on disease parameters. H&E stained sections of the lung revealed that WT mice exposed to SEB exhibited numerous layers of infiltration interspersed with edema. Interestingly, miR-155 $^{-/-}$ mice exposed to SEB presented with almost normal lung architecture (Figure 2.3A). Additionally, the miR-155 deficient mice expressed

significantly decreased total numbers of mononuclear cells within the lung upon SEB exposure when compared to their WT counterparts. Upon closer examination of the mononuclear cell phenotype within the lungs, absolute numbers of CD4+ and CD8+ in the miR-155 $^{-/-}$ mice were decreased compared to WT mice (Figure 2.3B). Additionally, cytokine analysis of the broncheoalveolar lavage fluid (BALF) in the lungs of WT mice demonstrated high concentrations of pro-inflammatory cytokine IFN-γ. In contrast, IFN-γ levels were significantly diminished in miR-155$^{-/-}$ mice (Figure2.3C). Taken together, these results provided clear evidence that miR-155$^{-/-}$ mice were protected from SEB mediated ALI, suggesting that miR-155 plays a critical role in SEB-induced inflammation.

miR-155 expression is critically linked to IFN-γ production

Because SEB exposure leads to the release of copious amounts of IFN-γ and also results in increased miR-155 expression, we considered if there was a positive correlation between IFN-γ secretion and the expression of miR-155. To explore this possibility, we first assessed the expression of IFN-γ after transfection of LN T-cells with a synthetic miR-155 mimic. Interestingly, we found a substantial increase in IFN-γ levels not only in WT mice (Figure2. 4A) but also in miR-155 deficient mice that were transfected with the mimic (Figure 2.4B). Additionally, inhibition of miR-155 with a synthetic inhibitor conversely resulted in the diminished expression of IFN-γ (Figure 2.4C), suggesting a crucial link between miR-155 expression and that of IFN-γ after SEB exposure.

miR-155 targets Socs1, a negative regulator of IFN-γ

miRs regulate the expression of genes by binding the 3'UTR of their respective target mRNA. To examine the link between miR-155 and its potential target genes, we undertook a bioinformatics-based approach. First, IPA miRNA target filter tools were used, selecting only those miR-155 target genes that were relevant to cytokine signaling, cellular immune response, and cellular growth and proliferation. Thirty six targets common to the filtering criteria applied were selected (Figure 2.5A). Next, an IPA generated network was used to sort the targets based on those that were highly predicted and experimentally observed (Figure 2.5B). Conclusively, a gene known as suppressor of cytokine signaling-1 (*Socs1*) was found to be a prominent miR-155 target due to miR-155's ability to bind to the 3' UTR of the *Socs1*mRNA (Figure2. 5C). Because *Socs1* is induced by IFN-γ and acts a negative regulator of IFN-γ, the relationship between miR-155 and *Socs1* in the context of IFN-γ production was examined. miR-155$^{-/-}$ mice that were exposed to SEB had significantly increased expression of *Socs1* mRNA in lung infiltrating mononuclear cells when compared to WT (Figure 2.5D). Accordingly, we hypothesized that miR-155 may target *Socs1* to promote IFN-γ-mediated inflammation during SEB-induced inflammatory ALI. To confirm *Socs1* as a miR-155 target, we first measured relative luciferase activity after co-transfection of miR-155 mimic and plasmid containing the 3' UTR of *Socs1*. Compared to mimic control, miR-155 mimic led to a significant decrease in luciferase activity (Figure 2.6A) validating *Socs1* as a target for miR-155. Next, the impact of miR-155 mimic on *Socs1* levels was explored. We found that both, in WT (Figure 2.6B) and miR-155 deficient cells (Figure 2.6C) that were transfected with miR-155 mimic, *Socs1* levels remained suppressed .On the other hand,

whereas SEB activation continued to lead to a repression in *Socs1*, miR-155 inhibition of SEB-activated cells, resulted in its derepression (Figure 2.6D), confirming the role of miR-155 in suppressing *Socs1* during SEB-mediated activation of immune cells.

2.4 DISCUSSION

With the discovery of miR, a novel and exciting mechanism of gene regulation has arisen. miRs are small non-coding endogenous RNA molecules that bind 3' UTR of genes carrying complimentary sites. A single miR usually targets several mRNA, acting as a fine-tuner of gene regulation rather than an on-off system (Sonkoly *et al.*, 2009b). In the context of inflammation, miRs have been found within a variety of immune cells often targeting genes involved in the regulation of inflammatory response (Lindsay, 2008). In the current study, we closely examined the miR profile after inhalation exposure to SEB. We observed that amongst the miRs that were dysregulated in response to SEB, miR-155 was one of the most significantly altered. It has been reported that naïve CD4+T cells initially display low levels of miR-155, which is increased after the engagement of TCR by an antigen (Stahl *et al.*, 2009; Thai *et al.*, 2007). This is consistent with our observation that miR-155 was upregulated following SEB activation.

Recent studies have reported that miR-155$^{-/-}$ mice are resistant to EAE, demonstrating its importance in mediating disease development (Murugaiyan *et al.*). In other studies, miR-155$^{-/-}$ mice failed to control *H. pylori* infection due to defective Th1 signaling (Oertli *et al.*). Moreover, in a mouse model of collagen-induced arthritis (CIA), the deficiency of miR-155 led to a decrease in pathogenic T-cells. In humans, it has also been reported that soldiers undergoing a battle-field like stress program demonstrated an increase in hsa-miR-155 levels in leucocytes exposed to SEB *ex vivo* (Muhie *et al.*)

indicating that stress- related inflammation could also potentially lead to the increase in miR-155. The current study further suggests that the acute inflammatory response in the lungs to a bacterial superantigen is also regulated by miR-155, inasmuch as, SEB-exposed miR-155$^{-/-}$ mice having fewer infiltrating T-cells and almost normal lung histopathology.

Usually an appropriate regulation of IFN-γ is necessary for mediating Th1 responses and blunting infection (Schoenborn *et al.*, 2007). SEB exposure, however, causes an excessive release of IFN-γ. T-cells exposed to IFN-γ, proliferate further, thus perpetuating a cycle of inflammation (Krakauer, ; Lee *et al.*, 1990). Studies carried out with SEB activation of splenocytes have demonstrated that early cytokines released include IL-2 and TNF-α, followed by the massive production of IFN-γ by T-helper cells (Assenmacher *et al.*, 1998). Additionally, *in vitro* SEB activation of rat splenocytes results in the release of IFN-γ for up to 48 hours post-activation and promotes the proliferation of CD4+ T-cells, similar to that seen in mice and humans (Huang *et al.*, 1998). We have noted in the current model (*unpublished)* that the peak of acute inflammatory lung injury occurs at 48 hours after SEB exposure. In line with the typical kinetics of cytokine release seen with SEB activation, we did not detect early cytokines, TNF-α and IL-2, in the BALF at this time point (*data not shown*). However, our data indicated substantial release of SEB-induced IFN-γ in WT mice suggesting that this particular cytokine may significantly contribute to SEB-induced inflammation. Moreover, the correlation between decreased IFN-γ in the BALF of miR-155$^{-/-}$ mice exposed to SEB and lack of significant inflammation in the lungs is suggestive of a major role for IFN-γ in our model.

The relationship between miR-155 and IFN-γ has been briefly explored in previous studies. For example, when miR-155 is overexpressed in human NK cells, the subsequent downregulation of a target, SHIP-1, promotes IFN-γ expression (Trotta *et al.*). During collagen-induced arthritis, miR-155-/- mice display significantly lower number of IFN-γ producing cells than WT (Kurowska-Stolarska *et al.*). Likewise, our data demonstrated that while transfection with a synthetic miR-155 mimic, leads to the induction of IFN-γ, the blockade of miR-155, diminishes IFN-γ production. Our results clearly indicate that the SEB-mediated induction of IFN-γ can be explained, at least in part, by the induction of miR-155.

To uncover the relationship between miR-155 and IFN-γ in response to SEB exposure, we employed bioinformatics tools and conducted extensive literature search. These efforts suggested suppressor of cytokine signaling 1 (SOCS1) as a possible link between miR-155 and IFN-γ. SOCS1 belongs to a family of eight proteins (SOCS1–SOCS7) that regulate the production of several cytokines (Krebs *et al.*, 2001). In particular, SOCS1 is induced by IFN-γ for auto regulation of the IFN-γ pro-inflammatory response by inhibiting the JAK/STAT1 signaling pathway (Tamiya *et al.*). Recent experiments in numerous cell types have revealed that miR-155 targets SOCS1 (Cardoso *et al.*, ; Jiang *et al.*, ; Zhang *et al.*). For example, macrophages infected with an RNA virus demonstrated enhanced Type I interferon production due to miR-155 targeting of *Socs1* (Wang *et al.*). In the current study we noted that the miR-155$^{-/-}$ mice that are exposed to SEB, showed increased expression in *Socs1* mRNA levels compared to SEB exposed WT mice. The expression of *Socs1* correlated inversely with IFN-γ production in the BALF. In addition,

our gain and loss of function studies with miR-155 mimic and inhibitor, clearly demonstrated that miR-155-mediated targeting of *Socs1* regulates IFN-γ production.

The results of the present study highlight the role of miR-155 in SEB induced acute inflammatory lung injury. Specifically, we demonstrate that the high levels of IFN-γ production associated with SEB exposure can be attributed to the miR-155 mediated repression of *Socs1*, a critical regulator of IFN-γ (Figure2. 7). Furthermore, the importance of miR-155 is made particularly evident as miR-155 deficient mice were found to be protected from SEB-mediated inflammation and acute lung injury, thereby suggesting that therapeutic targeting of miR-155 may be useful in the treatment of SEB-triggered acute inflammatory lung injury.

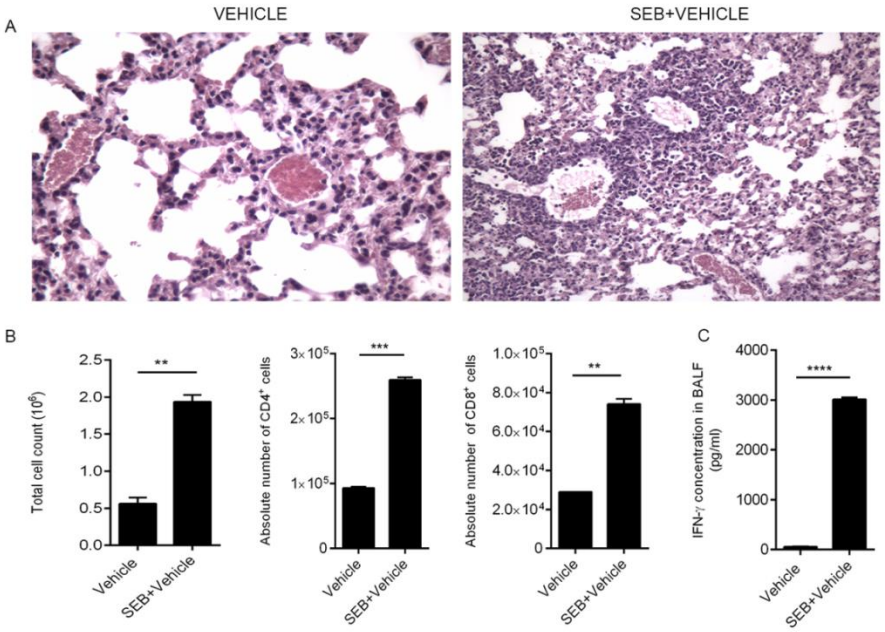

Figure 2. 1. SEB induces lung inflammation (A) Representative H&E images (20x) of cross sections of the lung from mice exposed to either Vehicle or SEB. (B) Lung infiltrating mononuclear cells obtained by density gradient centrifugation and total number of viable cells were counted using a hemocytometer. Cells were further stained with mAb to identify CD4+ and CD8+ cells and analyzed on a flow cytometer. The percentage of the immune cell subsets was multiplied by the total number of cells found in the lung and divided by 100 to yield the absolute cell numbers shown. (C) The concentration of IFN-γ protein present in the BALF was determined using a standard ELISA kit. Data are mean ± SEM (n=5) and are representative of three independent experiments. Statistical significance as compared to SEB + Vehicle is indicated as *p<0.05, ** p<0.01, *** P<0.001, **** p<0.0001.

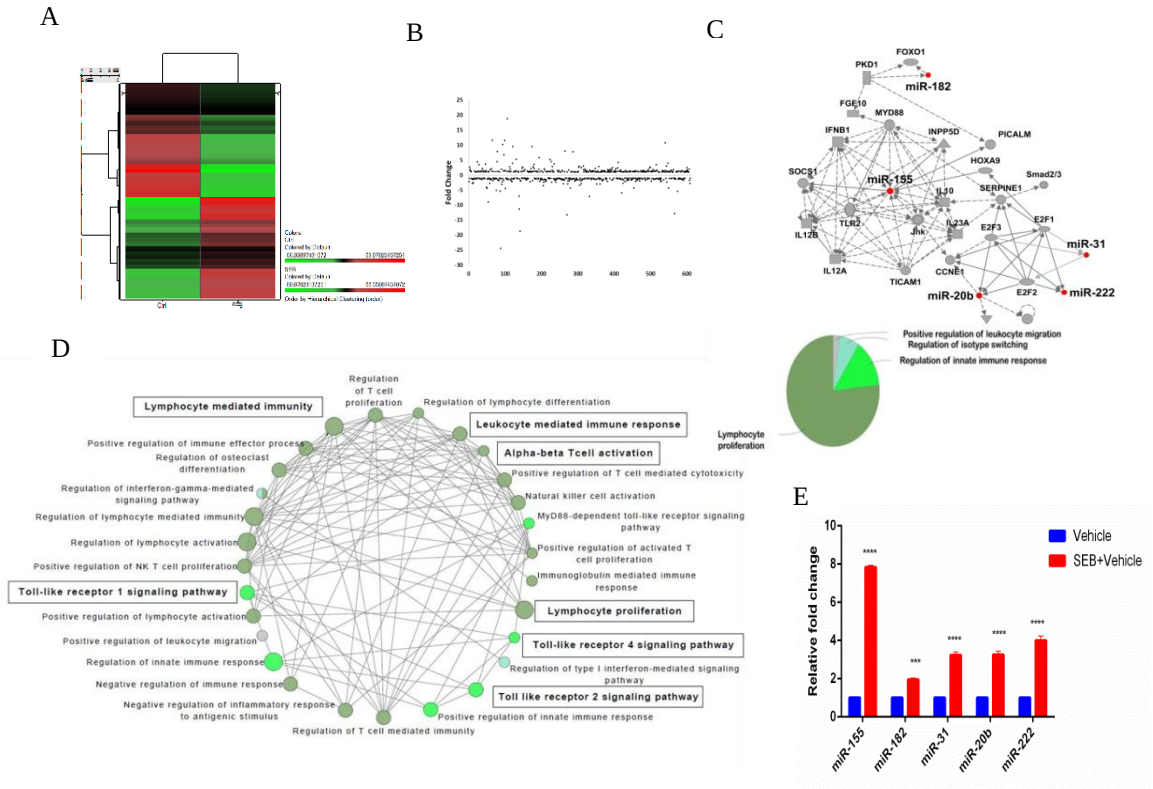

Figure 2.2. SEB exposure leads to dysregulation of miRNA. Forty- eight hours after vehicle or SEB administration, miRNA was isolated from lung infiltrating mononuclear cells. (A) Heatmap depicting differential expression of miRNA in the lungs of mice exposed to SEB +vehicle as compared to vehicle. (B) Fold change distribution of the 609 miRNA indicating several upregulated and downregulated miRNA (C) Ingenuity Pathway analysis generated 'Top network' with network function denoted as 'inflammatory response, cellular development, cellular growth and proliferation'. (D) Cytoscape generated Gene Ontology (GO) network based on Immunological processes for the molecules associated in 'Top Network' using ClueGo 2.0.7 application. Analysis criteria consisted of two-sided hypergeometric test with Benjamini Hochberg correction. Only results with kappa score = 0.3 are displayed. (E) qRT PCR validation of the IPA generated 'Top upregulated miRNA'. Total RNA was isolated from lung infiltrating mononuclear cells. Snord96a was used as the small RNA endogenous control and the expression level of SEB-induced miRNA shown here was normalized to vehicle. Data is represented as mean ± SEM from replicate samples (*p<0.05, **p <0.01 as compared to vehicle).

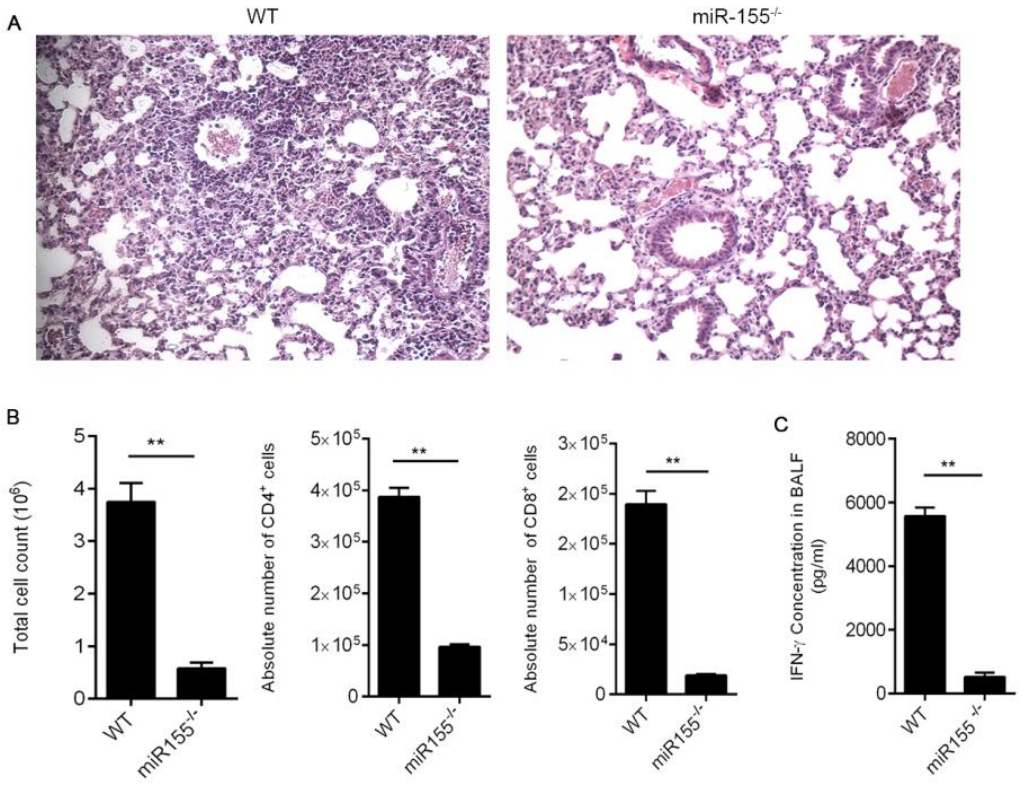

Figure 2.3. miR-155 plays a critical role in SEB-induced ALI. WT (C57BL/6) and miR-155$^{-/-}$ (B6.Cg-*Mir155* $^{tm1.1\ Rsky}$/J) mice were exposed to SEB and euthanized 48 hours later. (A) Representative H&E images (20x) of sections of lung indicating immune cell infiltration. (B) Phenotypic characterization of cells infiltrating the lung was determined by staining of mononuclear cells with fluorescent conjugated mAb against CD4 and CD8. (C) Levels of IFN-γ cytokine in the BALF was determined by ELISA. Data are mean ± SEM (n=5) and are representative of two independent experiments. Statistical significance as compared to WT is indicated as *p<0.05, ** p<0.01.

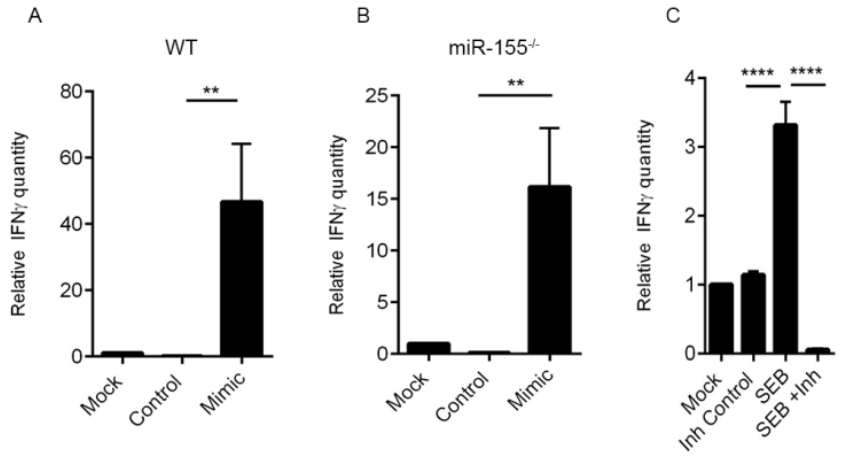

Figure 2.4. **IFN-γ forms a critical link between SEB and subsequent miR-155 induction**. (A) Lymph node (LN) T cells obtained from naïve wildtype (WT) mice were transfected either with miR-155 mimic (Mimic) or mimic control (Control) for 24 hours. IFN-γ levels were determined by RT-PCR. (B) LN T cells obtained from miR-155-/- were also transfected with 10nM miR-155 mimic or mimic control as indicated for 24 hours and IFN-γ levels were assessed. (C) LN cells were activated with SEB (1μg/ml) for 24 hours. Cells were then transfected with 50nM miR-155 inhibitor (Inh) or Inhibitor Control (Inh Control) for another 24 hours. IFN-γ levels were determined via RT-PCR. Data is represented as mean ± SEM from replicate samples. Statistical significance is indicated as *p<0.05, ** p<0.01, *** P<0.001, **** p<0.0001.

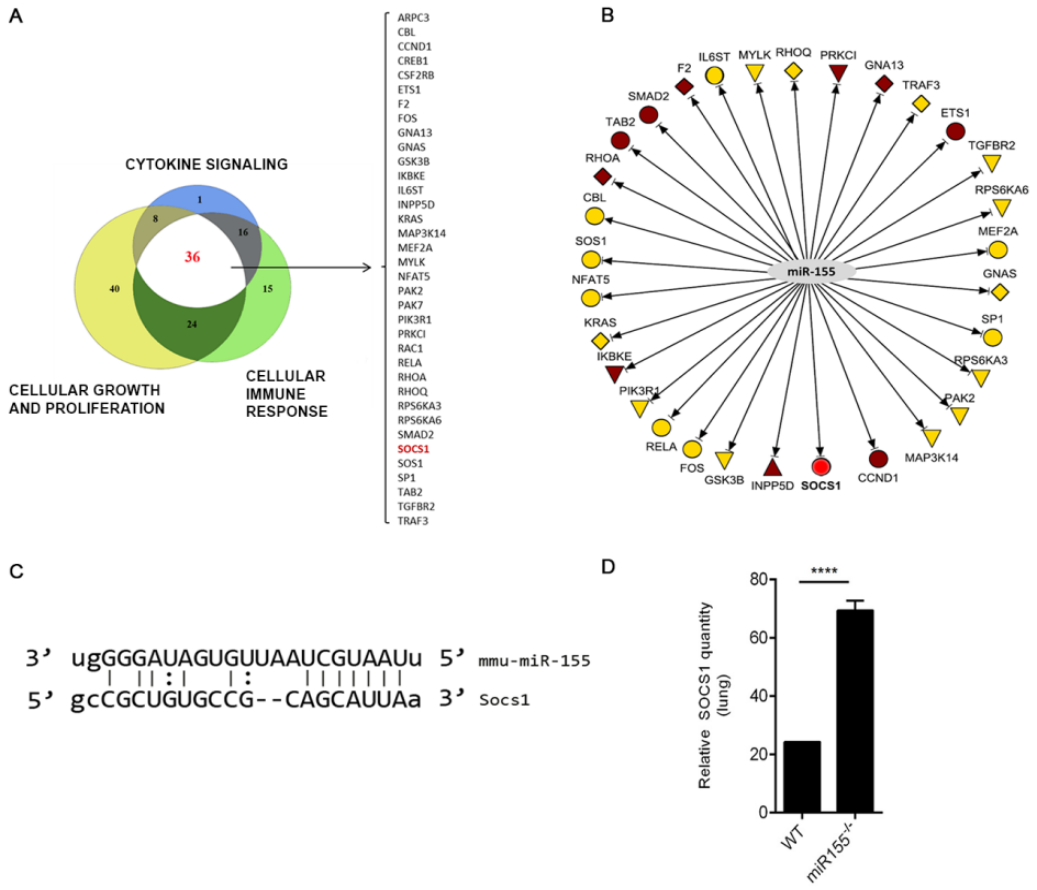

Figure 2.5. Identification of SEB-induced miR-155 targets. (A) miR-155 targets were filtered based on their role in cytokine signaling, cell growth and proliferation and cellular immune response using IPA. A proportional Venn diagram indicating the miR-155 targets common to all three filtering criteria was generated. The list of targets is indicated within brackets and *Socs1*, a highly predicted target is highlighted (red). (B) IPA network was generated highlighting the highly predicted (yellow) and experimentally observed (brown) miR-155 targets, in addition to *Socs1* (red), the target of interest. (C) Schematic illustration of the predicted target site for miR-155 within the 3' UTR of *Socs1* mRNA. (D) Total mRNA was isolated from lung-infiltrating mononuclear cells of WT and miR-155 $^{-/-}$ mice exposed to SEB. Relative expression of *Socs1* mRNA was determined by qRT PCR using β-actin as endogenous control. Data is represented as mean ± SEM from replicate samples .Statistical significance is indicated as *p<0.05, ** p<0.01, *** P<0.001, **** p<0.0001.

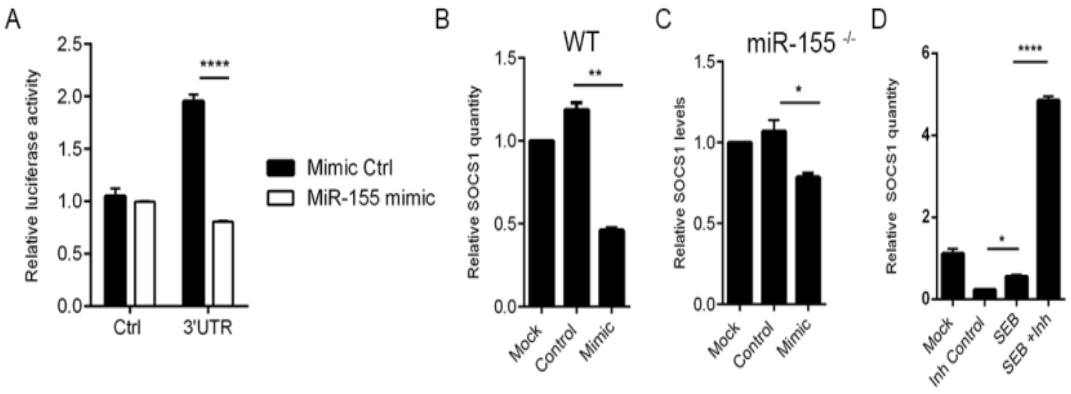

Figure 2. 6. miR-155 targets *Socs1*. (A) Chinese Hamster Ovary (CHO) cells were co-transfected with miR-155 mimic or mimic control along with plasmid containing either the 3'UTR of *Socs1* or control plasmid for 24 hours. Relative luciferase activity (firefly normalized to renilla) was determined following transfection. (B) Lymph nodes (LN) cells obtained from naïve wildtype (WT) mice were transfected either with 40nM miR-155 mimic (Mimic) or mimic control (Control) for 24 hours. *Socs1* levels were determined by RT-PCR. (C) LN cells obtained from miR-155-/- were also transfected with 40nM miR-155 mimic or mimic control as indicated for 24 hours and *Socs1* levels were assessed. (D) LN cells were activated with SEB (1μg/ml) for 24 hours. Cells were then transfected with 100nM miR-155 inhibitor (Inh) or Inhibitor Control (Inh Control) for another 24 hours. *Socs1* levels were determined via qRT-PCR. Data is represented as mean ± SEM from replicate samples statistical significance is indicated as *$p<0.05$, ** $p<0.01$, *** $P<0.001$, **** $p<0.0001$.

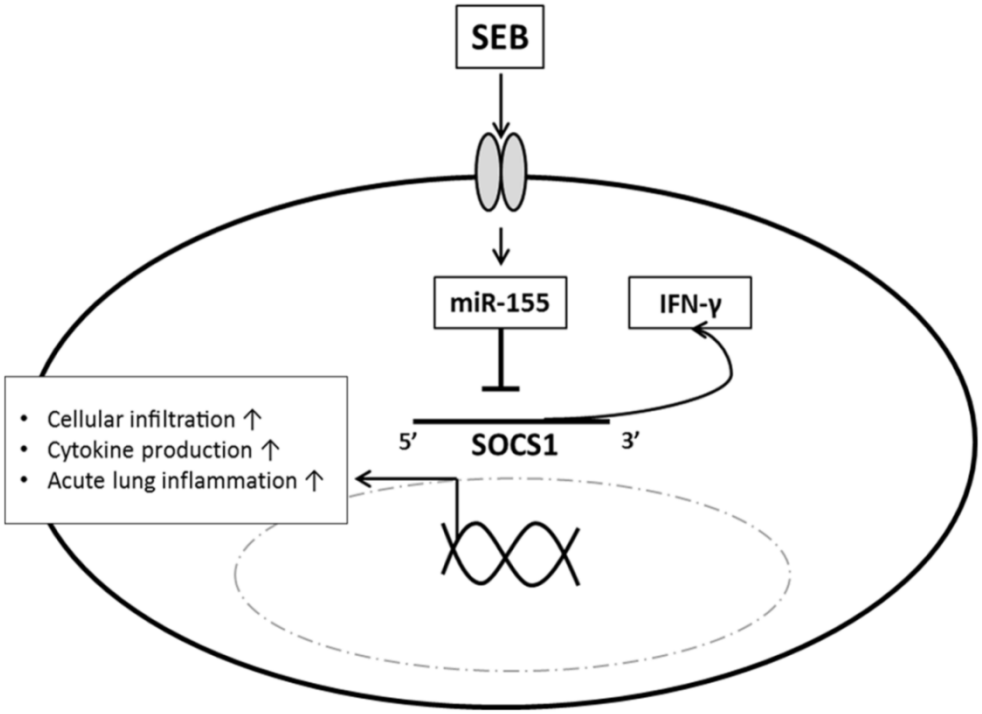

Figure 2.7. Schematic of SEB-mediated downregulation of *Socs1* via miR-155. SEB exposure leads to the release of IFN-γ and subsequent expression of miR-155. miR-155 mediated suppression of *Socs1* prevents appropriate control of IFN-γ leading to cell proliferation and sustained cytokine signaling and damage to the lung.

CHAPTER III: Role of miRNA in the Regulation of Inflammatory Genes in Staphylococcal enterotoxin B-Induced Acute Inflammatory Lung Injury and Mortality.

3.1 INTRODUCTION

Staphylococcus aureus is a commonly occurring gram positive pathogen implicated in a number of community and nosocomial infections ranging from skin infections, endocarditis, sepsis and toxic shock (Lowy, 1998). Its pathogenicity can be attributed to a number of virulence factors such as polysaccharides, proteases, cell surface proteins and in particular, its ability to secrete potent toxins such as Staphylococcal enterotoxin B (SEB) (Foster, 2004). Commonly referred to as a superantigen, SEB poses a threat as a biological weapon because it is effective at smaller quantities, is easily aerosolized and disseminated. Consequently the Center for Disease Control and Prevention has deemed SEB, a Category B select agent (Ulrich, 2001).

The consequences of SEB exposure are known to arise from an exaggerated immune response. Upon directly binding the non-polymorphic regions of the major histocompatibility complex class II (MHC II) on antigen presenting cells and Vβ8region of the T-cell receptor, SEB leads to the activation and clonal expansion of ~30-40% T-cells (Kozono *et al.*, 1995). Subsequently, a cytokine storm ensues leading to cellular infiltration, tissue damage, multi-organ failure and death(Strandberg *et al.*, ; Uchakina *et al.*). Although the impact of SEB exposure on key inflammatory signaling pathways such

as the NFκB, MAPK has been extensively studied (Krakauer), we have only recently been made aware of the possible role of microRNA (miRNA) in SEB-mediated inflammation.

microRNA are a unique class of small (18-25 nucleotides), single-stranded non-coding RNA molecules that have emerged as primary regulators of gene expression(Dai *et al.*, ; Davidson-Moncada *et al.*). Mammalian miRNA bind primarily to the 3' UTR of their respective target mRNA causing mRNA instability and degradation and/or the disruption of translation (Davidson-Moncada *et al.*). Although miRNAs are involved in the development and differentiation of cells, apoptosis and hematopoiesis under normal conditions, inflammatory cues leads to their dysregulation, thereby enabling the targeting of key regulators of inflammation (O'Connell *et al.*, 2010; Sonkoly *et al.*, 2008). For example, in rheumatoid arthritis, the overexpression of miR-146a in CD4+ T-cells obtained from the synovial fluid is associated with increased expression of TNFα (Li *et al.*). Similarly, the inhibition of miR-126 in a house dust mite induced model of asthma, leads to the decrease in allergic inflammation (Mattes *et al.*, 2009) . Conversely, while high levels of miR-125b are required to maintain a naïve state of T-cells, the activation of T-cells leads to its downregulation and subsequent expression of its target gene, *Ifng* (Rossi *et al.*).

Recently, our laboratory has demonstrated that intranasal exposure to SEB in C57BL/6 mice leads to the strong dysregulation of miRNA. miR-155 in particular promotes SEB-mediated acute inflammatory lung injury(Rao *et al.*). In the current study, we administered SEB as a 'Dual Hit' to C3H/HeJ mice which entails administering small quantities (5μg and 2 μg) of SEB intranasally and intraperitoneally respectively, two

hours apart that results in the hyperactivation of the immune system and 100% mortality of mice. Upon investigating the effect of SEB exposure on the miRNA profile, we observed the aberrant expression of several miRNA that could potentially contribute to SEB-mediated inflammation. Further, applying bioinformatics tools and q-RT PCR, we established important links between the miRNA and their respective target genes. Using gain -and -loss of function experiments we specifically demonstrate the possible role of miR-132 in mediating damage and death. Thus, our results provide further insights into the role of SEB-induced miRNA in contributing towards severe acute inflammatory lung injury and consequent mortality.

3.2 MATERIALS AND METHODS

Mice

Female C3H/HeJ mice (6-8 weeks) were obtained from the Jackson Laboratory. All mice were housed under pathogen free conditions in the Animal Resource facility (ARF), University of South Carolina, School of Medicine. All experiments using vertebrate animals were performed under protocols approved by the Institutional Animal Care and Use Committee (IACUC) at USC.

Administration of SEB

SEB was acquired from Toxin Technologies (Sarasota, FL). SEB was administered as a 'Dual- Hit' as described previously (Huzella *et al.*, 2009). The first dose of SEB was delivered by the intranasal (i.n) route at a concentration of 5 µg /mouse in a 25 µl volume. Two hours after, the second dose of SEB was administered intraperitoneally (i.p) at a concentration of 2 µg/mouse in a 100 µl volume. Control mice were similarly given PBS

(vehicle) as a dual dose. While mice were euthanized 72 hours after SEB exposure in all experiments, survival of mice was monitored up to 5 days after exposure to SEB and any moribund mice were immediately euthanized.

Lung Histopathology

72 hours after exposure to either Vehicle or SEB, lungs were excised and fixed in 10% formalin. Lung tissue was paraffin embedded and 5μm serial sections were made. Subsequently, the sections were deparaffinized by dissolving in xylene, rehydrated in alcohol (100%, 95%, and 90%). The sections were stained with hematoxylin and eosin (H&E) and assessed with Nikon E600 light microscope. Images were taken at 40X magnification.

Assessment of Vascular Leak

The percent of Vascular leakage in the lungs was determined as described previously (Rieder *et al.*, ; Saeed *et al.*). Briefly, 72 hours after Vehicle or SEB exposure, mice were administered 1% Evans Blue dye in sterile PBS intravenously (i.v). Two hours later, the mice were euthanized and lungs perfused with heparinized PBS. The lungs were incubated in formamide at 37 ° C for 24 hours to extract the dye. The optical density (O.D) of the supernatant was measured by a spectrophotometer at 620 nm. Percent increase in Vascular Leak was calculated using the following formula - ($O.D_{sample} - O.D_{control}/O.D_{control}$) x 100.

Preparation of lung infiltrating cells

72 hours after exposure to Vehicle or SEB, lungs were perfused with heparinized PBS and harvested. They were then homogenized using Stomacher 80 Biomaster blender from

Seward (Davie, FL) in 10 ml sterile PBS. Following washing with sterile PBS, the cells were separated by density gradient centrifugation at 500 x g for thirty minutes at 24 °C with the brake off. Mononuclear cell layer isolated was enumerated by the Trypan blue exclusion method using a hemocytometer.

Detection of Cytokines

Cytokines in the Broncheoalveolar lavage fluid (BALF) were obtained as described previously (Rao *et al.*). Briefly, 72 hours after Vehicle or SEB exposure, mice were euthanized. The trachea was bound with a suture and the lung was excised as an intact unit along with the bound trachea. Sterile ice-cold PBS was injected through the trachea to collect the BALF. Cytokine detection was carried out using Bio-Plex Pro ™ mouse cytokine 23-plex Assay from Biorad (Hercules, CA).

***In vitro* Assays**

Splenocytes from naïve C3H/HeJ mice were harvested and cultured in complete RPMI (10% FBS, 10mM L-glutamine, 10mM Hepes, 50 μM β-Mercaptoethanol, and 100 μg/mL penicillin). Cells were seeded at a density of $1x10^6$ cells in a 96 well plate and stimulated with either PBS (Vehicle) or SEB (1 μg/ ml) for 24 hours. The cells were then harvested to examine CD4, Vβ8 percentages or activation markers- CD69, CD28, CD62L, and CD86. Cellular proliferation was measured by similarly seeding and activating splenocytes for 48 hours. In the last twelve hours of incubation, ^{3}[H]-Thymidine (2μCi) was added to the cell culture. Cells were then collected using a harvester and thymidine incorporation was measured using a scintillation counter (Perkin Elmer).

Flow Cytometry and Antibodies

To determine the phenotypic characteristics of the lung infiltrating mononuclear cells and splenocytes obtained from *in vitro* cell culture assay above, cells were stained with the following fluorescent conjugated antibodies - Fluorescein isothiocyanate (FITC) - conjugated anti-CD8 (clone: 53-6.7), Phycoerthyrin (PE)-conjugated anti-CD4 (clone: GK 1.5), FITC-conjugated anti-CD69 (clone : H1.2F3), PE-Cy5-conjugated anti-CD28 (clone 37.51), PE-conjugated anti-CD62L (clone MEL-14), PE-conjugated anti-CD86 (clone Gl-1) from Biolegend (San Diego, CA) and (FITC-conjugated anti-Vβ8 (clone: K516) from Ebioscience (San Diego, CA). Stained cells were run and analyzed using Beckman Coulter 500 Flow Cytometer (Indianapolis, IN).

Total RNA extraction

Total RNA (including small RNA) was isolated from lung infiltrating mononuclear cells using the miRNAeasy kit from Qiagen (Valencia, CA) according to manufacturer's instructions. The purity and concentration of total RNA was confirmed spectrophotometrically by Nanodrop 2000c from Thermo Scientific (Wilmington, DE). The integrity of miRNA was further confirmed using Agilent 2100 BioAnalyzer (Agilent Tech, Palo Alto, CA).

miRNA expression profiling

To profile the miRNA expression in the lung after SEB exposure, the Affymetrix GeneChip® miRNA 3.0 array platform was used. The array identified 1111 mouse miRNA derived from the Sanger miRBase v17 (www.mirbase.org). Total RNA was labeled with Flash Tag ™ Biotin HSR labeling kit from Affymetrix (Santa Clara, CA)

according to manufacturer's instructions. Briefly, RNA spike control Oligos were added to the RNA and incubated with a Poly A Tailing master mix for 15 min. Next, the RNA was labeled with Biotin using FlashTag ™ Biotin HSR Ligation mix. For hybridization of the biotin-labeled samples to the array, a GeneChip ® Eukaryotic Hybridization Control kit comprising of bioB, bioC, bioD and cre was used to create the array hybridization cocktail. Following incubation at 99 °C for 5 min, then 45 °C for 5 min, a small volume (100 µl) was injected into an array. The arrays were further incubated at 48°C and 60 rpm for 16-18 hours. Post-hybridization, the array was washed and stained with fluorescent-conjugated streptavidin using the Fluidics Station 450. The stained chip was scanned on a GeneChip Scanner (Affymetrix) to generate the data summarization, normalization and quality control files. All microRNA microarray data was deposited into ArrayExpress database (www.ebi.ac.uk/arrayexpress/) under the ArrayExpress accession number E-MTAB-2641.

miRNA and mRNA target gene analysis

The fluorescent intensities obtained from the hybridization were log transformed, mean centered and visualized as a heatmap. Hierarchical clustering was carried out using Ward's method and similarity measurement was calculated using half square Euclidean distance. miRNA fold change differences between Vehicle and SEB as obtained from the microarray was plotted as a fold change distribution plot. Further, only miRNA that showed > 2 fold higher or lower values in SEB exposed lung infiltrating cells compared to control were considered for analysis. Proportional Venn diagram was created using Venn Diagram Plotter (http://omics.pnl.gov/software/venn-diagram-plotter). To further assess the biological functions and visualize miRNA interactions with its respective

target genes associated with the miRNA, we employed the use of the commercially available tool Ingenuity Systems, Ingenuity Pathway analysis (IPA) (Mountain View, CA). Additionally, to assign immunological functions to miRNA target genes, we used Cytoscape 3.0.1, an open source tool equipped with the Gene Ontology applications, ClueGO and CluePedia.

Real Time qPCR

Total RNA (miRNA and mRNA) obtained from lung infiltrating mononuclear cells or *in vitro* from splenocytes was converted to cDNA using miSript cDNA synthesis kit (Qiagen) according to manufacturer's instructions. To validate and detect miRNA, qPCR was carried out using miScript primer assays (miR-132, miR-155, miR-31, miR-222, miR-20b, let-7e, miR-192, miR-193*, miR-34a and control Snord96_a) that employs SYBR Green technology from Qiagen. Fold change was determined using the $2^{\Delta\Delta Ct}$ method and expressed relative to control. For mRNA validation, SSO advanced SYBR green PCR kit from Biorad (Hercules, CA) was used according to manufacturer's instructions. β-actin was used as the internal control. Primers (Table 3.1) were synthesized from Integrated DNA technologies (IDT).

Transfection with miR-132 mimic and inhibitor

Splenocytes from naïve C3H/HeJ mice were harvested and cultured in 10 ml of complete RPMI. Cells were seeded at 2 X 10^5 cells per well in 24 well plates and transfected with synthetic miR-132 mimic (40 nM) or mock transfected with Transfection reagent HiperFect from Qiagen for 24 hours. For miR-132 inhibition, cells were activated with SEB (1µg/ml) and transfected with either mock control or miR-132 inhibitor also

purchased from Qiagen. 24 hours after transfection, total RNA was collected for qRT PCR validation of miR-132 and target gene *Foxo3*.

Statistics

All statistical analyses were carried out using GraphPad Prism Software (San Diego, CA). In all experiments, the number of mice used was 4-5 per group, unless otherwise specified. Results are expressed as means ± SEM. Student's t-test was used to compare two-groups. A *p*-value of < 0.5 was considered statistically significant. Individual experiments were performed in triplicate and each experiment was performed independently at least three times to test reproducibility of results. Survival analysis was carried out using a Log-rank test**.**

3.3 RESULTS

SEB exposure leads to lung inflammation and acute mortality

The 'Dual Hit' model of SEB administration has been previously known to result in severe inflammation in the lungs and death of the mice (Huzella *et al.*, 2009). In this study, we found that SEB administration resulted in 100% mortality in mice between 96 and 120 hours (Figure 3.1A) when compared to mice exposed to vehicle. Pulmonary damage was characterized by the disruption of lung integrity, vascular leak and consequently edema. To quantitate the extent of damage to the lungs after SEB exposure, mice were administered Evans blue dye and vascular leak expressed as a percent increase over vehicle as described earlier (Rieder *et al.*, ; Saeed *et al.*) . Our results revealed that SEB exposure had almost an eight fold increase in vascular permeability compared to mice that were only exposed to vehicle (Figure 3.1B). Further, a consequence of SEB

exposure is the infiltration of immune cells around air vessels and bronchioles (Rao *et al.*, ; Rieder *et al.*). Accordingly, histopathological examination of the lungs confirmed the presence infiltrating immune cells after SEB exposure compared to vehicle alone (Figure 3.1C). Further, upon enumeration of the total number of infiltrating mononuclear cells in the lung, we found a profound increase in the number of cells post-SEB exposure compared to vehicle (Figure 3.1D). Because SEB exposure leads primarily to the clonal expansion of Vβ8+ T-cells, we further assessed the immune subsets (CD4, CD8 and Vβ8) by staining with fluorescein-conjugated antibodies and analyzed using flow cytometry. As expected, we found significantly increased absolute cell counts in all three subsets after SEB exposure (Figure 3.1E).

SEB, being a superantigen is known to result in the massive release of cytokines. Therefore, we obtained the broncheoalveolar lavage fluid (BALF) from mice that were exposed to vehicle or SEB and screened for several cytokines and chemokines such as IFN-γ, IL-6, IL-12, IL-1α, MCP-1, MIP-1, G-CSF, Eotaxin and KC (Figure 3.2) and found that SEB triggered significant levels of these mediators.

SEB exposure leads to the activation and proliferation of immune cells in vitro

To determine if SEB exposure can trigger activation of specific immune cell subsets, we exposed splenocytes with SEB *in vitro* for 24 hours and assessed activation by flow cytometry. Compared to vehicle, SEB lead to increased proportions of T-cell activation markers: Vβ8, CD28, CD69 and CD86 (Figure 3.3A). While we had earlier demonstrated that SEB administration leads to increased cell counts in the lung, we investigated if activation of splenocytes with SEB, could also lead to increased cellular proliferation. Indeed, activation with SEB for 48 hours resulted in significantly higher thymidine

counts as compared to vehicle (Figure 3.3B). Cellular proliferation and activation, especially of T-cells, is influenced by IL-2 production. Consequently we found exaggerated levels of IL-2 in the supernatants of cells activated with SEB. Similarly, IFN-γ, a hallmark cytokine associated with SEB exposure was measured and high concentrations (~2500 pg) was found upon SEB exposure (Figure 3.3C). These data indicate that SEB triggers the activation and proliferation of cells, *in vitro* in addition to in vivo.

SEB exposure results in the dysregulation of several microRNA

While miRNA are known to be induced during inflammation and play a critical role in its regulation, expression profile of miRNA during SEB-mediated lung inflammation and consequent death has not yet been investigated. Therefore, we extracted total RNA from the lung infiltrating mononuclear cells from mice that were either exposed to vehicle or SEB and performed miRNA microarray. The heatmap revealed a noticeable difference in fold change between vehicle and SEB-treated groups (Figure 3.4A). To visualize the distribution of the miRNA, a radial fold change distribution plot was generated demonstrating that while most miRNA remained unchanged and were found around the circumference of the plot, a few miRNA were highly upregulated (up to 56 fold) or highly downregulated (up to 22 fold) when compared to vehicle (Figure 3.4B). Amongst the miRNA assessed on the array, approximately 4% of the miRNA were either overexpressed or underexpressed greater than and equal to two-fold in SEB exposed cells compared to vehicle (Figure 3.4C). Next, Ingenuity Pathway analysis (IPA) was employed to analyze on this fraction of dysregulated miR, which yielded a list of top upregulated (miR-132, miR-155, miR-31, miR-20b, miR-222) and downregulated miRs

(miR-192, miR-193*, let -7e, miR-34a), whose fold change values as determined by the microarray, seed sequence and miRbase accession numbers were tabulated (Table 2). Next, the miRNA expression levels in the lung infiltrating mononuclear cells were validated by q-RT PCR. These results corroborated the expression pattern observed with the microarray (Figure 3.5).

Functional analysis of the dysregulated miRNA

To examine the possible biological functions associated with the over and underexpressed validated miRNA, IPA core analysis was conducted and statistically significant (Fishers exact test) biological functions were generated and -log [p-value] was plotted as a bar graph. We observed that cellular development, cell death and survival, cellular growth and proliferation, cell cycle, cell-cell signaling and interaction and gene expression were highly enriched functions associated with the SEB-mediated alterations in the miRNA (Figure 3.6A). A further dissection of these biological functions revealed that a majority of the molecules closely associated with the dysregulated miRs, were involved in very specific functions. For example, almost half of the molecules linked with cellular development were involved in the differentiation of mononuclear leukocytes and T-lymphocytes. Further, a vast majority (~45%) of the molecules associated with cellular growth and proliferation were linked specifically to propagation of T-lymphocytes. Similarly, cell-cell signaling and interactions predominantly comprised of the specific activation of T-lymphocytes and T-cell responses (Figure 3.6B), characteristic features of SEB-induced inflammation. Thus, our results suggested that the miRNA expression profile and its associated biological functions, as indicated *in silico*,

correlated with experimentally observed lung inflammation accompanying SEB exposure.

Predicted mRNA targets of the dysregulated miR after SEB exposure

Next, we identified possible miR targets by employing IPA. Highly predicted, experimentally observed as well as moderately predicted targets of the validated miRNA were filtered using the miRNA target filter tool. Only those molecules that were associated with the inflammatory process were considered for analysis. Amongst these target genes, we found that the upregulated miRNA were predicted or experimentally observed to target transcription factors and genes involved in the regulation of inflammation. For example, miR-132 and miR-155 targeted B-Cell CLL/Lymphoma 10 (BCL10), an inducer of apoptosis. Similarly, miR-20b and miR-222 target the suppressor of cytokine signaling (*Socs*) genes, which are negative regulators of several pro-inflammatory cytokines (Table 3.3). In contrast, the downregulated miRNA such as let 7-e, miR-34a, miR-192 and miR-193* were predicted to target pro-inflammatory molecules such as those involved in cellular proliferation, activation and cytokine production (Table 3.3). IPA pathway designer tool was also used to visualize the miRNA-mRNA interactions (Figure 3.7A) which provided further insight into how the over and underexpressed miRNA target key molecules and collectively act to regulate inflammation. Finally, to confirm the immunological functions of the miRNA target genes, Gene Ontology (GO) tool, ClueGo, was employed which yielded a map of highly enriched GO terms (Figure 3.7B) such as Lymphocyte activation (GO:0046649) , Positive regulation of lymphocyte activation (GO:0051251), Regulation of T-cell activation (GO:0050863) and Positive regulation of immune effector process

(GO:0002699). Together, these data indicated a strong role for key miRNA, induced by SEB, in the regulation of lung inflammation.

Experimental validation of mRNA target genes.

To validate and confirm some of the predicted target genes, q-RT PCR was carried out using mRNA from lung infiltrating mononuclear cells following exposure to vehicle or SEB. Interestingly, upon using microRNA.org (www.microRNA.org) miRNA-mRNA alignment tool, we observed that a few of the upregulated miRNA, aligned to the 3' UTR of some of these target genes. For example, miR-155, miR-132, miR-31 bind *Smad3*, while miR-20b and miR-222 aligned to the 3'UTR of *Runx1*. miR-132, which was highly induced following SEB exposure, aligned with the 3'UTR of *Foxo3*, with the potential to target it (Figure 3.8A). We observed significant downregulation of Smad family member 3 (*Smad3)*, Transforming Growth Factor, Beta 1 (*Tgfβ1*), Forkhead box O3 (*Foxo3*) and runt-related transcription factor 1 (*Runx1*) (Figure 3.8B), molecules that have been experimentally shown to regulate cellular proliferation, cell cycle progression and cytokine production when induced. Further, the microRNA.org tool suggested that a few underexpressed validated miRNA i.e., miR-192, miR-34a and let-7e aligned to the 3'UTR of these genes (Figure 3.8C) while several genes associated with the pro-inflammatory pathway such as T-box 21*(Tbx21)*, signal transducer and activation of transcription 3 (*Stat3*), prostaglandin-endoperoxidase synthase 2 (Ptgs2), nuclear factor kappa (*Nfκb*) and cell cycle progression genes such as Cyclin D1(*Ccnd1*) and Cyclin E1*(Ccne1*) were induced upon SEB exposure (Figure 3.8D). Altogether, our results indicated that SEB causes alterations in the expression profiles of a significant number of miRNA, which in turn may either allow for the expression of pro-inflammatory genes or

lead to the degradation of anti-inflammatory molecules, thereby collectively contributing to severe lung inflammation.

miR-132 targets Foxo3, an inhibitor of cellular proliferation and cell cycle progression

miRNA microarray analysis demonstrated that miR-132 was the most highly induced after SEB exposure (Table 3.2). Therefore, we rationalized that miR-132 may play a prominent role in mediating inflammation and damage in the current model. Additionally, amongst the many miR-132 predicted target genes, transcriptional factor *Foxo3,* was especially interesting not only because of its observed role in inhibiting cellular proliferation and curbing cell cycle progression, but due to the fact that miR-132 aligned to the 3'UTR of *Foxo3.* To confirm the binding of miR-132 to *Foxo3*, we transfected splenocytes with a miR-132 synthetic mimic. While the levels of miR-132 were highly increased with the mimic, *Foxo3* levels inversely correlated with its expression (Figure 3.9A). Similarly, SEB activation of splenocytes led to the expected increase in miR-132, but the inhibition of miR-132 resulted in the de-repression of *Foxo3* (Figure 3.9B). These results suggested that miR-132 targets *Foxo3,* thereby preventing the regulation of cellular proliferation seen upon SEB exposure.

3.4 DISCUSSION

The recent discovery of microRNA (miRNA) has propelled our understanding of gene regulation. These non-coding, evolutionarily conserved RNA molecules function primarily as repressors of gene expression and are estimated to regulate approximately 30% of all human genes (Lewis *et al.,* 2005). While the role of miRNA in mammalian

cells was first brought to the forefront in cancer (Calin *et al.*, 2002), their importance in a number of immune cell activation and functions has since been stressed (Baltimore *et al.*, 2008). With regards to inflammation, several changes in the transcriptional repertoire are accompanied with perturbation in miRNA(O'Connell *et al.*, 2010). As a result, it is conceivable that miRNA control several aspects of the inflammatory process.

In the current study, we have profiled the miRNA expression patterns following exposure to SEB. Using *in silico* analysis and q-RT PCR approaches we identified several miRNA that were altered in response to SEB. Importantly, these miRNA were found to be closely associated with key genes either involved in the control of inflammation or those that contributed directly to SEB-mediated inflammatory processes. By showcasing the effects of specific over and underexpressed miRNA, we provide evidence that the outcome of SEB exposure such as severe lung inflammation and death of mice can be explained, at least in part, to the intricate miRNA alterations and miRNA-mRNA interactions.

Following the unconventional binding of SEB to the major histocompatibility complex (MHC) class II on antigen presenting cells (APCs) and subsequent activation of Vβ8 region of the T-cell receptor, the immune system gets hyperactivated due to the presence of large proportions (~30%) of Vβ+T cells (Krakauer). As a consequence, such T-cells get clonally expanded resulting in a cytokine storm (Rajagopalan *et al.*, 2006). Although several murine models have been developed to study the toxic effects of SEB (Krakauer *et al.*), very few models exhibit mortality in the absence of the use of additional potentiating agents such as D-gal or LPS to mimic the consequence of exposure to the toxin in humans (Miethke *et al.*, 1992; Savransky *et al.*, 2003). The dual administration of SEB while addressing this concern, has previously been reported to result in severe

lung inflammation and the subsequent death of mice (Huzella *et al.*, 2009). In line with this previous observation, we found dual exposure to SEB, resulted in extensive inflammation of the lung characterized by immune cell infiltration, accumulation of cytokine and chemokines in the BALF, compromised lung function and eventually the mortality of mice.

Previously, we studied the effect of a single high dose (50 μg) administration of SEB intranasally in C57BL/6 mice and studied lung inflammation (Rao *et al.*). In this model, although mice exhibit symptoms of acute inflammatory lung injury, there is no mortality seen in mice exposed to SEB. Nonetheless, we demonstrated the predominant role of miR-155 in mediating acute inflammatory lung injury in this model (Rao *et al.*). The current "dual-hit" model, because of smaller quantities of SEB, and high mortality, is more relevant to SEB exposure in humans. It is for this reason that we aimed to highlight the miRNA profile after acute SEB exposure in this model. While we also observe the induction of miR-155 in the current model, we see a similar upregulation of other miRNA such as miR-31, miR-20b, miR-222 and miR-132 and the significant downregulation of miRNA such as let-7e, miR-34a, miR-192 and miR-193*. Interestingly, the expression of these miRNA has been associated with a variety of inflammatory conditions suggesting that they may collectively act to orchestrate the severe inflammation observed after SEB exposure. For example, miR-31 is overexpressed in psoriasis skin and mediates its pro-inflammatory role by targeting STK40, a negative regulator of NFκB (Xu *et al.*). Similarly, miR-155 expression correlates positively with that of NFκB activation in *Heliobacter pylori* infection and in a murine model of chronic alcohol consumption and inflammation (Bala *et al.*, ; Xiao *et al.*,

2009). Given that SEB exposure is known to activate the NFκB signaling pathway (Kissner *et al.*) and cause the expression of pro-inflammatory cytokines, as indicated by our results, it is possible that specific SEB-induced miRNA may function via the activation of NFkB.

Related to the expression of NFkB is the SEB-induced activation of the STAT family of proteins, especially STAT3 (Plaza *et al.*, 2004). Activated by cytokines such as IL-6, the STAT3 molecule, along with NFκB leads to cellular proliferation, cell survival, cytokine production and immune cell activation (Yu *et al.*, 2009), key inflammatory pathways we observed experimentally in this study. In addition to finding an increase in *Stat3* mRNA levels after SEB exposure, we demonstrate that miR-let7e, miR-34a and miR-193* that are predicted to target STAT3 are significantly downregulated, thereby facilitating its expression.

Previous reports indicated that the overexpression of miR-34a and miR-193* leads to cell cycle arrest and repression of cellular proliferation by the targeting of CCND1 (Chen *et al.*, ; Sun *et al.*, 2008). Similarly, while miR-192 is predicted to target CCNE1, let-7e has been experimentally validated to directly degrade it in hepatocellular carcinoma cells (Zhang *et al.*). Because these miRNA were specifically downregulated upon SEB activation, we observed the unrestrained expression of *Ccnd1* and *Ccne1* suggesting that the significant downregulation of these miRNA may contribute to cell cycle progression and cellular proliferation.

Consistent with previous studies (Busbee *et al.*, ; Green *et al.*, 1992), we have demonstrated that SEB exposure predominantly affects T-cells, leading to their activation (as indicated by assessment of activation markers) or their recruitment into the lung in

large numbers. Interestingly, our *in silico* analysis of dysregulated miRNA and its target genes primarily highlighted a number of T-cell specific functions, such as those that promote T-cell activation and proliferation. Of interest, Runx1, a transcriptional factor that drives various aspects of T-cell activation and differentiation was highlighted by our analysis. Functionally, Runx1 levels remain high in naïve CD4+ T-cells but the activation of T-cells turns off its expression (Wong *et al.*). Moreover, Runx1 deficiency leads to T-cell proliferation and the induction of IL-2 (Wong *et al.*). We observed that the SEB-induced down regulation of *Runx1* corresponded inversely with the induction of miR-20b and miR-222, miRNA that are specifically predicted to bind the 3'UTR of *Runx1*, suggesting that these miRNA may contribute to SEB-mediated T-cell proliferation and activation.

Comparable to the role of Runx1 in activated CD4+T-cells, the impairment of the TGFβ/SMAD3 pathway, also leads to the activation and proliferation of T-cells (Delisle *et al.*). Furthermore, TGFβ mediated cellular apoptosis and cell cycle arrest is known to occur through the activation of SMAD3 (Ten Dijke *et al.*, 2002) . Our data demonstrated a strong downregulation of *Smad3* and *Tgfβ* mRNA levels. Interestingly, three of the most highly overexpressed miRNA i.e. miR-132, miR-155 and miR-31 were predicted to align to the 3'UTR of *Smad3*, strongly suggesting a role of these miRNA in this pathway.

It is striking that the microarray results revealed a very high expression of miR-132, which was validated by q-RT-PCR. Although expressed in high levels in the brain with the capacity to influence neuronal differentiation and synaptic plasticity(Lungu *et al.*, ; Scott *et al.*), very few studies have explored its role in inflammation. In primary human preadipocytes, the overexpression of miR-132 results in the targeting of SIRT-1, the

subsequent activation of NFkB and induction of MCP-1 (Strum *et al.*, 2009). Following CD4+ T-cell activation, the overexpression of miR-132 facilitates HIV-1 replication (Chiang *et al.*). Because we witnessed the activation of CD4+ T-cells and the production of MCP-1 after SEB exposure, it is reasonable to believe that miR-132 may influence these immune processes. Moreover, the *in silico* analysis of the target genes pertaining to inflammation revealed that miR-132 could moderately target *Bcl10* and *Tgfb2*, but was highly predicted to target *Smad2*, *Smad5* and the *Foxo* set of transcriptional factors , especially *Foxo3*. It is known that FOXO3 overexpression leads to apoptosis and that one of its primary functions is to regulate unprecedented cellular proliferation (Hedrick *et al.*). Moreover, the absence of FOXO3 leads to hyperactivation of T-cells, autoimmunity and lymphoadenopathy (Lin *et al.*, 2004). Prompted by the importance of FOXO3 in controlling inflammation, we pursued the gain- and - loss of function experiments with synthetic miRNA mimic and inhibitors and found an inverse relationship between miR-132 and *Foxo3*. These data suggested that the targeting of *Foxo3* by the highly expressed miR-132 could offer an explanation for uninhibited cellular proliferation, the expression of cell cycle progression genes and the production of a number of cytokines and chemokines in response to SEB.

In summary, we have effectively profiled several miRNA following exposure to the superantigen, SEB. Our data revealed that SEB significantly altered the expression of miRNA predicted to have pro-inflammatory roles. With the consequence of SEB exposure being extensive lung inflammation and acute mortality of mice it is likely that several miRNA are acting in concert to enhance the severity of the disease. Additionally, since miRNA have several co-targets, its impact would be expected to be widespread and

involve the simultaneous activation and cross talk of a number of inflammatory signaling pathways as highlighted in the study. To the best of our knowledge, we are the first to report the differential regulation of miRNA in response to SEB in a murine model of acute inflammatory lung injury. While it would be interesting to identify a principal miRNA, the inhibition of which rescues mice from SEB-induced toxicity our results nevertheless point towards the potential therapeutic modulation of miRNA to mitigate SEB-induced toxicity.

Table 3.1. Real time qPCR primer list

Gene	Primer	Sequence 5'→3'
Tbx21	Tbx21-F	AAC CGC TTA TAT GTC CAC CCA
	Tbx21-R	CTT GTT GTT GGT GAG CTT TAG C
Tgfb1	Tgfb1-F	CCA CCT GCA AGA CCA TCG AC
	Tgfb1-R	CTG GCG AGC CTT AGT TTG GAC
Foxo3	Foxo3-F	GCA AGC CGT GTA CTG TGG A
	Foxo3-R	CGG GAG CGC GAT GTT ATC C
Stat3	Stat3-F	AAT ATA GCC GAT TCC TGC AGA G
	Stat3-R	TGG CTT CTC AAG ATA CCT GCT C
Nfκb	Nfκb --F	ATG GCA GAC GAT GAT CCC TAC
	Nfκb-R	TGT TGA CAG TGG TAT TTC TGG TG
Ccnd1	Ccnd1-F	GCG TAC CCT GAC ACC AAT CTC
	Ccnd1-R	ACT TGA AGT AAG ATA CGG AGG GC
CcnE1	CcnE1-F	GTG GCT CCG ACC TTT CAG TC
	CcnE1-R	CAC AGT CTT GTC AAT CTT GGC A
Cox2	Cox2-F	TGA GCA ACT ATT CCA AAC CAG C
	Cox2-R	GCA CGT AGT CTT CGA TCA CTA TC
Smad3	Smad3-F	AGG GGC TCC CTC ACG TTA TC
	Smad3-R	CAT GGC CCG TAA TTC ATG GTG
Runx1	Runx1-F	GCA GGC AAC GAT GAA AAC TAC T
	Runx1-R	GCA ACT TGT GGC GGA TTT GTA
β-actin	β-actin -F	GGC TGT ATT CCC CTC CAT CG
	β-actin -R	CCA GTT GGT AAC AAT GCC ATG T

Table 3.2.List of select differentially expressed (> 2 fold) miRNA in lung infiltrating mononuclear cells after SEB exposure compared to Vehicle control**.**

miRNA	**Fold change**	**Seed Sequence**	**Accession number**
Overexpressed			
mmu-miR-132	56.7	AACAGUC	MIMAT0000144
mmu-miR-155	38.8	UAAUGCU	MIMAT0000165
mmu-miR-31	15.2	GGCAAGA	MIMAT0000538
mmu-miR-20b	5.6	AAAGUGC	MIMAT0003187
mmu-miR-222	3.4	GCUACAU	MIMAT0000670
Underexpressed			
mmu-miR-193*	-22.3	GGGUCUU	MIMAT0004544
mmu-miR-192	-10.6	UGACCUA	MIMAT0000517
mmu-let-7e	-8.5	GAGGUAG	MIMAT0000524
mmu-miR-34a	-6.2	GGCAGUG	MIMAT0000542

Table 3.3. List of predicted or experimentally observed miRNA target genes associated with inflammation.

miRNA	Target genes
miR-132 ↑	*Foxo1, Foxo3, Tgfb2, Bcl10, Smad2, Smad5*
miR-155 ↑	*Bcl10, Foxo3, Socs1, Smad2,*
miR-20b ↑	*Runx1, Mcl1, Pten, Socs6, Socs7, Tgfbr2*
miR-222 ↑	*Foxo3, Gata4, Pten, Socs1, Socs3*
miR-31 ↑	*Foxp3, Smad3, Rorc*
let7e ↓	*Ccnd1, Ccne1 Cd80, Cd86, Cdkn1a, Il6, Il6r, Stat3*
miR-192 ↓	*Nfat5, Cxcr5, Traf5, Traf6,Zeb1,Ccne1*
miR-193* ↓	*Ccnd1, Ets1, Esr1, Il12rg, Cd247, Ptgs2*
miR-34a ↓	*Ccnd1,Bcl2, Il6r, Il2rb, Map2k1, Pik3r2*

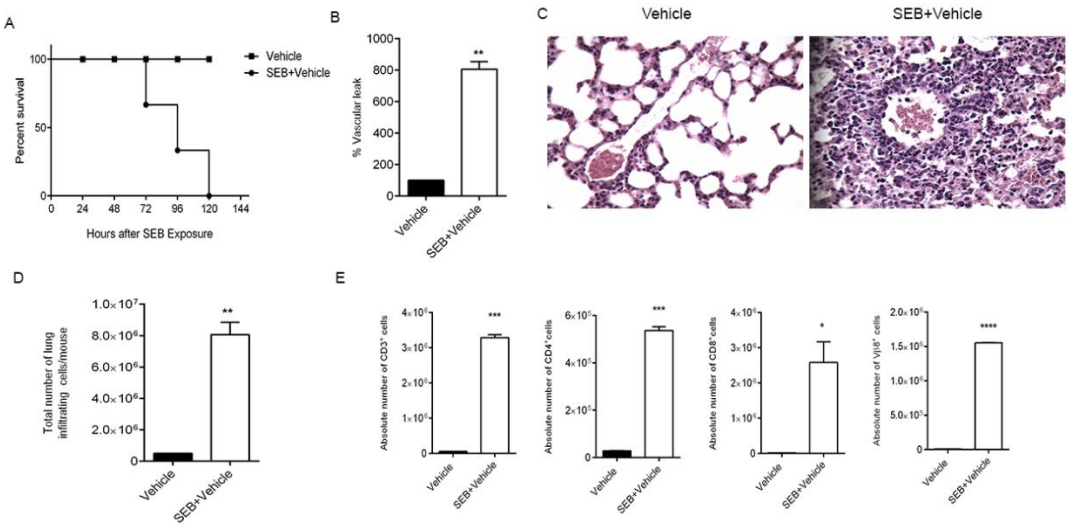

Figure 3.1. SEB exposure results in pulmonary inflammation and mortality of mice. C3H/HeJ mice were exposed to a 'Dual Hit' of SEB and euthanized 72 hours post exposure. (A) Survival curve of mice exposed to either vehicle or SEB. (B) Measurement of Vascular Leak 24 hours after exposure to the second dose of SEB. Mice were administered Evans blue dye and following perfusion, lungs were placed in formamide. Absorbance was recorded at 620 nm and the percentage of vascular leak was calculated and graphically represented. (C) Representative H&E (x 40) staining of sections of the lung demonstrating immune cell infiltration. (D) Total number of mononuclear cells infiltrating the lungs in vehicle or SEB exposed mice as determined by trypan blue exclusion method. (E) Phenotypic characterization of mononuclear cells infiltrating the lung determined by staining cells with fluorescein-conjugated antibodies against CD4, CD8 and Vβ8 and conducting flow cytometric analysis. Absolute cell counts are represented graphically. Data are means ±SEM (n=5) and are representative of three independent experiments. Statistical significance is indicated as follows *p<0.05, ** p<0.01, *** P<0.001, **** p<0.0001 (as compared to vehicle).

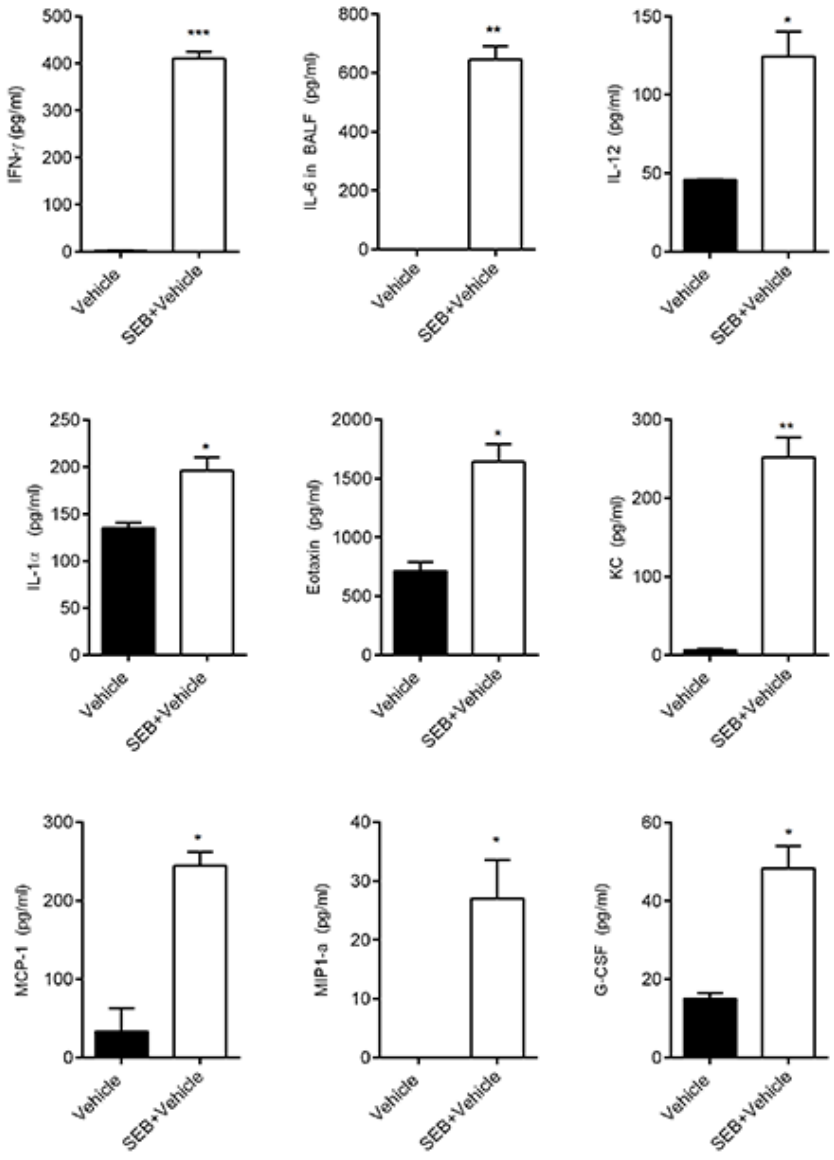

Figure 3.2. Exaggerated expression of chemokines and cytokines after SEB exposure. Mice were exposed to either vehicle or SEB for 72 hours and euthanized. The trachea was bound with a suture. Following the excision of the lung along with the trachea, 1 ml of ice-cold PBS was flushed through the trachea and collected as the Broncheoalveolar lavage fluid (BALF). Cytokine and chemokine expression was analyzed using a Bioplex and the concentration quantified in pg/ml. Data are means ±SEM (n=5) and are representative of three independent experiments. Data are means ±SEM (n=5) and are representative of two independent experiments. Statistical significance is indicated as follows *p<0.05, ** p<0.01, *** P<0.001, (as compared to vehicle).

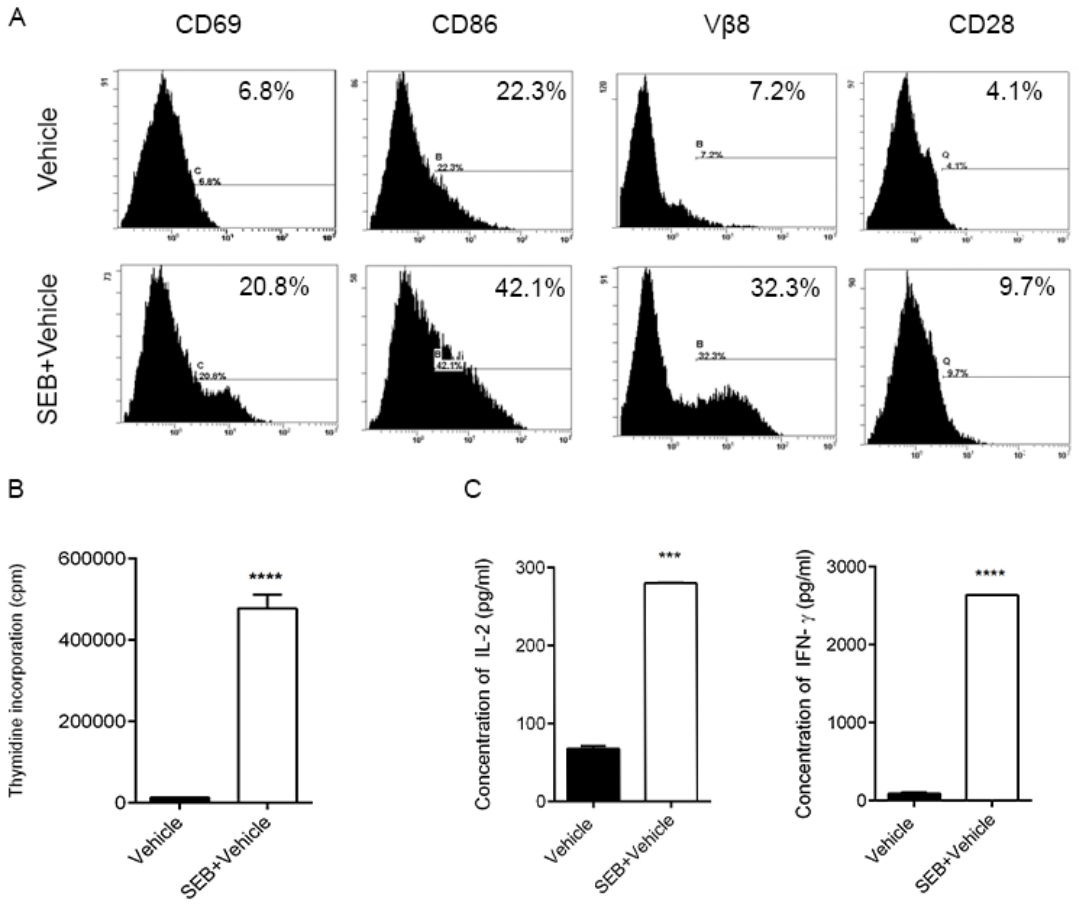

Figure 3.3. Effect of SEB activation *in vitro*. Splenocytes seeded at a density of 1X10 ^{6} cells were activated with 1 μg/ml of SEB. (A) Twenty four hours after activation, cells were harvested and stained with fluorescein-conjugated antibodies against Vβ8 and activation markers CD69, CD86 and CD28. The representative histograms are depicted (B) Cell proliferation assay as measured by the incorporation of thymidine in splenocytes that were activated with SEB for forty-eight hours. (C) Cytokine expression determined by ELISA. Samples were obtained from collecting the supernatants following SEB activation of splenocytes. For all experiments cells were plated in triplicates and data is representative of two independent experiments. Statistical significance is indicated as follows ** $p<0.01$, *** $P<0.001$, **** $p<0.0001$ (as compared to vehicle).

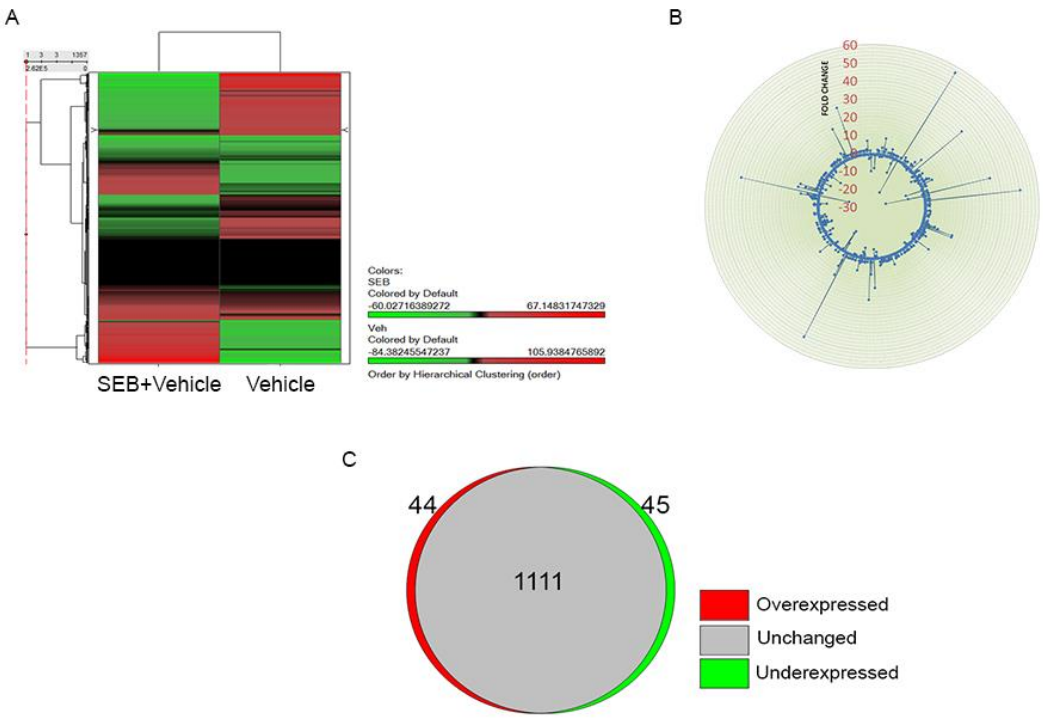

Figure 3. 4. SEB exposure leads to dysregulation of microRNA. Seventy-two hours after SEB exposure, total RNA was isolated from lung infiltrating mononuclear cells. (A) A Heatmap depicting the differential expression of miRNA in the lungs of SEB exposed mice compared to vehicle. The accompanying color scape depicts mean expression values that are overexpressed (red) or underexpressed (green) above or below the mean respectively. (B) Fold change distribution plot of 1111 mouse specific miRNA indicating several unchanged, upregulated or downregulated miRNA. (C) A proportional Venn diagram showing the number of miRNA that are overexpressed, underexpressed (< 2 fold) or unchanged after SEB exposure.

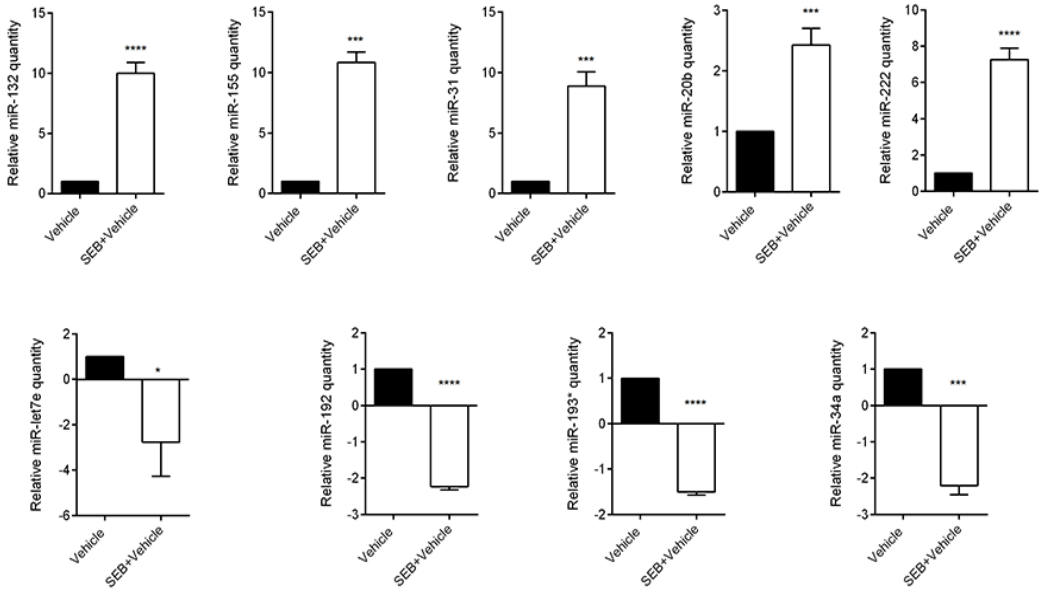

Figure 3.5. Experimental validation of Top overexpressed and underexpressed miRNA. Total RNA was obtained from the lung infiltrating mononuclear cells following exposure to either vehicle of SEB. (A) q-RT PCR validation of the IPA generated Top overexpressed miRNA. (B) q-RT PCR validation of the IPA generated Top underexpressed miRNA. Snord96a was used as the small endogenous control and expression of miRNA was normalized to vehicle. Data is represented as mean ± SEM from replicate samples. Lung infiltrating mononuclear cells were pooled from 5 mice in each group. Statistical significance is indicated as follows *p<0.05, *** P<0.001, **** p<0.0001 (as compared to vehicle).

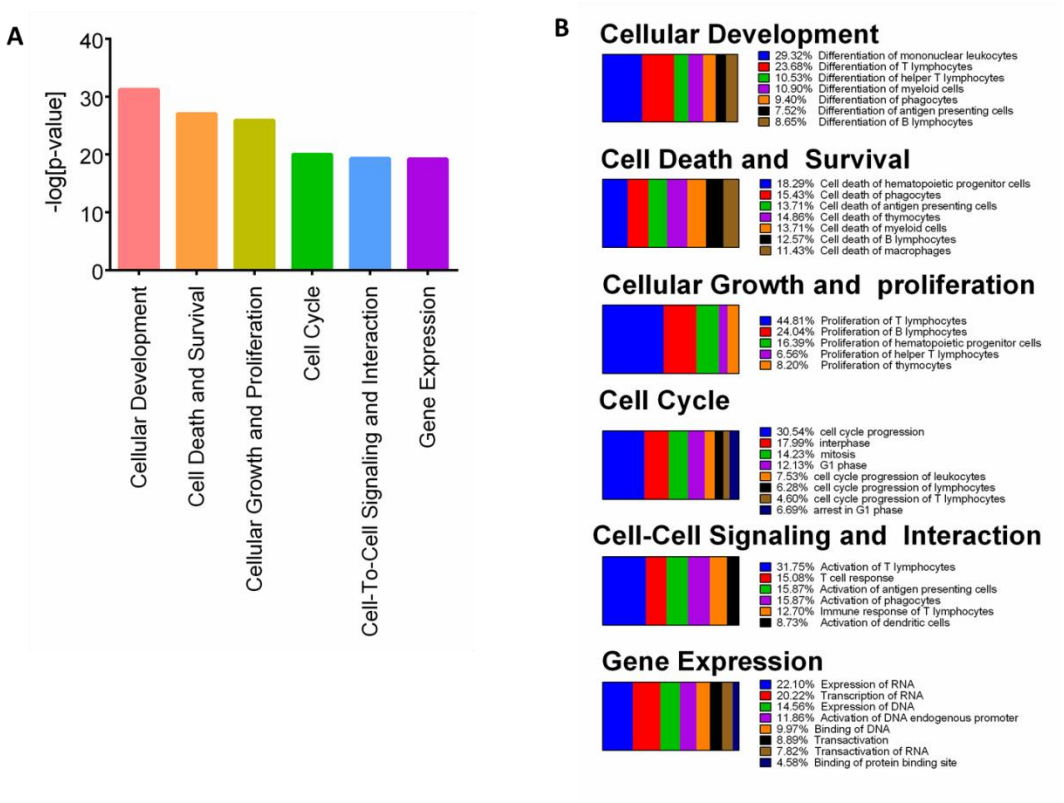

Figure 3.6. *In silico* analysis of SEB-dysregulated miRNA. Ingenuity pathway analysis (IPA) was used to analyze the miRNA that were significantly (<2 fold) altered. (A) Bar graph highlighting the overall biological functions associated with the dysregulated miRNA (B) Horizontal slice plot further depicting the percentage of the miRNA-associated molecules that can be attributed to specific biological functions.

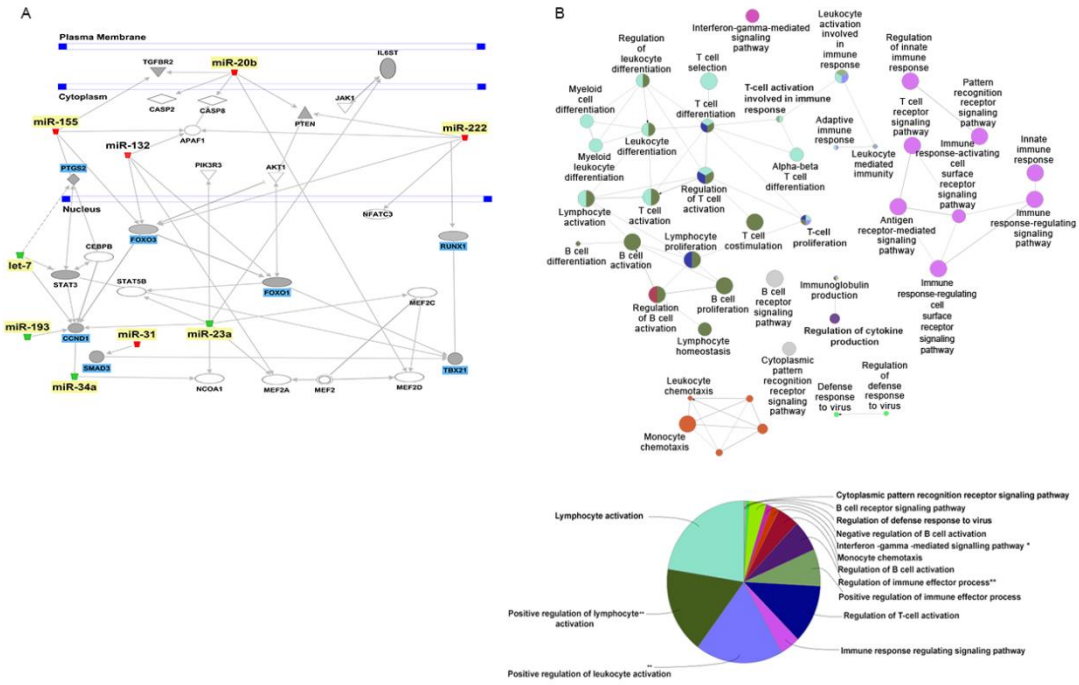

Figure 3.7. *In silico* analysis of the predicted mRNA targets. (A) IPA generated network highlighting the interaction between validated miRNA (yellow) and their respective target genes (blue). (B) Cytoscape generated network depicting Gene Ontology (GO) enrichment terms and mapped for GO category: Immune response, using Cytoscape with ClueGo and CluePedia applications. Two-sided hypergeometric test was performed with kappa score threshold setting of 0.4. Benjamini-Hochberg statistical test was used. The colored pie chart represents the highly enriched GO terms and the diameter of the node in the map is directly proportional to the number of miRNA target genes it contains.

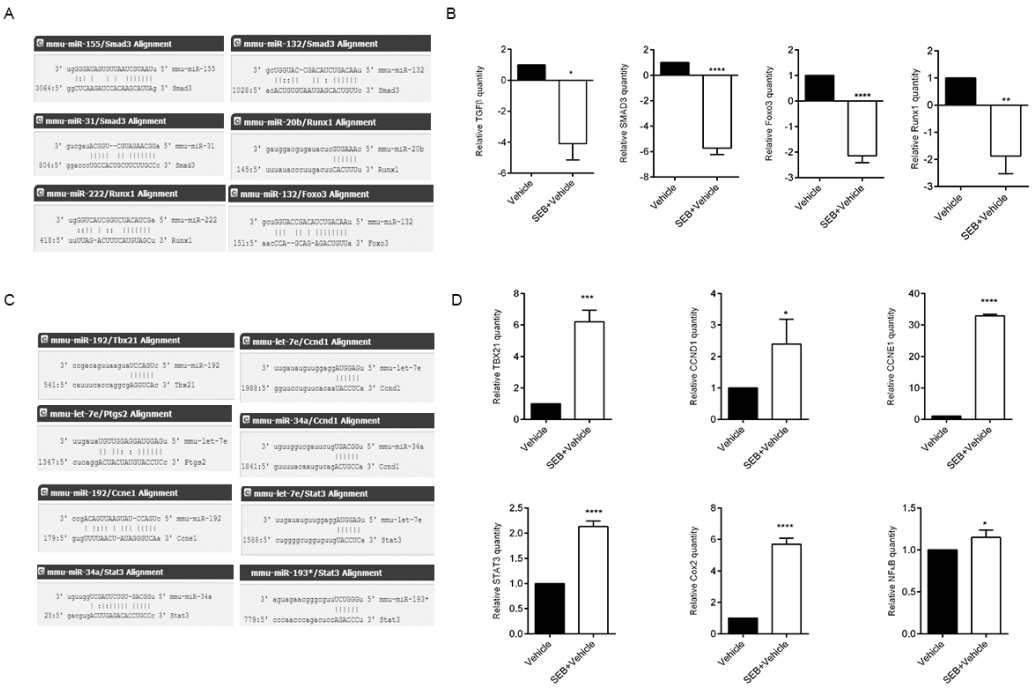

Figure 3.8. Experimental validation of miRNA target genes. (A) Schematic illustration of SEB-induced overexpressed miRNA targeting the 3'UTR of potential target genes. (B) q-RT PCR validation of SEB-induced miRNA mRNA targets. (C) Schematic illustration of SEB-induced underexpressed miRNA that target the 3' UTR of potential target genes. (D) q-RT PCR validation of SEB-induced miRNA mRNA targets. Data is represented as mean ± SEM from replicate samples. Lung infiltrating mononuclear cells were pooled from 5 mice in each group. *p<0.05, ** p<0.01, *** P<0.001, **** p<0.0001 (as compared to vehicle).

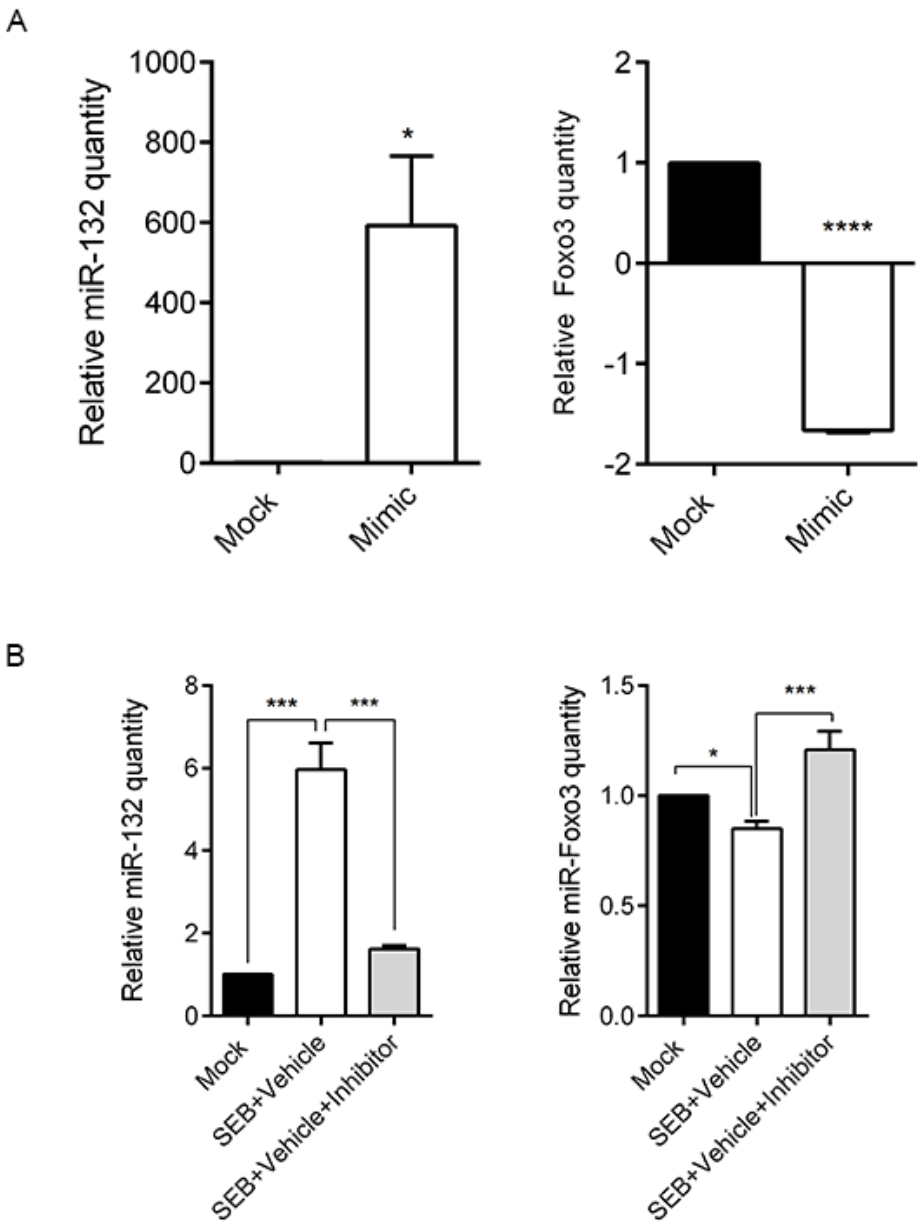

Figure 3.9. miR-132 targets *Foxo3*. (A) Splenocytes obtained from mice were transfected either with miR-132 mimic (Mimic) or Mock transfection control (Mock) for 24 hours. miR-132 and *Foxo3* levels were determined by RT-PCR. (B) Splenocytes were activated with (1μg/ml) and for 24 hours. Cells were then transfected with 100nM miR-132 inhibitor (Inhibitor) or Mock transfection control (Mock) for another 24 hours. *Foxo3* levels were determined via RT-PCR. For miRNA normalization, Snord96_a was used as internal control. For mRNA, β-actin was used as the internal control. Data is represented as mean ± SEM from replicate samples statistical significance is indicated as *p<0.05,**p<0.01,***P<0.001,****p<0.0001.

CHAPTER IV: Δ^9Tetrahydrocannabinol attenuates Staphylococcal enterotoxin B-induced inflammatory lung injury and prevents mortality in mice by modulation of miR-17-92 cluster and induction of T-regulatory cells.

4.1 INTRODUCTION

Staphylococcal enterotoxin B (SEB) is a potent activator of the immune system resulting in the clonal expansion of 5-30% of the T-cell pool and massive release of cytokines (Choi *et al.*, 1989; Faulkner *et al.*, 2005). As a consequence, it is associated with a number of diseases ranging from food poisoning, multi-organ failure and lethal toxic-shock (Alouf *et al.*, 2003; Dinges *et al.*, 2000; Larkin *et al.*, 2009). When inhaled, the combination of cellular infiltration and cytokine production, results in vascular leak, pulmonary edema, tissue damage and eventually acute inflammatory lung injury (Rao *et al.*, ; Rieder *et al.*). Due to its ability to be easily aerosolized and for its possible role as a biological weapon, SEB is considered a Center for Disease Control and Prevention - Category B select agent (Ulrich, 2001). While it is known that the interaction of SEB with the T-cell receptor results in the activation of inflammatory pathways such as the PI3K, MAPK and NFκB (Krakauer), a recent study from our laboratory has suggested that microRNA (miRNA) may play an important role in SEB-mediated inflammation (Rao *et al.*).

miRNA are ~22 nucleotide, small, non-coding RNA that target mRNA, leading to its degradation and/or translational repression (Guo *et al.*). Consequently, they control the development and differentiation of various immune cells thereby leading to the regulation of immune responses (Lindsay, 2008). Upon receiving inflammatory signals , active changes occur within the transcriptional repertoire accompanied with altered expression of a number of miRNA resulting in the up or downregulation of several important genes (O'Connell *et al.*). One such modulator of gene expression is the miR-17-92 cluster. Originally recognized as an oncogenic miRNA, this cluster that comprises of six miRNA (miR-17, miR-18a, miR-19a, miR-20a, miR-19b-1 and miR-92a-1) is known to be an important regulator of B and T-cell responses (Olive *et al.*). For example, miR-17-92 transgenic mice that express the cluster in both B and T cells develop lymphoproliferative disease (Xiao *et al.*, 2008). In addition, miR-19b and miR-17 within the cluster are reported to regulate CD4 + T-cells and enhance Th1 responses (Liu *et al.*), thereby demonstrating an important role for the cluster during inflammation.

Although current therapeutic strategies against SEB include the use of intravenous antibodies as well as neutralizing antibodies against SEB-induced cytokines (Larkin *et al.*, ; Larkin *et al.*, ; Matthys *et al.*, 1995; Miethke *et al.*, 1992) it's efficacy remains inefficient (Darenberg *et al.*, 2004). Additionally, corticosteroids have been shown to attenuate SEB-induced toxic shock and acute lung injury (Huzella *et al.*, 2009; Krakauer *et al.*, 2006) , but the immunosuppressive property of corticosteroids is either accompanied by a number of side-effects or have remained ineffective clinically (Bernard *et al.*, 1987; Meduri *et al.*, 1998; Wajanaponsan *et al.*, 2007) . As a result, there is a need

for alternative agents that mitigate SEB-triggered inflammation with the potential to modulate SEB-induced inflammatory miRNA.

Δ^9-Tetrahydrocannabinol (THC) is a marijuana plant-derived cannabinoid known for its robust anti-inflammatory properties (Klein, 2005; Nagarkatti *et al.*, ; Nagarkatti *et al.*, 2009). It mediates its action by binding to two main cannabinoid receptors, CB1 and CB2, found primarily in the brain and on immune cells respectively (Felder *et al.*, 1998). Previously, we have demonstrated that THC induces apoptosis in Jurkat leukemia T-cells and dendritic cells (Do *et al.*, 2004). THC suppresses the production of Th1 cytokines IFN-γ and TNF-α (Klein, 2005; Klein *et al.*, 1995; Srivastava *et al.*, 1998; Sun *et al.*, 2008) , while increasing Th2 cytokines, IL-10 and TGF-β (Sun *et al.*, 2008). Additionally, while we have earlier reported that THC induces the production of myeloid derived suppressor cells (MDSCs) (Nagarkatti *et al.*), we have for the first time demonstrated that THC-mediated miRNA control the development of these MDSCs (Nagarkatti *et al.*). Taken together, THC, by virtue of its anti-inflammatory properties and its recently discovered ability to regulate miRNA expression could serve as an effective therapeutic agent in the attenuation of SEB-mediated lung injury.

Thus, in the current study, we tested the hypothesis that THC treatment ameliorates SEB-induced toxicity through regulation of miRNA. Our data demonstrate that THC treatment downregulates the members of the miR-17-92 cluster and ameliorates inflammatory symptoms associated with SEB-exposure in the lungs.

4.2 MATERIALS AND METHODS

Mice

Female C3H/HeJ mice (6-8 weeks) were purchased from The Jackson laboratory. All mice were housed at the Animal Resource Facility (ARF), University of South Carolina, under specific pathogen free conditions. All experiments involving the use of vertebrate animals were conducted under protocols approved by the Institutional Animal Care and Use Committee (IACUC) at USC.

SEB administration and THC treatment schedule

THC was provided by National Institute on Drug Abuse (Bethesda, MD) and SEB was procured from Toxin Technologies (Sarasota, Florida). The treatment schedule comprised of first injecting Vehicle or THC intraperitoneally (i.p) at a concentration of 20 mg/kg body weight in a 100 µl volume dissolved in ethanol (Day 1). The following day (Day 2), THC (20 mg/kg) was once again administered via the i.p route. Thirty minutes later, SEB was delivered as a 'Dual Dose' as described previously (Huzella *et al.*, 2009). Briefly, SEB dissolved in sterile PBS (2 mg/mL) was administered first by the intranasal (i.n) route at a concentration of 5µg/mouse in a volume of 25 µL. Two hours later, a second dose of SEB was delivered i.p at a concentration of 2 µg/mouse in a 100 µl volume. On Day 3, mice were treated i.p. with THC (20 mg/kg). Survival of mice was monitored up to 5 days after SEB exposure and any moribund mice were immediately euthanized.

Assessment of lung damage and function

Vascular leak in the lungs was determined as described (Rieder *et al.*, ; Rieder *et al.*, ; Saeed *et al.*, 2012). Briefly, mice were injected with 1% Evans blue in sterile PBS intravenously (i.v) seventy-two hours after the second dose of SEB. Two hours later, mice were euthanized and lungs were perfused with heparinized PBS. Lungs were incubated in formamide at 37 ° C for 24 hours to extract the dye. The optical density (O.D) of the supernatant was measured spectrophotometrically at 620 nm and percent increase in vascular leak was calculated using the following formula - ($O.D_{sample}$ - $O.D_{control}$/$O.D_{control}$) x 100. Airway resistance was measured using whole body plethysmography (Buxco, Troy, NY). Each mouse was restrained in a two-chamber plethysmographic tube and were first allowed to acclimatize, followed by exposure to saline for 2 minutes. This was followed by a 2 minute exposure to increasing doses of methalcholine. The sRaw measurement at each methalcholine dose was calculated and plotted as percent airway resistance. To examine lung morphology and histology, lungs were fixed in 10% formalin, paraffin embedded and stained with hematoxylin and eosin (H&E). The slides were observed under a light microscope at 20 x magnification.

Cell preparation and Flow cytometry

Vehicle, SEB+Vehicle and SEB+THC mice (5 mice per group) were euthanized 72 hours after dual exposure to SEB. The lungs were perfused with heparinized PBS, harvested and homogenized using Stomacher® 80 Biomaster blender from Seward (Davie, FL) in 10 ml of sterile PBS. Following washing with sterile PBS, cells were layered carefully onto Ficoll-Histopaque ®-1077 from Sigma-Aldrich (St Louis, MO) at a 1:1 ratio. Mononuclear cells were separated by density gradient centrifugation as a distinct layer as

described (Rao *et al.*, ; Rieder *et al.*) and enumerated by Trypan blue exclusion. To determine the phenotypic characteristics of the infiltrating cells, mononuclear cells were stained with the following fluorescent conjugated antibodies- Fluorescein isothiocyanate (FITC) -conjugated anti-CD8 (clone: 53-6.7), anti-CD3 (clone: 145.2 C11). Phycoerthyrin (PE)-conjugated anti-CD4 (clone: GK 1.5), anti NK1.1 (clone: PK136) from Biolegend (San Diego, CA). FITC-conjugated anti-Vβ8 (clone: K516) from Ebioscience (San Diego, CA). Intracellular staining of Foxp3 was carried out using Biolegend's Foxp3 Fix/Perm buffer set following manufacturer's instructions and using anti-foxp3 alexa flour 488 (clone MF-14) from Biolegend.

Cytokine Analysis

To assess serum cytokines, mice were bled three hours after dual exposure to SEB. Cytokines from the BALF were obtained at the time by binding the trachea with a suture and excising the lung along with the trachea, as described (Rao *et al.*, ; Rieder *et al.*). Sterile, ice-cold PBS was injected through the trachea to aspirate the fluid. The samples were centrifuged to obtain the supernatants. All cytokine levels were measured using Biolegend (San Diego, CA) ELISA MAX ™ standard kits.

miRNA target predictions and transfections

miRNA target candidate *Pten* was predicted using Ingenuity Pathway Analysis (IPA) software from Ingenuity Systems ® (Mountain View CA). Briefly, highly predicted and experimentally observed targets of the individual miRNA in the miR-17-92 cluster were selected. A core analysis was carried out and significant (fishers exact test) biological functions associated with the data set was generated. Additionally, a bar graph highlighting key canonical pathways associated with the dataset was also generated.

miRSVR score and alignment of miR-18a with *Pten* was obtained from www.microRNA.org , target prediction website. To validate *Pten* as a target of miR-18a, splenocytes from naïve C3H/HeJ mice were harvested and cultured in complete (10% FBS, 10mM L-glutamine, 10mM Hepes, 50 μM β-Mercaptoethanol , and 100 μg/mL penicillin) RPMI 1640 medium (Gibco Laboratories, Grand Island, NY). Cells were seeded at 2 x 10^5 cells per well in a 24 well plate and transfected for 24 hours with 40nM synthetic mmu-miR-18a (MSY0000528) or mock transfected with HiperFect transfection reagent from Qiagen (Valencia, CA). For inhibition of miR-18a, SEB-activated cells were similarly transfected for 24 hours with 100 nM synthetic mmu-miR-18a (MIN0000528) or mock transfected.

Total RNA extraction and q-RT PCR

Total RNA (including small RNA) was isolated from lung-infiltrating mononuclear cells or in vitro from splenocytes using miRNeasy kit from Qiagen (Valencia, CA) following manufacturers instruction. The purity and concentration of the RNA was confirmed spectrophotometrically using Nanodrop 2000c from Thermo Scientific (Wilmington, DE). For miRNA validation and quantification, we used SYBR Green PCR kit (Qiagen) and for mRNA validation, SSO Advanced ™ SYBR green PCR kit from Biorad (Hercules, CA). Fold change of miRNA was determined by normalization to Snord96_a internal control, whereas, mRNA levels were normalized to β-actin. The following q-RT PCR primers were used: *β-actin* (F) 5'GGCTGTATTCCCCTCCAT G-3' and (R) 5'-CCAGTT GGTAACAATGCCATGT-3'; *Foxp3* (F) 5' AGCAGTCCACTTCACCAAGG 3' and (R) 5' GGATAACGCCAGAGGAGCTG 3'; *Pten* (F) 5'

TGGATTCGACTTAGACTTGACCT 3' and (R) 5' GCGGTGTCATAATGTCTCTCAG 3'.

In vitro cell culture assays

Splenocytes from naïve C3H/HeJ mice were harvested and cultured in complete RPMI. Cells were seeded at $1x10^6$ cells per well of a 96 well plate and either left unstimulated or stimulated with SEB (1μg/ml). Cell were either treated with THC (20μM) or with AKT 1/2 kinase inhibitor (A6730) from Sigma-Aldrich at the doses indicated. Twenty-four hours later cells were harvested and centrifuged. The cell supernatants were collected for assessment of IFN-γ levels by ELISA and the cell pellets were used for total RNA extraction and q-RT PCR. Cell proliferation was determined by incubating the cells as described above for forty-eight hours. ^{3}[H]-Thymidine (2μCi) was added to the cell cultures in the last 12 hours of incubation. Cultures were collected using a cell harvester and thymidine incorporation was measured using a scintillation counter (Perkin Elmer).

Statistical analysis

All statistical analyses were carried out using GraphPad Prism Software (San Diego, CA). In all experiments, the number of mice used was 4-5 per group, unless otherwise specified. Results are expressed as means ± SEM. Student's t-test was used to compare two-groups, whereas multiple comparisons were made using one-way analysis of variance (ANOVA), followed by *post hoc* analysis using Tukey's method. A P-value of < 0.5 was considered statistically significant. Individual experiments were performed in triplicate and each experiment was performed independently at least three times to test reproducibility of results**.** Survival analysis was carried out using a Log-rank test.

4.3 RESULTS

THC strongly attenuates SEB-mediated inflammation and prevents acute mortality

Dual SEB exposure has been previously used to study acute lung injury leading to 100% death in C3H/HeJ mice (Huzella *et al.*, 2009). In the current study, we found that 100% of the mice exposed to SEB died between 96 and 120 hours. Remarkably, in THC treated groups, all mice survived (Figure 4.1A). SEB exposed mice displayed signs of lethargy, hunching, ruffled fur and respiratory stress; whereas THC treated mice appeared healthier. To gauge the extent of pulmonary damage , we measured airway resistance using whole body plethysmography and found that SEB exposure resulted in a significant percent increase in airway resistance, while THC treated mice recorded specific airway resistance (sRAW) values similar to Vehicle alone (Figure 4.1B). Further, we measured the percent increase in vascular leak by administration of Evans blue dye. Evans blue binds to serum albumin and is a measure of vascular permeability, as shown previously (Rieder *et al.*). Our results demonstrated that while SEB exposure had a profound increase in vascular leak when compared to Vehicle only, THC treatment caused a significant decrease in vascular leak (Figure 4.1C). Acute inflammatory lung injury is characterized by massive immune cell infiltration into the lung. Accordingly, we found an increase in the total number of mononuclear cells after SEB exposure and a subsequent decrease with THC treatment (Figure 4.1D). This was confirmed by histopathological examination of the lungs whereby SEB exposed mice displayed an increase in infiltrating immune cells around the bronchioles and air vessels while the THC treated mice, yielded significantly fewer layers (Figure 4.1E). To identify the immune subsets amongst the infiltrating mononuclear cells, we stained the cells with

various fluorescein-conjugated anti-mouse antibodies. We found that exposure to SEB resulted in increased CD3+ (T-cells), CD4+ (T-helper cells), CD8+ (Cytotoxic T-cells), Vβ8+ NK+ (Natural Killer cells) and NK1.1+CD3+ (Natural killer T-cells), THC treatment caused an overall decrease in the absolute cell numbers (Fig 4.1F).

A hallmark of SEB-mediated inflammation is the abundant release of cytokines. To determine if THC was able to blunt cytokine secretion, we first analyzed the concentration of early cytokines IL-2 and MCP-1 in the serum. Mice were bled at 3 hours, 6 hours, and 24 hours after SEB exposure. While IL-2 and MCP-1 peaked at 3 hours (data not shown), we found that the THC treated group showed diminished secretion of both IL-2 and MCP-1 as early as 3 hours after SEB exposure (Figure 4.2A), supporting the potent anti-inflammatory role of THC in this model. Moreover, an examination of cytokines in the broncheoalveolar lavage fluid (BALF) revealed that THC treatment led to the substantial decrease in IFN-γ, IL-6, IL-12 and IL-10 (Figure 4.2B). Overall, these data suggest that THC attenuates SEB-induced immune cell infiltration, decreases early and late cytokine secretion, and prevents mortality of the mice.

THC modulates the expression of the miR-17-92 cluster

Antigenic stimulation and the activation of the T-cell receptor is known to result in the induction of miR-17-92 cluster (Wu *et al.*, 2012). Consequently, we reasoned that SEB exposure would lead to the expression of this prominent miRNA cluster. Seventy two hours after exposure to SEB, we measured miRNA expression in mononuclear cells isolated from the lung by q-RT PCR. Interestingly, we observed high levels (up to 600 fold) of the miRNA cluster, although individual miRNA were induced to different levels. More interestingly, THC treatment was able to down-regulate the individual members of

the cluster significantly (Figure 4.3), strongly suggesting that THC may exhibit its powerful anti-inflammatory activity through the modulation of inflammatory miRNA.

miR-17-92 cluster is linked to the activation of the PI3K/AKT/ pathway

Because SEB exposure resulted in the strong induction of the miR-17-92 cluster, we sought to explore the significance of this particular cluster in our study. Therefore, we carried out computational analysis on the highly predicted and experimentally observed targets of the cluster (miR-17, miR-18a, miR-19a, miR-20a, miR-19b-1, and miR-92a-1) using Ingenuity Pathway analysis (IPA). IPA results suggested that the members of the cluster were involved in a number of biological functions relevant to the expansion of T-helper lymphocytes, the development of regulatory T-cells, the proliferation of cells and apoptotic processes (Figure 4.4A). In addition, analysis of the canonical pathways associated with the cluster indicated the involvement of the MAPK, NFκB, and PI3K/AKT signaling pathways, (processes that are all reported to be SEB-triggered). Interestingly, while the PTEN signaling and mTOR pathways were highlighted by IPA as significant (Figure 4.4B), pathway analysis also indicated that the miRNA in the cluster are highly predicted or experimentally observed to converge on *Pten* (Figure 4.4C). As a result, we reasoned that the SEB-induced miRNA cluster is involved in the activation of the PI3K/AKT signaling pathway while THC mediated down-regulation of this cluster inhibits the aforementioned activation. To test if the cluster was indeed involved in the activation of the PI3K/AKT pathway, we activated splenocytes with SEB and treated them with an AKT1/2 inhibitor. Amongst the individual members of the cluster that were upregulated by SEB activation (*data not shown*), miR-18a in particular was significantly

downregulated upon AKT1/2 inhibition (Figure 4.5A). This indicated the involvement of miR-18a in SEB-mediated activation of the PI3K/AKT pathway.

miR-18a targets Pten, a negative regulator of the PI3K/AKT Pathway

Previous reports have established that a principal target of the miR-17-92 cluster is PTEN (phosphatase and tensin homologue), an antagonist of the PI3K/AKT pathway (Liu *et al.*, ; Xiao *et al.*, 2008) . Using www.miRNA.org alignment tool, we found that miR18a is predicted to target the 3' UTR of *Pten* with a good miRSVR score of -0.1453 (Figure 4.5B). To assess if miR-18a indeed targets *Pten*, we first transfected splenocytes with synthetic miR-18a mimic. Interestingly, we found that miR-18a mimic repressed *Pten* (Figure 4.5C). Further, the inhibition of SEB-activated cells with a miR-18a synthetic inhibitor led to the derepression of *Pten* (Figure 4.5D), suggesting that miR-18a, belonging to the cluster, plays a prominent role in the repression of *Pten* and consequently results in the activation of SEB-triggered PI3K/AKT pathway. Earlier we observed that THC was able to dramatically decrease the expression of the miRNA cluster (Figure 4.3). Therefore, we wondered if THC treatment would be able to subsequently restore the SEB-induced suppression of *Pten*. Upon assessing *Pten* expression in lung infiltrating mononuclear cells by q-RT PCR, we observed that while SEB exposure indeed resulted in the repression of *Pten*, THC treatment led to its increase (Figure 4.5E). Taken together, these data indicated that THC, via down-regulation of miR-18a, leads to the release of *Pten* and in doing so, may act as an AKT inhibitor.

THC functions as an AKT inhibitor

The activation of the PI3K/AKT pathway leads to cellular proliferation, the release of IFN-γ and inhibition of T-regulatory cells. Our results suggested that by antagonizing the

PI3K/AKT axis via the down-regulation of miR-18a and the subsequent release of *Pten*, THC may mimic the properties of an AKT inhibitor. To confirm this notion, we first compared the properties of THC with an AKT inhibitor on IFN-γ production *in vitro*. Splenocytes were activated with SEB and treated with THC or AKT inhibitor. The resulting concentration of IFN-γ was measured by ELISA. As expected, AKT inhibition led to the dose dependent decrease of IFN-γ (Figure 4.6A). Interestingly, THC treatment also demonstrated a trend in the dose-dependent decrease of IFN-γ, with a significant blunting of this cytokine at the highest dose (Figure 4.6A). Further, when cellular proliferation of cells was assayed by thymidine incorporation, we observed a similar dose-dependent decrease in cellular proliferation (Figure 4.6B) with THC and the AKT inhibitor. Moreover, the interruption of AKT signaling results in the induction of CD4+Foxp3+ T-regulatory cells (Merkenschlager *et al.*, ; Sauer *et al.*, 2008). Upon activating splenocytes with SEB in vitro and treating with either the AKT inhibitor or THC, we found significant induction of foxp3 (Figure 4.6C) compared to SEB alone. The induction was further confirmed by flow cytometric analysis and q-RT PCR of lung infiltrating mononuclear cells (Figure 4.6D). Taken together, these data indicate that THC inhibits AKT signaling by modulating miR-18a and allowing for the release of *Pten*. The resulting decrease in cellular proliferation, IFN-γ production and induction T-regulatory cells, prevent SEB-mediated acute inflammatory lung injury and death.

4.4 DISCUSSION

In the current study, we investigated the role of THC in preventing SEB-induced inflammatory lung injury and subsequent mortality via the modulation of miRNA. Through the use of q-RT PCR and computational tools, we found that the SEB-induced miRNA 17-92 cluster which was overexpressed in the lungs is down-regulated with THC treatment. Specifically, by performing gain-and loss-of function analysis using synthetic mimic and inhibitor, we confirmed the predominant role of miR-18a in the SEB-mediated activation of the PI3K/AKT pathway. Our studies also suggested that THC may function as an antagonist of the AKT pathway, at least in part, by its ability to significantly decrease the expression of miR-18a. Our results highlight the role of miRNA in facilitating severe inflammation and the ability of cannabinoids to suppress its expression. Importantly, we show that the previously reported potent anti-inflammatory role of THC can be explained, at least in part, by its ability to act upon SEB-mediated miRNA.

SEB specifically expands a large number of T cells, by virtue of engaging the Vβ8 region of the T-cell receptor (TCR) following binding to the MHC II on antigen presenting cells (APCs) (Choi *et al.*, 1989; Hurley *et al.*, 1995). Consequently, SEB exposure leads to the massive release of inflammatory cytokines, proliferation of T cells, tissue damage and SEB-mediated shock (DeVries *et al.*, 2011; Kissner *et al.*, 2011; Miethke *et al.*, 1992). Most models developed to study the effects of SEB exposure in mice, have employed the use of transgenic mice or external agents such as LPS or D-galactosamine to potentiate SEB-mediated inflammatory response (DaSilva *et al.*, 2002; Savransky *et al.*, 2003). In the dual administration of SEB as used in this study,

microgram quantities of SEB were sufficient to cause inflammatory symptoms and toxicity reminiscent of SEB exposure in humans (Huzella *et al.*, 2009). In this model, mice succumb to SEB-mediated shock and severe respiratory damage (Huzella *et al.*, 2009). Consistent with these reports, we observed an overall increase in mononuclear cells in the lung, particularly T cells. We also found SEB-mediated release of early monocyte and T-cell recruiting cytokines IL-2 and MCP-1 in the serum. Additionally, we noted the abundant release of late cytokines, especially IFN-γ in the BALF of the lungs resulting in compromised vascular permeability and the ultimate death of mice.

Earlier studies have reported that the molecular mechanism of action behind SEB-mediated inflammation and toxicity begins soon after the activation of the TCR (Goldbach-Mansky *et al.*, 1992; Linsley *et al.*, 1993). Following the increase in co-stimulatory molecules, a number of signaling pathways such as the MAPK, ERK, JNK, and PI3K/AKT are simultaneously activated (Krakauer). These pathways culminate in the stimulation of various transcription factors such as NFκB and NFAT (Trede *et al.*, 1995; Tsytsykova *et al.*, 2000). However, with the recent discovery of miRNA, our understanding of the molecular mechanisms that govern gene regulation has been revolutionized. It is now evident that these small single- stranded RNA molecules are capable of targeting the 3' UTR of mRNA thereby regulating biological processes such as cellular proliferation, differentiation and development(Davidson-Moncada *et al.*). miRNA are also induced upon a number of inflammatory cues and subsequently influence immune responses and immune cell development (Dai *et al.*).

The miR-17-92 cluster found on mouse chromosome 14 is amongst the many miRNA that are found to be overexpressed under inflammatory conditions (Sonkoly *et al.*,

2009a). It is transcribed as a single polycistronic unit and comprises of six miRNA- miR-17, miR-18a, miR-19a, miR-19b-1, miR-20a, and miR-92-1(Wu *et al.*). Previously, it has been shown that naïve CD4+ T-cells polarized under Th1 inducing conditions show a significant increase in the miR-17-92 cluster. (Sasaki *et al.*, 2010) Further, a recent report demonstrated the critical role of the cluster in the expansion of T-cells upon antigenic-stimulation, although they observed that individual miRNA within the cluster have differential roles in promoting Th1 responses.(Liu *et al.*) Prompted by these reports, we first investigated the role of miRNA in facilitating SEB-mediated lethality in mice and found that SEB exposure led to the overexpression of the miR-17-92 cluster in lung infiltrating mononuclear cells. Similar to previous studies, we also found that the members of the cluster, were expressed to different levels, suggesting that one or more miRNA within the cluster may play a more prominent role.

It was reported that the overexpression of miR-17-92 cluster causes lymphoproliferation, autoimmunity and premature death of mice by targeting *Pten*, a well-established antagonist of the PI3K/AKT pathway (Xiao *et al.*, 2008). In the present study, we demonstrate that *Pten* is suppressed after SEB exposure. Whereas previous studies have shown a primary role for miR-19b in the targeting of *Pten* (Liu *et al.*, ; Olive *et al.*, 2009), we attribute the SEB-mediated suppression of *Pten* to the predominant role of miR-18a. These data are surprising because while we demonstrate a clear reversal in the suppression of *Pten* using a miR-18a inhibitor, a few reports have demonstrated its role in inhibiting cellular proliferation(Liu *et al.*, ; Tsang *et al.*, 2009). It is possible that the functional targets of miRNA may differ based on the type of antigenic stimulation. Alternatively, the critical timing of SEB dual administration could contribute to the

specific regulation of *Pten* by miR-18a. Moreover, it is also possible that because the cluster comprises of six miRNA with several predicted target genes, *Pten* is simply one of many genes simultaneously targeted during the course of inflammation. Nevertheless, our results show a clear induction of the miR-17-92 cluster and specifically the suppression of *Pten* by miR-18a.

The anti-inflammatory and immunosuppressive effects of THC are diverse and function effectively to abrogate a number of inflammatory processes. For example, THC has previously been reported to prevent the development of a murine model of multiple sclerosis and colitis (Jamontt *et al.*, 2010; Lyman *et al.*, 1989). In a mouse model of Con-A induced hepatitis, we have demonstrated its ability to act on acute inflammation, where it not only decreased the production of inflammatory cytokines, but also reduced cellular proliferation(Hegde *et al.*, 2008). Consistent with these reports, our data demonstrate a significant reduction in infiltrating immune cells in the lung, blunting of cytokines as early as 3 hours after SEB exposure and more astonishingly, the 100% survival of mice.

We have previously demonstrated that THC's anti-inflammatory properties can be credited, in part, to the induction of immunosuppressive cells such as regulatory T-cells (T-regs) and myeloid derived suppressor cells (MDSC) (Hegde *et al.*, 2008; Nagarkatti *et al.*). Recently, we have identified a novel role for THC in modulating miRNA involved in the development of MDSCs (Nagarkatti *et al.*), a finding that could shed mechanistic light on THC's mode of action . Thus, we rationalized that THC could potentially exert its strong anti-inflammatory activities by modulating SEB-induced miRNA. Our present findings validate our hypothesis and we observed a potent down-regulation of the miR-17-92 cluster. Inversely, our results demonstrate the derepression of *Pten* suggesting that

THC, via the down regulation of the cluster might be an inhibitor of the PI3K/AKT pathway. Interestingly, earlier studies in cancer models have demonstrated that THC disrupts the PI3K/AKT signaling pathway (Greenhough *et al.*, 2007; Leelawat *et al.*, 2010). However, in light of our current observation that it modulates key miRNA, its anti-inflammatory properties via its role as a PI3K/AKT inhibitor, is made more evident.

The disruption of the PI3K/AKT/mTOR axis using AKT inhibitors has been previously reported to decrease cellular proliferation, induce apoptosis and decrease IFN-γ production (Mandal *et al.*, 2005; Shin *et al.*, 2002). Further, Rapamycin, an inhibitor of mTORC1, specifically diminishes SEB-induced IL-2 ,IFN-γ and T-cell proliferation (Krakauer *et al.*, ; Krakauer *et al.*). In line with these reports, our results also demonstrated decreased cellular proliferation and IFN-γ production with THC treatment. Additionally, the PI3K/AKT activation of PTEN deficient T-cells, led to the suppression of CD4+Foxp3+ T-cells, which was reversed with PI3K/AKT inhibition (Sauer *et al.*, 2008). Similarly, we observed the induction of T-regulatory cells in the lung upon THC treatment, further confirming that THC is an inhibitor of the PI3K/AKT signaling pathway, and that part of its mechanism involves down-regulation of the miR-17-92 cluster, particularly miR-18a.

Taken together, our data demonstrate that THC is a strong anti-inflammatory agent capable of rescuing mice from SEB-mediated toxicity and death. By affecting the SEB-induced miR-17-92 cluster, it restores *Pten,* and enables the proper regulation of the PI3K/AKT signaling pathway. Consequently, it reduces cellular proliferation, diminishes the production of pro-inflammatory cytokine and induces T-regulatory cells (Figure 4.7).

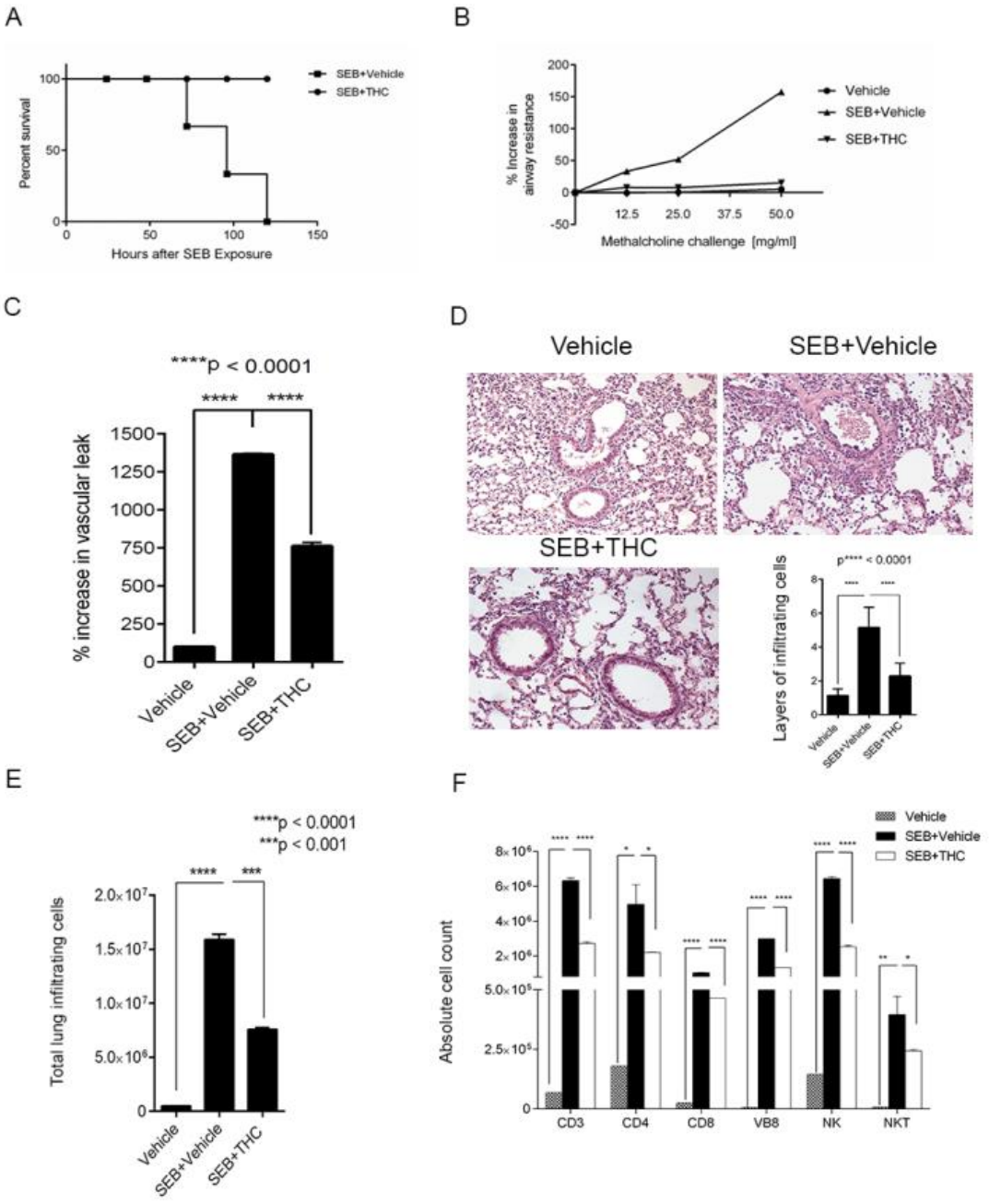

Figure 4.1. THC prevents mortality and alleviates SEB-induced inflammation in the lung (A) Survival curve of mice receiving SEB+ Vehicle when compared to mice treated with SEB+THC. (B) Measurement of airway hyperreactivity [sRAW] using whole body plethysmography. Mice were acclimatized in a two-chamber plethysmograph tube and

were first exposed to aerosolized saline followed by increasing doses of methalcholine. Data was recorded for 4 minutes and the sRAW value was calculated over saline. (C) Assessment of vascular leak in the lungs was carried out 72 hours after SEB exposure. Mice were injected with 1% Evans blue i.v. Two hours later, the lungs were perfused and placed in formamide at 37 °C for 48 hours. Percent vascular leak was calculated by measuring absorbance at 620 nm. (D) Total number of infiltrating mononuclear cells were determined 72 hours after SEB exposure. Lungs were mechanically macerated and the suspension was placed on a Ficoll gradient. Mononuclear cells thus obtained, were counted by trypan blue exclusion method and enumerated. (E) Histopathological examination of lungs as determined by Hemotoxylin and Eosin staining. Arrows indicate infiltrating immune cells around a capillary. Total layers of infiltrating cells were counted around 10 different capillaries and enumerated in the bar graph. (F) Flow cytometric analysis to identify immune subsets was carried out. Mononuclear cells were stained with antibodies against T-cells (CD3), T-helper cells (CD4), cytotoxic T-cells (CD8), Vβ8-region of the T-cell receptor (Vβ8), natural killer cells (NK) and natural killer T-cells (NKT). Absolute cell numbers of various subpopulations was calculated using the formula: Total number of cells isolated from the lungs x percent of specific cells/100, and plotted as a bar graph. Bar graphs summarize the means ±SEM from 3-5 independent experiments.

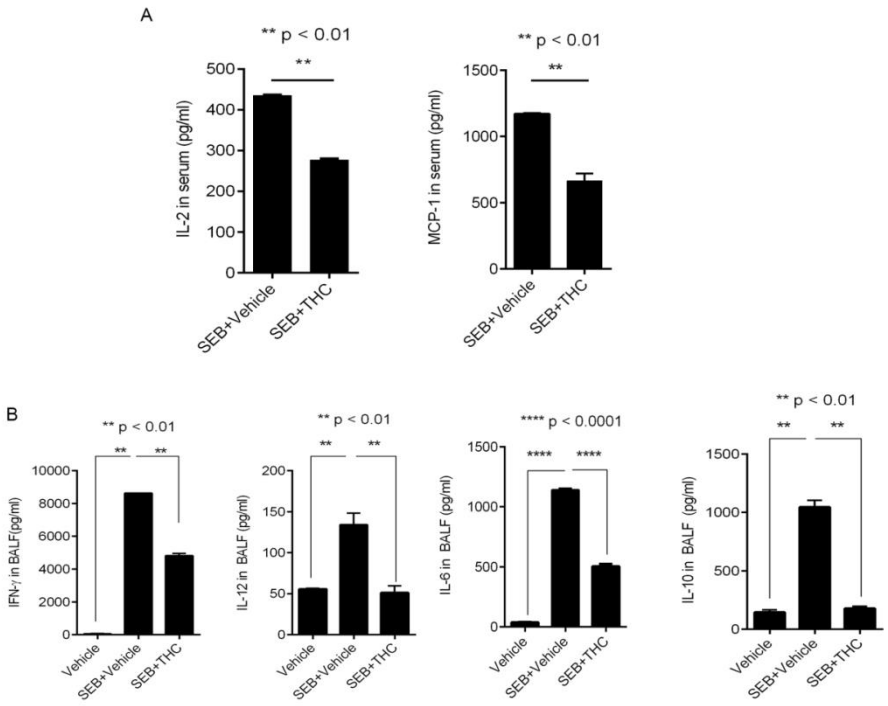

Figure 4.2: THC decreases SEB-induced cytokine secretion (A) Measurement of early cytokines, IL-2 and MCP-1 in serum 3 hours after SEB exposure. (B) Cytokine measurement of IFN-γ, IL-12, IL-10 and IL-6 in the broncheoalveloar lavage fluid (BALF). All cytokines concentrations were determined using Enzyme linked immunosorbent assay (ELISA). Bar graphs summarize the means ±SEM from 3-5 independent experiments. For cytokines from the serum, unpaired, two-tailed t-test was used to determine significance from SEB.

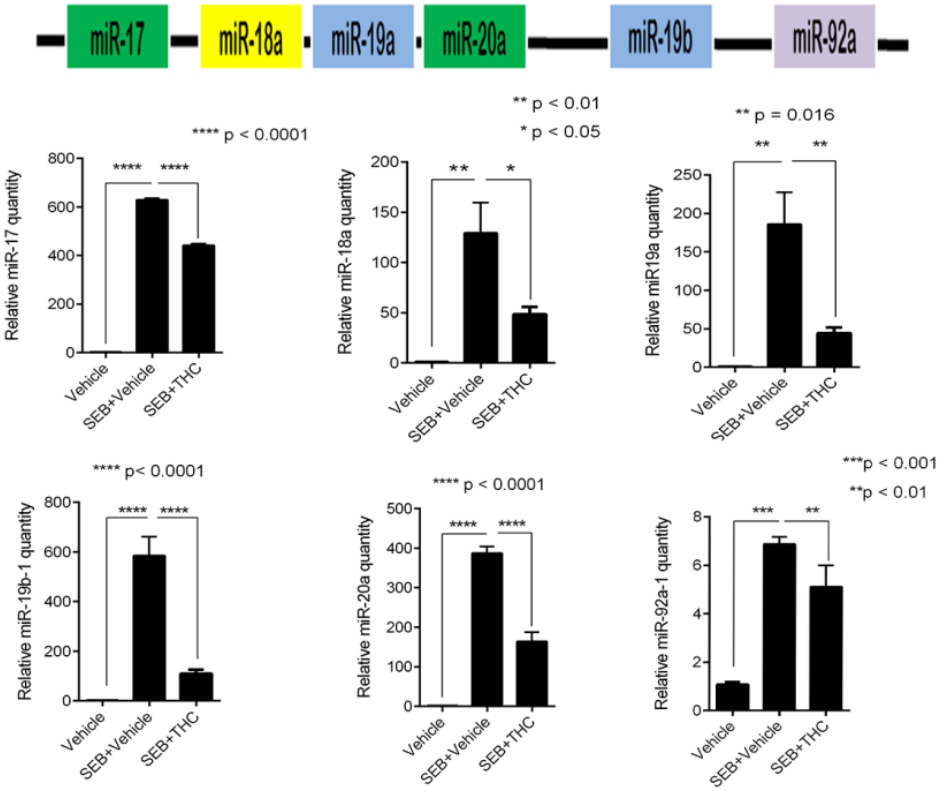

Figure 4.3: THC significantly down-regulates SEB-induced expression of the miR-17-92 cluster. Real time (RT) PCR validation of the individual miRNA (miR-17, miR-18a, miR-19a, miR-19b-1, miR20a and miR-92a-1) of the miR-17-92 cluster obtained from lung infiltrating mononuclear cells. Data are normalized to internal control Snord_96a. Statistical significance was assessed using ANOVA, tukey's multiple comparison test.

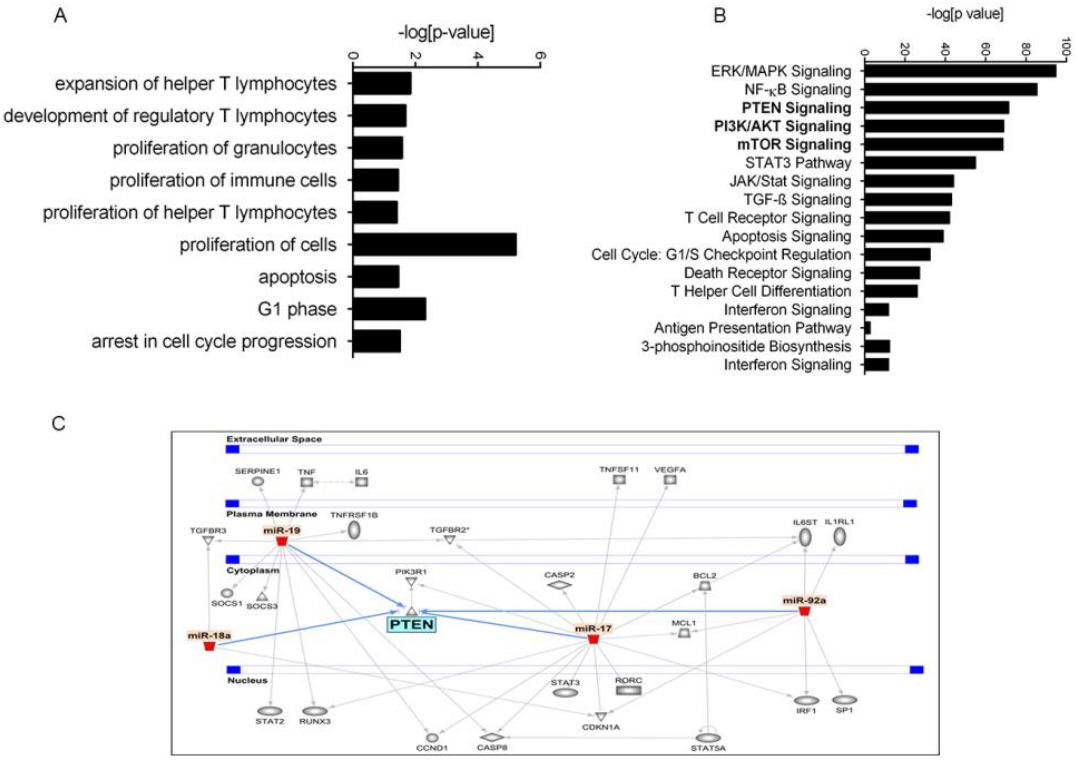

Figure 4.4: The involvement of the miR-17-92 cluster in key biological pathways (A) Graphical representation of the biological functions associated with significantly upregulated SEB-induced miRNA as determined by Ingenuity ® pathway analysis (IPA) (B) Canonical pathways associated with miRNA target genes. IPA was used to filter highly predicted and experimentally observed targets of only the significantly upregulated miRNA in response to SEB. A graphical representation of the significant (fisher's exact test) pathways of these particular target genes was generated. (C) IPA pathway demonstrating the convergence of the members of the miR-17-92 cluster on *Pten.*

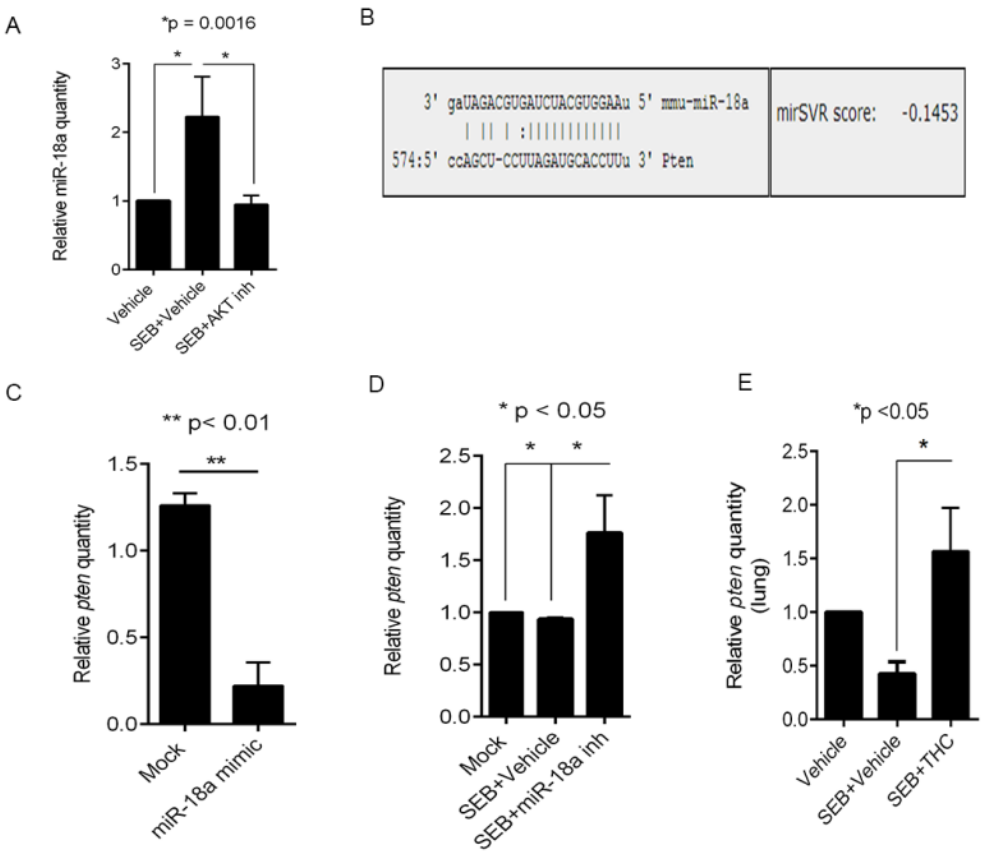

Figure 4.5: **miR-18a targets *Pten*, an inhibitor of the PI3K/AKT pathway.** (A) RT-PCR of miR-18a levels in splenocytes that were activated with SEB and treated with AKT inhibitor. miRNA levels measured relative to Snord_96a internal control (B) Target prediction of miR-18a using miRanda (www.microrna.org), showing the alignment of the mature miRNA to the 3' UTR of *Pten* mRNA. The miRSVR score represents the probability of mRNA target down-regulation and the cut-off for a good score was set at ≤ -0.01. (C) RT-PCR quantification of miR-18a and its target *Pten*. Splenocytes were transfected with 40 nm of miR-18a mimic for 24 hours. (D) RT-PCR quantification of miR-18a and *Pten* after transfection with a synthetic miR-18a inhibitor. Splenocytes that were activated with SEB (1μg/ml) were also transfected with miR-18a inhibitor for 24 hours. (E) Real-time PCR quantification of *Pten* levels in lung infiltrating mononuclear cells. All miRNA levels were measured relative to internal control Snord_96a and mRNA levels were normalized to β-actin. Statistical significance was assessed using ANOVA, tukey's multiple comparison test.

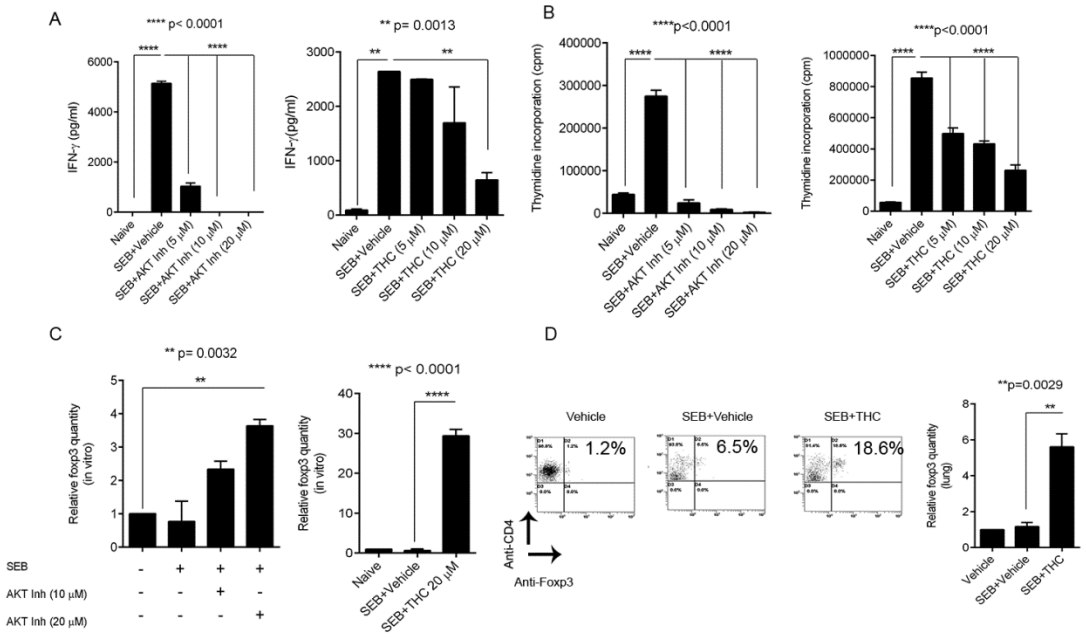

Figure 4.6 : THC is an inhibitor of the AKT pathway and leads to the induction of CD4+Foxp3+ T-regulatory cells (A) IFN-γ levels in supernatants of splenocytes that were activated with SEB and treated with varying doses of THC or AKT inhibitor. (B) Thymidine incorporation to measure proliferation of splenocytes activated with SEB or treated with the indicated doses of THC or AKT inhibitor. (C) RT-PCR of Foxp3 levels in splenocytes that were treated either with THC or AKT. mRNA levels measured relative to β-actin. (D) Flow cytometric analysis of CD4+Foxp3+ T-regulatory cells in lung infiltrating mononuclear cells for the groups indicated. The bar graph represents the RT-PCR expression of Foxp3 in lung infiltrating mononuclear cells. In all in vitro experiments, Splenocytes were activated with 1μg/ml SEB. Statistical significance was assessed using ANOVA, tukey's multiple comparison test.

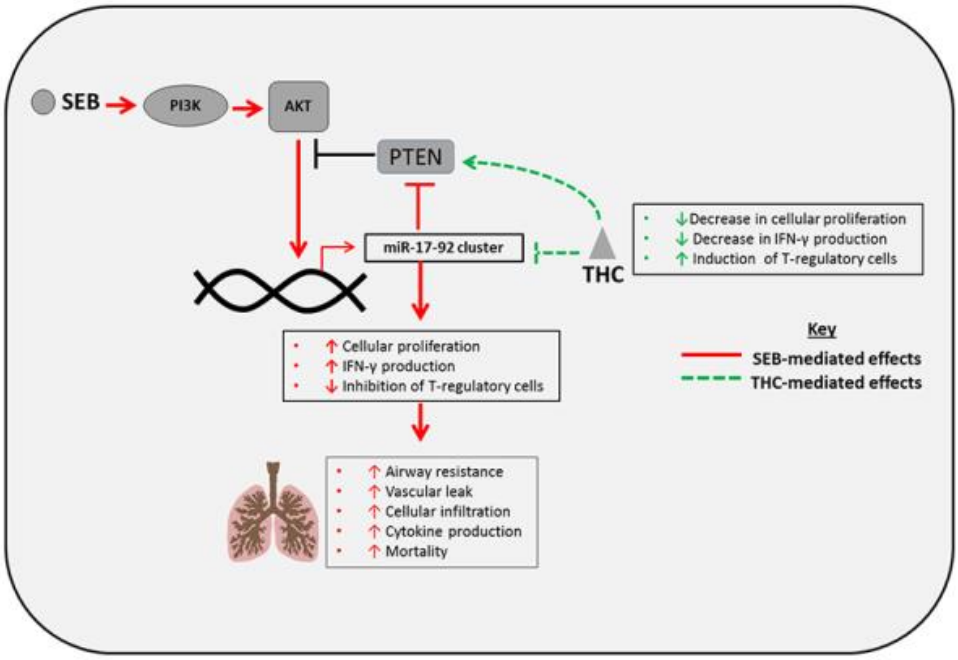

Figure 4.7: Schematic of the proposed working model. SEB administration leads to the activation of the PI3K/AKT pathway via the induction of the miR-17-92 cluster and the subsequent down-regulation of *Pten*. As a result, SEB exposure leads to increased cellular proliferation, cytokine production, pulmonary damage and the acute mortality. The down regulation of the cluster by THC restores *Pten* levels and allows for the inhibition of the PI3K/AKT axis. This leads to attenuation of acute inflammatory lung injury and induction of T-regulatory cells, which together prevent SEB-induced mortality.

CHAPTER V: SUMMARY AND CONCLUSION

It is evident that the scientific community is making great strides in the study of miRNA. In nearly a decade, these novel regulators of gene expression have been recognized for their ability to control almost every biological process. In naïve conditions, they exist to maintain homeostasis, influence cellular development and commitment to specific lineages. In stress and inflammation, their impact is made even more apparent, as their massive dysregulation contributes significantly to worsening of disease. miRNA biology is made complex given that a single miRNA can have hundreds of target genes and that inflammatory conditions lead to the alteration of a number of miRNA. Thus, it is imperative that we first present an overview of the importance of the miRNA signaling pathways and then begin to dissect the involvement of individual miRNA. In doing so, we can identify unique miRNA biomarkers and aim to develop therapeutic agents that directly or indirectly target miRNA.

In the studies undertaken here, we have explored the impact of SEB exposure in mouse models of acute inflammatory lung injury. Although, previous studies have demonstrated that SEB, a superantigen causes an exaggerated immune response and subsequent damage, the molecular mechanism behind its actions were attributed to inflammatory signaling pathways downstream of TCR activation. We hypothesized that if inflammatory cues are known to induce miRNA, then SEB-induced antigenic stimulation

should also lead to expression of miRNA. Indeed, our studies in two mouse models of SEB-induced lung injury confirmed the dysregulation of miRNA. *In silico* analysis revealed that these miRNA perform biological functions pertaining to cellular proliferation, T-cell activation, and cytokine production. The interaction between miRNA and their respective target genes was further found to involve the activation of key inflammatory signaling pathways known to be associated with SEB activation experimentally. Additionally, we focused on the role of highly overexpressed miRNA to determine its involvement to SEB-mediated damage. In the less severe form of acute inflammation, we found that miR-155 and its respective target gene *Socs1* could explain the copious amounts of IFN-γ produced and the subsequent damage inflicted to the lung. In the model that resulted in the death of mice, we observed that a miRNA cluster (miR-17-92) commonly studied in cancer, was activated following SEB exposure. Identification of the role of this cluster in inflammation, led us to the SEB mediated activation of the PI3K/AKT signaling pathway via the suppression of *Pten*, a negative regulator of AKT signaling. We also found that overexpression of miR-132 was linked with repression of *Foxo3*, a regulator of T-cell proliferation and activation.

Since SEB is a strong pro-inflammatory inducing agent, we sought to counter its effects with an equally potent anti-inflammatory compound, THC. In choosing this particular therapeutic agent, we were aware that some of its previously studied functions included its ability to decrease inflammatory cytokines, inhibit cellular proliferation and induce immunosuppressive cells such as the MDSCs or T-regs. Indeed, we demonstrated that THC could prevent SEB-triggered acute mortality of mice by ameliorating inflammation

and inducing T-regs, however, for the first time we established that it does so by modulating miRNA. In conclusion, our studies have helped understand that the miRNA control of gene expression lies at the heart of pro-inflammatory (SEB-induced) and anti-inflammatory (THC-mediated) immune responses. By further studying the role of these small RNA molecules and their dynamic interaction with their target genes, we can better develop miRNA related therapeutics to prevent and treat inflammatory diseases.

REFERENCES

(2011). In *Guide for the Care and Use of Laboratory Animals*. Washington (DC).

ALOUF, J.E. & MULLER-ALOUF, H. (2003). Staphylococcal and streptococcal superantigens: molecular, biological and clinical aspects. *Int J Med Microbiol*, **292,** 429-40.

ARCHER, G.L. (1998). Staphylococcus aureus: a well-armed pathogen. *Clin Infect Dis*, **26,** 1179-81.

ARGUDIN, M.A., MENDOZA, M.C. & RODICIO, M.R. (2010). Food poisoning and Staphylococcus aureus enterotoxins. *Toxins (Basel)*, **2,** 1751-73.

ASSENMACHER, M., LOHNING, M., SCHEFFOLD, A., MANZ, R.A., SCHMITZ, J. & RADBRUCH, A. (1998). Sequential production of IL-2, IFN-gamma and IL-10 by individual staphylococcal enterotoxin B-activated T helper lymphocytes. *Eur J Immunol*, **28,** 1534-43.

BALA, S., MARCOS, M., KODYS, K., CSAK, T., CATALANO, D., MANDREKAR, P. & SZABO, G. Up-regulation of microRNA-155 in macrophages contributes to increased tumor necrosis factor {alpha} (TNF{alpha}) production via increased mRNA half-life in alcoholic liver disease. *J Biol Chem*, **286,** 1436-44.

BALABAN, N. & RASOOLY, A. (2000). Staphylococcal enterotoxins. *Int J Food Microbiol*, **61,** 1-10.

BALTIMORE, D., BOLDIN, M.P., O'CONNELL, R.M., RAO, D.S. & TAGANOV, K.D. (2008). MicroRNAs: new regulators of immune cell development and function. *Nat Immunol*, **9,** 839-45.

BAVARI, S. & ULRICH, R.G. (1995). Staphylococcal enterotoxin A and toxic shock syndrome toxin compete with CD4 for human major histocompatibility complex class II binding. *Infect Immun*, **63,** 423-9.

BERNARD, G.R., LUCE, J.M., SPRUNG, C.L., RINALDO, J.E., TATE, R.M., SIBBALD, W.J., KARIMAN, K., HIGGINS, S., BRADLEY, R., METZ, C.A. & ET AL. (1987). High-dose corticosteroids in patients with the adult respiratory distress syndrome. *N Engl J Med*, **317,** 1565-70.

BETTE, M., SCHAFER, M.K., VAN ROOIJEN, N., WEIHE, E. & FLEISCHER, B. (1993). Distribution and kinetics of superantigen-induced cytokine gene expression in mouse spleen. *J Exp Med*, **178,** 1531-9.

BUSBEE, P.B., NAGARKATTI, M. & NAGARKATTI, P.S. Natural indoles, indole-3-carbinol and 3,3'-diindolymethane, inhibit T cell activation by staphylococcal enterotoxin B through epigenetic regulation involving HDAC expression. *Toxicol Appl Pharmacol*, **274,** 7-16.

CAI, Y., YU, X., HU, S. & YU, J. (2009). A brief review on the mechanisms of miRNA regulation. *Genomics Proteomics Bioinformatics*, **7,** 147-54.

CALIN, G.A., DUMITRU, C.D., SHIMIZU, M., BICHI, R., ZUPO, S., NOCH, E., ALDLER, H., RATTAN, S., KEATING, M., RAI, K., RASSENTI, L., KIPPS, T., NEGRINI, M., BULLRICH, F. & CROCE, C.M. (2002). Frequent deletions and down-regulation of

micro- RNA genes miR15 and miR16 at 13q14 in chronic lymphocytic leukemia. *Proc Natl Acad Sci U S A*, **99,** 15524-9.

CARDOSO, A.L., GUEDES, J.R., PEREIRA DE ALMEIDA, L. & PEDROSO DE LIMA, M.C. miR-155 modulates microglia-mediated immune response by down-regulating SOCS-1 and promoting cytokine and nitric oxide production. *Immunology*, **135,** 73-88.

CHEN, J., FEILOTTER, H.E., PARE, G.C., ZHANG, X., PEMBERTON, J.G., GARADY, C., LAI, D., YANG, X. & TRON, V.A. MicroRNA-193b represses cell proliferation and regulates cyclin D1 in melanoma. *Am J Pathol*, **176,** 2520-9.

CHIANG, K., LIU, H. & RICE, A.P. miR-132 enhances HIV-1 replication. *Virology*, **438,** 1-4.

CHOI, Y.W., KOTZIN, B., HERRON, L., CALLAHAN, J., MARRACK, P. & KAPPLER, J. (1989). Interaction of Staphylococcus aureus toxin "superantigens" with human T cells. *Proc Natl Acad Sci U S A*, **86,** 8941-5.

DAI, R. & AHMED, S.A. MicroRNA, a new paradigm for understanding immunoregulation, inflammation, and autoimmune diseases. *Transl Res*, **157,** 163-79.

DAI, R. & AHMED, S.A. (2011). MicroRNA, a new paradigm for understanding immunoregulation, inflammation, and autoimmune diseases. *Transl Res*, **157,** 163-79.

DARENBERG, J., SODERQUIST, B., NORMARK, B.H. & NORRBY-TEGLUND, A. (2004). Differences in potency of intravenous polyspecific immunoglobulin G against streptococcal and staphylococcal superantigens: implications for therapy of toxic shock syndrome. *Clin Infect Dis*, **38,** 836-42.

DaSilva, L., Welcher, B.C., Ulrich, R.G., Aman, M.J., David, C.S. & Bavari, S. (2002). Humanlike immune response of human leukocyte antigen-DR3 transgenic mice to staphylococcal enterotoxins: a novel model for superantigen vaccines. *J Infect Dis*, **185,** 1754-60.

Davidson-Moncada, J., Papavasiliou, F.N. & Tam, W. MicroRNAs of the immune system: roles in inflammation and cancer. *Ann N Y Acad Sci*, **1183,** 183-94.

Davidson-Moncada, J., Papavasiliou, F.N. & Tam, W. (2010). MicroRNAs of the immune system: roles in inflammation and cancer. *Ann N Y Acad Sci*, **1183,** 183-94.

Delisle, J.S., Giroux, M., Boucher, G., Landry, J.R., Hardy, M.P., Lemieux, S., Jones, R.G., Wilhelm, B.T. & Perreault, C. The TGF-beta-Smad3 pathway inhibits CD28-dependent cell growth and proliferation of CD4 T cells. *Genes Immun*, **14,** 115-26.

DeVries, A.S., Lesher, L., Schlievert, P.M., Rogers, T., Villaume, L.G., Danila, R. & Lynfield, R. (2011). Staphylococcal toxic shock syndrome 2000-2006: epidemiology, clinical features, and molecular characteristics. *PLoS One*, **6,** e22997.

Dinges, M.M., Orwin, P.M. & Schlievert, P.M. (2000). Exotoxins of Staphylococcus aureus. *Clin Microbiol Rev*, **13,** 16-34, table of contents.

Do, Y., McKallip, R.J., Nagarkatti, M. & Nagarkatti, P.S. (2004). Activation through cannabinoid receptors 1 and 2 on dendritic cells triggers NF-kappaB-dependent apoptosis: novel role for endogenous and exogenous cannabinoids in immunoregulation. *J Immunol*, **173,** 2373-82.

FAULKNER, L., COOPER, A., FANTINO, C., ALTMANN, D.M. & SRISKANDAN, S. (2005). The mechanism of superantigen-mediated toxic shock: not a simple Th1 cytokine storm. *J Immunol*, **175,** 6870-7.

FELDER, C.C. & GLASS, M. (1998). Cannabinoid receptors and their endogenous agonists. *Annu Rev Pharmacol Toxicol*, **38,** 179-200.

FLEISCHER, B., GERARDY-SCHAHN, R., METZROTH, B., CARREL, S., GERLACH, D. & KOHLER, W. (1991). An evolutionary conserved mechanism of T cell activation by microbial toxins. Evidence for different affinities of T cell receptor-toxin interaction. *J Immunol*, **146,** 11-7.

FLORQUIN, S., AMRAOUI, Z. & GOLDMAN, M. (1995). T cells made deficient in interleukin-2 production by exposure to staphylococcal enterotoxin B in vivo are primed for interferon-gamma and interleukin-10 secretion. *Eur J Immunol*, **25,** 1148-53.

FOSTER, T.J. (2004). The Staphylococcus aureus "superbug". *J Clin Invest*, **114,** 1693-6.

FRANK, D.N., FEAZEL, L.M., BESSESEN, M.T., PRICE, C.S., JANOFF, E.N. & PACE, N.R. (2010). The human nasal microbiota and Staphylococcus aureus carriage. *PLoS One*, **5,** e10598.

GOLDBACH-MANSKY, R., KING, P.D., TAYLOR, A.P. & DUPONT, B. (1992). A co-stimulatory role for CD28 in the activation of CD4+ T lymphocytes by staphylococcal enterotoxin B. *Int Immunol*, **4,** 1351-60.

GORDON, R.J. & LOWY, F.D. (2008). Pathogenesis of methicillin-resistant Staphylococcus aureus infection. *Clin Infect Dis*, **46 Suppl 5,** S350-9.

GREEN, J.M., TURKA, L.A., JUNE, C.H. & THOMPSON, C.B. (1992). CD28 and staphylococcal enterotoxins synergize to induce MHC-independent T-cell proliferation. *Cell Immunol*, **145,** 11-20.

GREENHOUGH, A., PATSOS, H.A., WILLIAMS, A.C. & PARASKEVA, C. (2007). The cannabinoid delta(9)-tetrahydrocannabinol inhibits RAS-MAPK and PI3K-AKT survival signalling and induces BAD-mediated apoptosis in colorectal cancer cells. *Int J Cancer*, **121,** 2172-80.

GUO, H., INGOLIA, N.T., WEISSMAN, J.S. & BARTEL, D.P. (2010). Mammalian microRNAs predominantly act to decrease target mRNA levels. *Nature*, **466,** 835-40.

HEDRICK, S.M., HESS MICHELINI, R., DOEDENS, A.L., GOLDRATH, A.W. & STONE, E.L. FOXO transcription factors throughout T cell biology. *Nat Rev Immunol*, **12,** 649-61.

HEGDE, V.L., HEGDE, S., CRAVATT, B.F., HOFSETH, L.J., NAGARKATTI, M. & NAGARKATTI, P.S. (2008). Attenuation of experimental autoimmune hepatitis by exogenous and endogenous cannabinoids: involvement of regulatory T cells. *Mol Pharmacol*, **74,** 20-33.

HERMAN, A., KAPPLER, J.W., MARRACK, P. & PULLEN, A.M. (1991). Superantigens: mechanism of T-cell stimulation and role in immune responses. *Annu Rev Immunol*, **9,** 745-72.

HUANG, W. & KOLLER, L.D. (1998). Superantigen activation and kinetics of cytokines in the Long-Evans rat. *Immunology*, **95,** 331-8.

HURLEY, J.M., SHIMONKEVITZ, R., HANAGAN, A., ENNEY, K., BOEN, E., MALMSTROM, S., KOTZIN, B.L. & MATSUMURA, M. (1995). Identification of class II major histocompatibility complex and T cell receptor binding sites in the superantigen toxic shock syndrome toxin 1. *J Exp Med*, **181,** 2229-35.

HUZELLA, L.M., BUCKLEY, M.J., ALVES, D.A., STILES, B.G. & KRAKAUER, T. (2009). Central roles for IL-2 and MCP-1 following intranasal exposure to SEB: a new mouse model. *Res Vet Sci*, **86,** 241-7.

JAMONTT, J.M., MOLLEMAN, A., PERTWEE, R.G. & PARSONS, M.E. (2010). The effects of Delta-tetrahydrocannabinol and cannabidiol alone and in combination on damage, inflammation and in vitro motility disturbances in rat colitis. *Br J Pharmacol*, **160,** 712-23.

JIANG, S., ZHANG, H.W., LU, M.H., HE, X.H., LI, Y., GU, H., LIU, M.F. & WANG, E.D. MicroRNA-155 functions as an OncomiR in breast cancer by targeting the suppressor of cytokine signaling 1 gene. *Cancer Res*, **70,** 3119-27.

KISSNER, T.L., RUTHEL, G., ALAM, S., ULRICH, R.G., FERNANDEZ, S. & SAIKH, K.U. (2011). Activation of MyD88 signaling upon staphylococcal enterotoxin binding to MHC class II molecules. *PLoS One*, **6,** e15985.

KISSNER, T.L., RUTHEL, G., ALAM, S., ULRICH, R.G., FERNANDEZ, S. & SAIKH, K.U. Activation of MyD88 signaling upon staphylococcal enterotoxin binding to MHC class II molecules. *PLoS One*, **6,** e15985.

KLEIN, T.W. (2005). Cannabinoid-based drugs as anti-inflammatory therapeutics. *Nat Rev Immunol*, **5,** 400-11.

KLEIN, T.W., NEWTON, C., ZHU, W., DAAKA, Y. & FRIEDMAN, H. (1995). delta 9-Tetrahydrocannabinol, cytokines, and immunity to Legionella pneumophila. *Proc Soc Exp Biol Med,* **209,** 205-12.

KOZONO, H., PARKER, D., WHITE, J., MARRACK, P. & KAPPLER, J. (1995). Multiple binding sites for bacterial superantigens on soluble class II MHC molecules. *Immunity,* **3,** 187-96.

KRAKAUER, T. PI3K/Akt/mTOR, a pathway less recognized for staphylococcal superantigen-induced toxicity. *Toxins (Basel),* **4,** 1343-66.

KRAKAUER, T. Update on staphylococcal superantigen-induced signaling pathways and therapeutic interventions. *Toxins (Basel),* **5,** 1629-54.

KRAKAUER, T. & BUCKLEY, M. (2006). Dexamethasone attenuates staphylococcal enterotoxin B-induced hypothermic response and protects mice from superantigen-induced toxic shock. *Antimicrob Agents Chemother,* **50,** 391-5.

KRAKAUER, T. & BUCKLEY, M. Intranasal rapamycin rescues mice from staphylococcal enterotoxin B-induced shock. *Toxins (Basel),* **4,** 718-28.

KRAKAUER, T., BUCKLEY, M. & FISHER, D. Murine models of staphylococcal enterotoxin B-induced toxic shock. *Mil Med,* **175,** 917-22.

KRAKAUER, T., BUCKLEY, M., ISSAQ, H.J. & FOX, S.D. Rapamycin protects mice from staphylococcal enterotoxin B-induced toxic shock and blocks cytokine release in vitro and in vivo. *Antimicrob Agents Chemother,* **54,** 1125-31.

KREBS, D.L. & HILTON, D.J. (2001). SOCS proteins: negative regulators of cytokine signaling. *Stem Cells,* **19,** 378-87.

KUEHNERT, M.J., KRUSZON-MORAN, D., HILL, H.A., MCQUILLAN, G., MCALLISTER, S.K., FOSHEIM, G., MCDOUGAL, L.K., CHAITRAM, J., JENSEN, B., FRIDKIN, S.K., KILLGORE, G. & TENOVER, F.C. (2006). Prevalence of Staphylococcus aureus nasal colonization in the United States, 2001-2002. *J Infect Dis*, **193,** 172-9.

KUROWSKA-STOLARSKA, M., ALIVERNINI, S., BALLANTINE, L.E., ASQUITH, D.L., MILLAR, N.L., GILCHRIST, D.S., REILLY, J., IERNA, M., FRASER, A.R., STOLARSKI, B., MCSHARRY, C., HUEBER, A.J., BAXTER, D., HUNTER, J., GAY, S., LIEW, F.Y. & MCINNES, I.B. MicroRNA-155 as a proinflammatory regulator in clinical and experimental arthritis. *Proc Natl Acad Sci U S A*, **108,** 11193-8.

LARKIN, E.A., CARMAN, R.J., KRAKAUER, T. & STILES, B.G. (2009). Staphylococcus aureus: the toxic presence of a pathogen extraordinaire. *Curr Med Chem*, **16,** 4003-19.

LARKIN, E.A., STILES, B.G. & ULRICH, R.G. Inhibition of toxic shock by human monoclonal antibodies against staphylococcal enterotoxin B. *PLoS One*, **5,** e13253.

LEE, C.L., LEE, S.H., JAY, F.T. & ROZEE, K.R. (1990). Immunobiological study of interferon-gamma-producing cells after staphylococcal enterotoxin B stimulation. *Immunology*, **70,** 94-9.

LEELAWAT, S., LEELAWAT, K., NARONG, S. & MATANGKASOMBUT, O. (2010). The dual effects of delta(9)-tetrahydrocannabinol on cholangiocarcinoma cells: anti-invasion activity at low concentration and apoptosis induction at high concentration. *Cancer Invest*, **28,** 357-63.

LEWIS, B.P., BURGE, C.B. & BARTEL, D.P. (2005). Conserved seed pairing, often flanked by adenosines, indicates that thousands of human genes are microRNA targets. *Cell*, **120,** 15-20.

LI, J., WAN, Y., GUO, Q., ZOU, L., ZHANG, J., FANG, Y., ZHANG, J., ZHANG, J., FU, X., LIU, H., LU, L. & WU, Y. Altered microRNA expression profile with miR-146a upregulation in CD4+ T cells from patients with rheumatoid arthritis. *Arthritis Res Ther*, **12,** R81.

LIN, L., HRON, J.D. & PENG, S.L. (2004). Regulation of NF-kappaB, Th activation, and autoinflammation by the forkhead transcription factor Foxo3a. *Immunity*, **21,** 203-13.

LINDSAY, M.A. (2008). microRNAs and the immune response. *Trends Immunol*, **29,** 343-51.

LINSLEY, P.S. & LEDBETTER, J.A. (1993). The role of the CD28 receptor during T cell responses to antigen. *Annu Rev Immunol*, **11,** 191-212.

LIU, S.Q., JIANG, S., LI, C., ZHANG, B. & LI, Q.J. miR-17-92 Cluster Targets Phosphatase and Tensin Homology and Ikaros Family Zinc Finger 4 to Promote TH17-mediated Inflammation. *J Biol Chem*, **289,** 12446-56.

LOWY, F.D. (1998). Staphylococcus aureus infections. *N Engl J Med*, **339,** 520-32.

LUNGU, G., STOICA, G. & AMBRUS, A. MicroRNA profiling and the role of microRNA-132 in neurodegeneration using a rat model. *Neurosci Lett*, **553,** 153-8.

LYMAN, W.D., SONETT, J.R., BROSNAN, C.F., ELKIN, R. & BORNSTEIN, M.B. (1989). Delta 9-tetrahydrocannabinol: a novel treatment for experimental autoimmune encephalomyelitis. *J Neuroimmunol*, **23,** 73-81.

MANDAL, M., KIM, S., YOUNES, M.N., JASSER, S.A., EL-NAGGAR, A.K., MILLS, G.B. & MYERS, J.N. (2005). The Akt inhibitor KP372-1 suppresses Akt activity and cell proliferation and induces apoptosis in thyroid cancer cells. *Br J Cancer*, **92,** 1899-905.

MATTES, J., COLLISON, A., PLANK, M., PHIPPS, S. & FOSTER, P.S. (2009). Antagonism of microRNA-126 suppresses the effector function of TH2 cells and the development of allergic airways disease. *Proc Natl Acad Sci U S A*, **106,** 18704-9.

MATTHYS, P., MITERA, T., HEREMANS, H., VAN DAMME, J. & BILLIAU, A. (1995). Anti-gamma interferon and anti-interleukin-6 antibodies affect staphylococcal enterotoxin B-induced weight loss, hypoglycemia, and cytokine release in D-galactosamine-sensitized and unsensitized mice. *Infect Immun*, **63,** 1158-64.

MEDURI, G.U., HEADLEY, A.S., GOLDEN, E., CARSON, S.J., UMBERGER, R.A., KELSO, T. & TOLLEY, E.A. (1998). Effect of prolonged methylprednisolone therapy in unresolving acute respiratory distress syndrome: a randomized controlled trial. *Jama*, **280,** 159-65.

MERKENSCHLAGER, M. & VON BOEHMER, H. PI3 kinase signalling blocks Foxp3 expression by sequestering Foxo factors. *J Exp Med*, **207,** 1347-50.

MIETHKE, T., DUSCHEK, K., WAHL, C., HEEG, K. & WAGNER, H. (1993). Pathogenesis of the toxic shock syndrome: T cell mediated lethal shock caused by the superantigen TSST-1. *Eur J Immunol*, **23,** 1494-500.

MIETHKE, T., WAHL, C., HEEG, K., ECHTENACHER, B., KRAMMER, P.H. & WAGNER, H. (1992). T cell-mediated lethal shock triggered in mice by the superantigen

staphylococcal enterotoxin B: critical role of tumor necrosis factor. *J Exp Med*, **175,** 91-8.

MIYATA, A., NATSUAKI, M. & YAMANISHI, K. (2008). Staphylococcal enterotoxin B enhances a flare-up reaction of murine contact hypersensitivity through up-regulation of interferon-gamma. *Exp Dermatol*, **17,** 843-8.

MUHIE, S., HAMMAMIEH, R., CUMMINGS, C., YANG, D. & JETT, M. Transcriptome characterization of immune suppression from battlefield-like stress. *Genes Immun*, **14,** 19-34.

MURUGAIYAN, G., BEYNON, V., MITTAL, A., JOLLER, N. & WEINER, H.L. Silencing microRNA-155 ameliorates experimental autoimmune encephalomyelitis. *J Immunol*, **187,** 2213-21.

NAGARKATTI, M., RIEDER, S.A., HEGDE, V.L., KANADA, S. & NAGARKATTI, P. Do cannabinoids have a therapeutic role in transplantation? *Trends Pharmacol Sci*, **31,** 345-50.

NAGARKATTI, P., PANDEY, R., RIEDER, S.A., HEGDE, V.L. & NAGARKATTI, M. (2009). Cannabinoids as novel anti-inflammatory drugs. *Future Med Chem*, **1,** 1333-49.

NEUMANN, B., ENGELHARDT, B., WAGNER, H. & HOLZMANN, B. (1997). Induction of acute inflammatory lung injury by staphylococcal enterotoxin B. *J Immunol*, **158,** 1862-71.

O'CONNELL, R.M., KAHN, D., GIBSON, W.S., ROUND, J.L., SCHOLZ, R.L., CHAUDHURI, A.A., KAHN, M.E., RAO, D.S. & BALTIMORE, D. (2010). MicroRNA-155 promotes autoimmune inflammation by enhancing inflammatory T cell development. *Immunity*, **33,** 607-19.

O'CONNELL, R.M., RAO, D.S. & BALTIMORE, D. (2012). microRNA regulation of inflammatory responses. *Annu Rev Immunol*, **30,** 295-312.

OERTLI, M., ENGLER, D.B., KOHLER, E., KOCH, M., MEYER, T.F. & MULLER, A. MicroRNA-155 is essential for the T cell-mediated control of Helicobacter pylori infection and for the induction of chronic Gastritis and Colitis. *J Immunol*, **187,** 3578-86.

OLIVE, V., BENNETT, M.J., WALKER, J.C., MA, C., JIANG, I., CORDON-CARDO, C., LI, Q.J., LOWE, S.W., HANNON, G.J. & HE, L. (2009). miR-19 is a key oncogenic component of mir-17-92. *Genes Dev*, **23,** 2839-49.

OLIVE, V., JIANG, I. & HE, L. mir-17-92, a cluster of miRNAs in the midst of the cancer network. *Int J Biochem Cell Biol*, **42,** 1348-54.

PINCHUK, I.V., BESWICK, E.J. & REYES, V.E. (2010). Staphylococcal enterotoxins. *Toxins (Basel)*, **2,** 2177-97.

PLAZA, R., RODRIGUEZ-SANCHEZ, J.L. & JUAREZ, C. (2007). Staphylococcal enterotoxin B in vivo modulates both gamma interferon receptor expression and ligand-induced activation of signal transducer and activator of transcription 1 in T cells. *Infect Immun*, **75,** 306-13.

PLAZA, R., VIDAL, S., RODRIGUEZ-SANCHEZ, J.L. & JUAREZ, C. (2004). Implication of STAT1 and STAT3 transcription factors in the response to superantigens. *Cytokine*, **25,** 1-10.

RAJAGOPALAN, G., SEN, M.M., SINGH, M., MURALI, N.S., NATH, K.A., IIJIMA, K., KITA, H., LEONTOVICH, A.A., GOPINATHAN, U., PATEL, R. & DAVID, C.S. (2006).

Intranasal exposure to staphylococcal enterotoxin B elicits an acute systemic inflammatory response. *Shock,* **25,** 647-56.

RAO, R., NAGARKATTI, P. & NAGARKATTI, M. Staphylococcal enterotoxin B (SEB) - induced microRNA-155 targets suppressor of cytokine signaling-1 (SOCS1) to promote acute inflammatory lung injury. *Infect Immun.*

RIEDER, S.A., NAGARKATTI, P. & NAGARKATTI, M. CD1d-independent activation of invariant natural killer T cells by staphylococcal enterotoxin B through major histocompatibility complex class II/T cell receptor interaction results in acute lung injury. *Infect Immun,* **79,** 3141-8.

RIEDER, S.A., NAGARKATTI, P. & NAGARKATTI, M. Multiple anti-inflammatory pathways triggered by resveratrol lead to amelioration of staphylococcal enterotoxin B-induced lung injury. *Br J Pharmacol,* **167,** 1244-58.

ROSSI, R.L., ROSSETTI, G., WENANDY, L., CURTI, S., RIPAMONTI, A., BONNAL, R.J., BIROLO, R.S., MORO, M., CROSTI, M.C., GRUARIN, P., MAGLIE, S., MARABITA, F., MASCHERONI, D., PARENTE, V., COMELLI, M., TRABUCCHI, E., DE FRANCESCO, R., GEGINAT, J., ABRIGNANI, S. & PAGANI, M. (2011). Distinct microRNA signatures in human lymphocyte subsets and enforcement of the naive state in CD4+ T cells by the microRNA miR-125b. *Nat Immunol,* **12,** 796-803.

ROSSI, R.L., ROSSETTI, G., WENANDY, L., CURTI, S., RIPAMONTI, A., BONNAL, R.J., BIROLO, R.S., MORO, M., CROSTI, M.C., GRUARIN, P., MAGLIE, S., MARABITA, F., MASCHERONI, D., PARENTE, V., COMELLI, M., TRABUCCHI, E., DE FRANCESCO, R., GEGINAT, J., ABRIGNANI, S. & PAGANI, M. Distinct microRNA signatures in

human lymphocyte subsets and enforcement of the naive state in CD4+ T cells by the microRNA miR-125b. *Nat Immunol*, **12,** 796-803.

SAEED, A.I., RIEDER, S.A., PRICE, R.L., BARKER, J., NAGARKATTI, P. & NAGARKATTI, M. (2012). Acute lung injury induced by Staphylococcal enterotoxin B: disruption of terminal vessels as a mechanism of induction of vascular leak. *Microsc Microanal*, **18,** 445-52.

SAEED, A.I., RIEDER, S.A., PRICE, R.L., BARKER, J., NAGARKATTI, P. & NAGARKATTI, M. Acute lung injury induced by Staphylococcal enterotoxin B: disruption of terminal vessels as a mechanism of induction of vascular leak. *Microsc Microanal*, **18,** 445-52.

SASAKI, K., KOHANBASH, G., HOJI, A., UEDA, R., MCDONALD, H.A., REINHART, T.A., MARTINSON, J., LOTZE, M.T., MARINCOLA, F.M., WANG, E., FUJITA, M. & OKADA, H. (2010). miR-17-92 expression in differentiated T cells - implications for cancer immunotherapy. *J Transl Med*, **8,** 17.

SAUER, S., BRUNO, L., HERTWECK, A., FINLAY, D., LELEU, M., SPIVAKOV, M., KNIGHT, Z.A., COBB, B.S., CANTRELL, D., O'CONNOR, E., SHOKAT, K.M., FISHER, A.G. & MERKENSCHLAGER, M. (2008). T cell receptor signaling controls Foxp3 expression via PI3K, Akt, and mTOR. *Proc Natl Acad Sci U S A*, **105,** 7797-802.

SAVRANSKY, V., ROSTAPSHOV, V., PINELIS, D., POLOTSKY, Y., KOROLEV, S., KOMISAR, J. & FEGEDING, K. (2003). Murine lethal toxic shock caused by intranasal administration of staphylococcal enterotoxin B. *Toxicol Pathol*, **31,** 373-8.

SCHOENBORN, J.R. & WILSON, C.B. (2007). Regulation of interferon-gamma during innate and adaptive immune responses. *Adv Immunol*, **96,** 41-101.

SCOTT, H.L., TAMAGNINI, F., NARDUZZO, K.E., HOWARTH, J.L., LEE, Y.B., WONG, L.F., BROWN, M.W., WARBURTON, E.C., BASHIR, Z.I. & UNEY, J.B. MicroRNA-132 regulates recognition memory and synaptic plasticity in the perirhinal cortex. *Eur J Neurosci*, **36,** 2941-8.

SHIN, I., YAKES, F.M., ROJO, F., SHIN, N.Y., BAKIN, A.V., BASELGA, J. & ARTEAGA, C.L. (2002). PKB/Akt mediates cell-cycle progression by phosphorylation of p27(Kip1) at threonine 157 and modulation of its cellular localization. *Nat Med*, **8,** 1145-52.

SONKOLY, E. & PIVARCSI, A. (2009a). Advances in microRNAs: implications for immunity and inflammatory diseases. *J Cell Mol Med,* **13,** 24-38.

SONKOLY, E. & PIVARCSI, A. (2009b). microRNAs in inflammation. *Int Rev Immunol,* **28,** 535-61.

SONKOLY, E., STAHLE, M. & PIVARCSI, A. (2008). MicroRNAs and immunity: novel players in the regulation of normal immune function and inflammation. *Semin Cancer Biol*, **18,** 131-40.

SRIVASTAVA, M.D., SRIVASTAVA, B.I. & BROUHARD, B. (1998). Delta9 tetrahydrocannabinol and cannabidiol alter cytokine production by human immune cells. *Immunopharmacology*, **40,** 179-85.

STAHL, H.F., FAUTI, T., ULLRICH, N., BOPP, T., KUBACH, J., RUST, W., LABHART, P., ALEXIADIS, V., BECKER, C., HAFNER, M., WEITH, A., LENTER, M.C., JONULEIT, H., SCHMITT, E. & MENNERICH, D. (2009). miR-155 inhibition sensitizes CD4+ Th cells for TREG mediated suppression. *PLoS One*, **4,** e7158.

STRANDBERG, K.L., ROTSCHAFER, J.H., VETTER, S.M., BUONPANE, R.A., KRANZ, D.M. & SCHLIEVERT, P.M. Staphylococcal superantigens cause lethal pulmonary disease in rabbits. *J Infect Dis*, **202,** 1690-7.

STRUM, J.C., JOHNSON, J.H., WARD, J., XIE, H., FEILD, J., HESTER, A., ALFORD, A. & WATERS, K.M. (2009). MicroRNA 132 regulates nutritional stress-induced chemokine production through repression of SirT1. *Mol Endocrinol*, **23,** 1876-84.

SUN, F., FU, H., LIU, Q., TIE, Y., ZHU, J., XING, R., SUN, Z. & ZHENG, X. (2008). Downregulation of CCND1 and CDK6 by miR-34a induces cell cycle arrest. *FEBS Lett*, **582,** 1564-8.

TAMIYA, T., KASHIWAGI, I., TAKAHASHI, R., YASUKAWA, H. & YOSHIMURA, A. Suppressors of cytokine signaling (SOCS) proteins and JAK/STAT pathways: regulation of T-cell inflammation by SOCS1 and SOCS3. *Arterioscler Thromb Vasc Biol*, **31,** 980-5.

TEN DIJKE, P., GOUMANS, M.J., ITOH, F. & ITOH, S. (2002). Regulation of cell proliferation by Smad proteins. *J Cell Physiol*, **191,** 1-16.

THAI, T.H., CALADO, D.P., CASOLA, S., ANSEL, K.M., XIAO, C., XUE, Y., MURPHY, A., FRENDEWEY, D., VALENZUELA, D., KUTOK, J.L., SCHMIDT-SUPPRIAN, M., RAJEWSKY, N., YANCOPOULOS, G., RAO, A. & RAJEWSKY, K. (2007). Regulation of the germinal center response by microRNA-155. *Science*, **316,** 604-8.

TILAHUN, A.Y., HOLZ, M., WU, T.T., DAVID, C.S. & RAJAGOPALAN, G. (2011). Interferon gamma-dependent intestinal pathology contributes to the lethality in bacterial superantigen-induced toxic shock syndrome. *PLoS One*, **6,** e16764.

TREDE, N.S., TSYTSYKOVA, A.V., CHATILA, T., GOLDFELD, A.E. & GEHA, R.S. (1995). Transcriptional activation of the human TNF-alpha promoter by superantigen in human monocytic cells: role of NF-kappa B. *J Immunol*, **155,** 902-8.

TROTTA, R., CHEN, L., CIARLARIELLO, D., JOSYULA, S., MAO, C., COSTINEAN, S., YU, L., BUTCHAR, J.P., TRIDANDAPANI, S., CROCE, C.M. & CALIGIURI, M.A. miR-155 regulates IFN-gamma production in natural killer cells. *Blood*, **119,** 3478-85.

TSANG, W.P. & KWOK, T.T. (2009). The miR-18a* microRNA functions as a potential tumor suppressor by targeting on K-Ras. *Carcinogenesis*, **30,** 953-9.

TSYTSYKOVA, A.V. & GOLDFELD, A.E. (2000). Nuclear factor of activated T cells transcription factor NFATp controls superantigen-induced lethal shock. *J Exp Med*, **192,** 581-6.

UCHAKINA, O.N., CASTILLEJO, C.M., BRIDGES, C.C. & MCKALLIP, R.J. The role of hyaluronic acid in SEB-induced acute lung inflammation. *Clin Immunol*, **146,** 56-69.

ULRICH, R.G., S. SIDELL, T.J.TAYLOR, C.L WILHELMSEN AND D.R FRANZ. (2001). *Textbook of military medicine: medical aspects of chemical and biological warfare.*

WAJANAPONSAN, N., READE, M.C. & MILBRANDT, E.B. (2007). Steroids in late ARDS? *Crit Care*, **11,** 310.

WANG, P., HOU, J., LIN, L., WANG, C., LIU, X., LI, D., MA, F., WANG, Z. & CAO, X. Inducible microRNA-155 feedback promotes type I IFN signaling in antiviral innate immunity by targeting suppressor of cytokine signaling 1. *J Immunol*, **185,** 6226-33.

WERTHEIM, H.F., MELLES, D.C., VOS, M.C., VAN LEEUWEN, W., VAN BELKUM, A., VERBRUGH, H.A. & NOUWEN, J.L. (2005). The role of nasal carriage in Staphylococcus aureus infections. *Lancet Infect Dis*, **5,** 751-62.

WHEELER, A.P. & BERNARD, G.R. (2007). Acute lung injury and the acute respiratory distress syndrome: a clinical review. *Lancet*, **369,** 1553-64.

WONG, W.F., KOHU, K., CHIBA, T., SATO, T. & SATAKE, M. Interplay of transcription factors in T-cell differentiation and function: the role of Runx. *Immunology*, **132,** 157-64.

WONG, W.F., KOHU, K., NAKAMURA, A., EBINA, M., KIKUCHI, T., TAZAWA, R., TANAKA, K., KON, S., FUNAKI, T., SUGAHARA-TOBINAI, A., LOOI, C.Y., ENDO, S., FUNAYAMA, R., KUROKAWA, M., HABU, S., ISHII, N., FUKUMOTO, M., NAKATA, K., TAKAI, T. & SATAKE, M. Runx1 deficiency in CD4+ T cells causes fatal autoimmune inflammatory lung disease due to spontaneous hyperactivation of cells. *J Immunol*, **188,** 5408-20.

WU, T., WIELAND, A., ARAKI, K., DAVIS, C.W., YE, L., HALE, J.S. & AHMED, R. (2012). Temporal expression of microRNA cluster miR-17-92 regulates effector and memory CD8+ T-cell differentiation. *Proc Natl Acad Sci U S A*, **109,** 9965-70.

XIAO, B., LIU, Z., LI, B.S., TANG, B., LI, W., GUO, G., SHI, Y., WANG, F., WU, Y., TONG, W.D., GUO, H., MAO, X.H. & ZOU, Q.M. (2009). Induction of microRNA-155 during Helicobacter pylori infection and its negative regulatory role in the inflammatory response. *J Infect Dis*, **200,** 916-25.

XIAO, C., SRINIVASAN, L., CALADO, D.P., PATTERSON, H.C., ZHANG, B., WANG, J., HENDERSON, J.M., KUTOK, J.L. & RAJEWSKY, K. (2008). Lymphoproliferative

disease and autoimmunity in mice with increased miR-17-92 expression in lymphocytes. *Nat Immunol*, **9,** 405-14.

XU, N., MEISGEN, F., BUTLER, L.M., HAN, G., WANG, X.J., SODERBERG-NAUCLER, C., STAHLE, M., PIVARCSI, A. & SONKOLY, E. MicroRNA-31 is overexpressed in psoriasis and modulates inflammatory cytokine and chemokine production in keratinocytes via targeting serine/threonine kinase 40. *J Immunol*, **190,** 678-88.

YU, H., PARDOLL, D. & JOVE, R. (2009). STATs in cancer inflammation and immunity: a leading role for STAT3. *Nat Rev Cancer*, **9,** 798-809.

ZHANG, M., ZHANG, Q., LIU, F., YIN, L., YU, B. & WU, J. MicroRNA-155 may affect allograft survival by regulating the expression of suppressor of cytokine signaling 1. *Med Hypotheses*, **77,** 682-4.

ZHANG, X., HU, S., ZHANG, X., WANG, L., ZHANG, X., YAN, B., ZHAO, J., YANG, A. & ZHANG, R. MicroRNA-7 arrests cell cycle in G1 phase by directly targeting CCNE1 in human hepatocellular carcinoma cells. *Biochem Biophys Res Commun*, **443,** 1078-84.